Brigham Young University

BYU ScholarsArchive

2021-08-12

Inflammation and Altered Signaling in Obstetric Pathologies

Ya-Fang Tsai
Brigham Young University

Inflammation and Altered Signaling in Obstetric Pathologies

Ya-Fang Tsai

A dissertation submitted to the faculty of
Brigham Young University
in partial fulfillment of the requirements for the degree of

Doctor of Philosophy

Juan A. Arroyo, Chair
Benjamin T. Bikman
Paul R. Reynolds
Sterling N. Sudweeks
Brian D. Pool

Department of Physiology and Developmental Biology

Brigham Young University

ABSTRACT

Inflammation and Altered Signaling in Obstetric Pathologies

Ya-Fang Tsai
Department of Physiology and Developmental Biology, BYU
Doctor of Philosophy

The purpose of this research project was to elucidate the molecular interactions and detail the signaling pathways in obstetric pathologies. This work first seeks to understand inflammation related complications relevant to obstetrics. Prior research in our lab identified the implications of the receptor of advanced glycation end products (RAGE) during inflammatory response in the placenta. Current work identified the presence of DNA double-strand breaks (DNA-DSBs) in inflammation associated pregnancy complications of preeclampsia (PE) and preterm labor (PTL) and demonstrated the positive role of RAGE in repairing the damage.

The confluent relevance of disrupted mitochondrial function and inflammation has been recognized in the etiology of numerous chronic diseases. Our current studies aim to understand the connections between energy metabolism and inflammation in pathologies of pregnancy complications. Previous research conducted in our laboratory has demonstrated the mediation of the Gas6/Axl pathway on the mechanistic target of rapamycin (mTOR), an important metabolic molecule. We observed the negative regulation of Gas6 treatment on the mTOR pathway and its negative effects on trophoblast cell invasion. In the current study looking at the aspect of energy regulation, we identified the activation of placental mTOR in gestational diabetes mellitus (GDM) and its decrease during PE and intrauterine growth restriction (IUGR). We further evaluated the regulation of mTOR on its downstream effector pyruvate kinase M2 (PKM2). We found that inhibition of mTOR decreased PKM2 activation; while PKM2 activation positively regulated trophoblastic invasion and rescued negative effects observed in our second-hand smoke IUGR murine model.

Our work has opened a new direction of placental research, especially in pregnancy complications stemming from genomic instability. We also clarified details of mTOR and PKM2 meditated metabolic signaling that are crucial for future investigation on the dynamic metabolic regulation during pregnancy.

Keywords: RAGE, DNA-DSB, mTOR, PKM2, preeclampsia, preterm labor, intrauterine growth restriction, gestational diabetes mellitus, placenta, pregnancy, trophoblast

ACKNOWLEDGEMENTS

My deep gratitude goes first to my mentors, Dr. Arroyo and Dr. Reynolds, who adapted my way of learning and expertly guided me through my graduate studies. They have shown their invaluable qualities as leaders by having my best interest at heart and setting me up for success. My gratitude also extends to teachers, students, colleagues, and friends who have made an impact in my life and shaped who I am today. Furthermore, I am thankful for my family who love me unconditionally and provide support in every aspect. Finally, I would like to pay my special regards to those mentioned above and many more whose assistance was a milestone in my life and in the completion of this project.

TABLE OF CONTENTS

LIST OF FIGURES

LIST OF TABLES

CHAPTER 1: Introduction

The importance of pathology research has been recognized in recent years. Knowledge of pathological pathways bridges the gap between basic science and clinical applications and underpins every aspect of patient care from prevention and diagnosis to treatment options and post-treatment care (Rodriguez-Canales et al., 2011; Sanfilippo, 2014). One of the major successes in modern health science was the identification of the contributions of inflammation and altered metabolism in disease developments. This discovery provides advanced knowledge in disease prevention and makes many treatment options available (Osborn & Olefsky, 2012). While most obstetric complications are linked to inflammatory and metabolic issues, their pathological pathways remain largely unexplored (Challis et al., 2009; Do et al., 2019). Our research primarily focuses on the inflammatory and metabolic signaling pathways during pregnancy complications.

The Placenta

During gestation, appropriate communication between the mother and the fetus is essential for a successful pregnancy. This connection is governed by the organ of the placenta. The major functions of the placenta include nutrient delivery and barrier protection between the mother and the fetus and are carried out by trophoblast cells (Turco & Moffett, 2019). The two main trophoblast cell types that make up the placenta are syncytiotrophoblasts and cytotrophoblasts. Syncytiotrophoblasts (SCT) are specialized epithelial cells that provide immune protection in direct contact with the maternal side. In the intervillous space, SCT becomes the outer lining of placental villi and allows maternal and fetal nutrient and waste exchange. The invasive cytotrophoblasts invade the endometrium and myometrium, remodeling spiral arteries from high to low resistance vasculature for larger oxygen and nutrient delivery

(Knöfler et al., 2019). Thus, the survival and functions of trophoblast cells are critical in maintaining a healthy placenta and allowing proper adaptation as pregnancy progresses (Maltepe & Fisher, 2015).

Pregnancy Complications

Pregnancy complications are issues that arise during gestation which complicate maternal and fetal health. A healthy placenta is critical to protect fetuses from maternal immune attack and allow appropriate nutrient and waste exchange. Expectedly, most obstetric complications share the common feature of a pathological placenta (Brosens et al., 2011; Fisher, 2000).

Preeclampsia (PE)

Preeclampsia complicates 2-8% of pregnancies globally (Espinoza et al., 2020). Though the exact pathology remains unclear, advanced research reveals features of placental ischemia and underdeveloped placenta as results for insufficient trophoblast invasion in preeclamptic pregnancies. Clinical manifestations of PE include maternal hypertension, proteinuria, and signs of liver and kidney damage. Depending on its severity, preeclampsia treatment usually focuses on anti-hypertensive therapy, yet the only conclusive treatment is to remove the placenta. Because of the need for placental removal, premature delivery often leaves lifelong effects on the health and development of the infants (Rana et al., 2019).

Pre-term Labor (PTL)

Pre-term birth is defined as delivery before 37 weeks of gestation which occurs in 5-18% of pregnancies worldwide. Current research suggests the immunopathogenesis theory, where compromised immune adaptation causes the bidirectional inflammation in mother and fetus and

results in the onset of delivery (Green & Arck, n.d.). Premature birth increases the risks of infant mortality and disability later in life (Anderson & Cacola, 2017).

Intrauterine Growth Restriction (IUGR)

After preterm delivery, IUGR is the second leading cause of perinatal mortality and morbidity (Nardozza et al., 2017). IUGR, as suggested by the name, is under desired fetal growth in consequence of aberrant vasculature development and decreased vascular density in the placental villi (Arroyo & Winn, 2008). This results in poor placental perfusion which alters fetal nutrition leading to developmental adaptation that changes the physiology and metabolism of the offspring (Guerby & Bujold, 2020).

Gestational Diabetes Mellitus (GDM)

Affecting 7-10% of pregnancies worldwide, GDM is when diabetes occurs during pregnancy (Behboudi-Gandevani et al., 2019). Current treatments focus on metabolic control through insulin or lifestyle/diet change (Desoye & Hauguel-De Mouzon, 2007). GDM is characterized by an enlarged placenta and nutritional oversupply to the fetus. Excessive fetal growth and increased risk of type 2 diabetes in the mother are often the results (Vince et al., 2020).

Most pregnancy complications share the common feature of a pathological placenta as a consequence of impaired trophoblast cell functions. Systemic inflammation and metabolic imbalance are known to be deleterious to cell functions and have been linked to undesired pregnancy outcomes. Thus, research on inflammatory and metabolic pathways in the placenta is essential for advanced disease prevention and treatments.

Receptor for Advanced Glycation End-Products

In the uterus, the extent of inflammation will determine the reception or rejection of the semi-allogeneic fetus. Though some is required for uterine receptivity and parturition, excessive inflammation is involved in the development of many pregnancy complications such as PE, PTL, and IUGR (Negishi et al., 2020). Significantly, the pathologies in these complications have been linked to the receptor for advanced glycation end-products (RAGE) –mediated inflammatory signaling pathway (Alexander et al., 2016; Buhimschi et al., 2009; Lewis et al., 2017; Noguchi et al., 2010).

RAGE is a member of the immunoglobulin superfamily, consisting of a cytosolic tail, a single hydrophobic transmembrane domain, and an extracellular region. The extracellular region contains two C-type and one V-type immunoglobulin domain, wherein the V-type domain allows three-dimensional recognition rather than specific amino acid sequences (Chuah et al., 2013). Thus, RAGE is often referred to as a pattern recognition receptor and harbors a group of ligands. Besides binding to advanced glycation end products (AGEs), RAGE also binds with amyloid β-peptide, high mobility group box protein 1 (HMGB1), and S100. The ligand-receptor interaction is a common cellular pathway in inducing inflammatory response which implicates disease progression such as pulmonary diseases, cancers, type 2 diabetes, and pregnancy complications (Alexander et al., 2016; Buhimschi et al., 2009; Lewis et al., 2017; Marie Schmidt et al., n.d.; Noguchi et al., 2010; Tadesse et al., 2014).

Although RAGE primarily functions as a cell surface receptor, different isoforms of RAGE have also been identified such as soluble RAGE (sRAGE) and nuclear RAGE (nRAGE) (Kumar et al., 2017; Mulrennan et al., 2015). sRAGE corresponds to the extracellular region of RAGE. Lacking transmembrane and cytosolic domains, sRAGE is produced either through

alternative splicing or proteolytic processing of the membrane RAGE (Mulrennan et al., 2015).

Because of the conserved extracellular region, sRAGE shares the same ligand-binding specificity and is able to alleviate inflammatory signaling by competitively preventing ligands from binding to membrane RAGE (Koyama et al., 2007). This counteraction principle of sRAGE to membrane receptor RAGE has been incorporated in RAGE-associated therapeutic target research by utilizing RAGE neutralizing antibody and semi-synthetic glycosaminoglycan ethers (SAGEs) (Strieder-Barboza et al., 2019; Tsai et al., 2019).

On the other hand, the nuclear isoform of RAGE was identified and shown to have a role in DNA double-strand breaks (DNA-DSBs) repair in the lung tissue (Kumar et al., 2017). DNA damage can be a part of the natural cell cycle. If left unrepaired, accumulative DNA defects can induce tissue inflammation and disturb normal organ functions such as those reported in preeclampsia (Shimizu et al., 2014; Tadesse et al., 2014). Therefore, identifying a placental DNA repair pathway is critical in understanding disease progression and allows potential treatment developments.

mTOR

mTOR is a member of the PI3k-assocaited kinase protein family and serves as a core component of mTOR complex 1 and 2 (Sabatini, 2017). Functioning as the common downstream effector of RAGE and AXL, mTOR regulates cell proliferation, survival and migration by coordinating nutrients availability (Eva et al., 2020; Hirschi et al., 2019; Hou et al., 2014). mTOR is expressed in placental trophoblast cells and mediates trophoblast proliferation, placental growth, and nutrient transfer through the placental barriers from the mother to the fetus (Jansson et al., 2012; Wen et al., 2005). mTOR is also a positive regulator of pyruvate kinase M2 (PKM2) (Sun et al., 2011). PKM2 catalyzes the last step of glycolysis and is responsible for ATP

production under hypoxia condition (Vaupel & Harrison, 2004). mTOR has been shown to be implicated during nutrient overload in GDM and oxidative stress in preeclampsia; in addition, PKM2 is elevated during preeclampsia (Huang et al., 2020; Nguyen-Ngo et al., 2019). Thus, the mTOR pathway and its effects on PKM2 are essential in understanding both physiological and pathological placental and fetal developments.

Our work has identified the pathology of pregnancy complications stemming from genomic instability and detailed the involvement of RAGE during placental DNA-DSBs repair. We also described the effect of altered metabolic regulations on trophoblast functions in different pregnancy complications. These findings offer a foundation for future research in the investigation of DNA repair mechanisms in the placenta and metabolism-imbalance-associated pathologies in obstetric complications.

References

Alexander, K. L., Mejia, C. A., Jordan, C., Nelson, M. B., Howell, B. M., Jones, C. M., Reynolds, P. R., & Arroyo, J. A. (2016). Differential Receptor for Advanced Glycation End Products Expression in Preeclamptic, Intrauterine Growth Restricted, and Gestational Diabetic Placentas. *American Journal of Reproductive Immunology*, *75*(2), 172–180. https://doi.org/10.1111/aji.12462

Anderson, C., & Cacola, P. (2017). Implications of Preterm Birth for Maternal Mental Health and Infant Development. *The American Journal of Maternal/Child Nursing*, *42*(2), 108–114.

Arroyo, J. A., & Winn, V. D. (2008). Vasculogenesis and Angiogenesis in the IUGR Placenta. In *Seminars in Perinatology* (Vol. 32, Issue 3, pp. 172–177). https://doi.org/10.1053/j.semperi.2008.02.006

Axelrod, H., & Pienta, K. J. (2014). Oncotarget 8818 www.impactjournals.com/oncotarget Axl as a mediator of cellular growth and survival. In *Oncotarget* (Vol. 5, Issue 19). www.impactjournals.com/oncotarget/

Behboudi-Gandevani, S., Amiri, M., Bidhendi Yarandi, R., & Ramezani Tehrani, F. (2019). The impact of diagnostic criteria for gestational diabetes on its prevalence: A systematic review and meta-analysis. In *Diabetology and Metabolic Syndrome* (Vol. 11, Issue 1). BioMed Central Ltd. https://doi.org/10.1186/s13098-019-0406-1

Brosens, I., Pijnenborg, R., Vercruysse, L., & Romero, R. (2011). The "great Obstetrical Syndromes" are associated with disorders of deep placentation. *American Journal of Obstetrics and Gynecology*, *204*(3), 193–201. https://doi.org/10.1016/j.ajog.2010.08.009

Buhimschi, C. S., Baumbusch, M. A., Dulay, A. T., Oliver, E. A., Lee, S., Zhao, G., Bhandari, V., Ehrenkranz, R. A., Weiner, C. P., Madri, J. A., & Buhimschi, I. A. (2009). Characterization of RAGE, HMGB1, and S100β in inflammation-induced preterm birth and fetal tissue injury. *American Journal of Pathology*, *175*(3), 958–975. https://doi.org/10.2353/ajpath.2009.090156

Challis, J. R., Lockwood, C. J., Myatt, L., Norman, J. E., Strauss, J. F., & Petraglia, F. (2009). Inflammation and pregnancy. *Reproductive Sciences*, *16*(2), 206–215. https://doi.org/10.1177/1933719108329095

Chuah, Y. K., Basir, R., Talib, H., Tie, T. H., & Nordin, N. (2013). Receptor for advanced glycation end products and its involvement in inflammatory diseases. In *International Journal of Inflammation* (Vol. 2013). https://doi.org/10.1155/2013/403460

Cooke, C. L. M., Brockelsby, J. C., Baker, P. N., & Davidge, S. T. (2003). The Receptor for Advanced Glycation End Products (RAGE) Is Elevated in Women with Preeclampsia. *Hypertension in Pregnancy*, *22*(2), 173–184. https://doi.org/10.1081/PRG-120021068

Desoye, G., & Hauguel-De Mouzon, S. (2007). The human placenta in gestational diabetes mellitus: The insulin and cytokine network. *Diabetes Care*, *30*(SUPPL. 2). https://doi.org/10.2337/dc07-s203

Do, M., Lima, C. P., Suely, A., Melo, O., Santos Sena, A. S., De Oliveira Barros, V., & Ramos Amorim, M. M. (2019). Metabolic syndrome in pregnancy and postpartum: prevalence and associated factors. *REV ASSOC MED BRAS*, *65*(12), 1489–1495. https://doi.org/10.1590/1806-9282.65.12.1489

Espinoza, J., Vidaeff, A., Pettker, C. M., & Simhan, H. (2020). *ACOG PRACTICE BULLETIN Clinical Management Guidelines for Obstetrician-Gynecologists*. http://journals.lww.com/greenjournal

Eva, T. A., Barua, N., Chowdhury, M. M., Yeasmin, S., Rakib, A., Islam, M. R., Emran, T. Bin, & Simal-Gandara, J. (2020). Perspectives on signaling for biological- and processed food-related advanced glycation end-products and its role in cancer progression. *Critical Reviews in Food Science and Nutrition*, 1–18. https://doi.org/10.1080/10408398.2020.1856771

Fisher, S. J. (2000). *+1(212)*.

Green, E. S., & Arck, P. C. (n.d.). *Pathogenesis of preterm birth: bidirectional inflammation in mother and fetus*. https://doi.org/10.1007/s00281-020-00807-y/Published

Guerby, P., & Bujold, E. (2020). Early detection and prevention of intrauterine growth restriction and its consequences. In *JAMA Pediatrics* (Vol. 174, Issue 8, pp. 749–750). American Medical Association. https://doi.org/10.1001/jamapediatrics.2020.1106

Hirschi, K. M., Fang Tsai, K. Y., Edwards, M. M., Hall, P., Mejia, J. F., Mejia, C. A., Reynolds, P. R., & Arroyo, J. A. (2019). The mTOR Family of Proteins and the Regulation of Trophoblast Invasion by Gas6. *Journal of Cell Signaling*, *04*(02). https://doi.org/10.35248/2576-1471.19.4.203

Hou, X., Hu, Z., Xu, H., Xu, J., Zhang, S., Zhong, Y., He, X., & Wang, N. (2014). Advanced glycation endproducts trigger autophagy in cadiomyocyte Via RAGE/PI3K/AKT/mTOR pathway. *Cardiovascular Diabetology*, *13*(1). https://doi.org/10.1186/1475-2840-13-78

Huang, J., Zheng, L., Wang, F., Su, Y., Kong, H., & Xin, H. (2020). Mangiferin ameliorates placental oxidative stress and activates PI3K/Akt/mTOR pathway in mouse model of preeclampsia. *Archives of Pharmacal Research*, *43*(2), 233–241. https://doi.org/10.1007/s12272-020-01220-7

Jansson, T., Aye, I. L. M. H., & Goberdhan, D. C. I. (2012). The emerging role of mTORC1 signaling in placental nutrient-sensing. *Placenta*, *33*(SUPPL. 2). https://doi.org/10.1016/j.placenta.2012.05.010

Knöfler, M., Haider, S., Saleh, L., Pollheimer, J., Gamage, T. K. J. B., & James, J. (2019). Human placenta and trophoblast development: key molecular mechanisms and model systems. In *Cellular and Molecular Life Sciences* (Vol. 76, Issue 18, pp. 3479–3496). Birkhauser Verlag AG. https://doi.org/10.1007/s00018-019-03104-6

Koyama, H., Yamamoto, H., & Nishizawa, Y. (2007). RAGE and soluble RAGE: Potential therapeutic targets for cardiovascular diseases. In *Molecular Medicine* (Vol. 13, Issues 11–12, pp. 625–635). https://doi.org/10.2119/2007-00087.Koyama

Kumar, V., Fleming, T., Terjung, S., Gorzelanny, C., Gebhardt, C., Agrawal, R., Mall, M. A., Ranzinger, J., Zeier, M., Madhusudhan, T., Ranjan, S., Isermann, B., Liesz, A., Deshpande, D., Häring, H. U., Biswas, S. K., Reynolds, P. R., Hammes, H. P., Peperkok, R., … Nawroth, P. P. (2017). Homeostatic nuclear RAGE-ATM interaction is essential for efficient DNA repair. *Nucleic Acids Research*, *45*(18), 10595–10613. https://doi.org/10.1093/nar/gkx705

Lewis, J. B., Mejia, C., Jordan, C., Monson, T. D., Bodine, J. S., Dunaway, T. M., Egbert, K. M., Lewis, A. L., Wright, T. J., Ogden, K. C., Broberg, D. S., Hall, P. D., Nelson, S. M., Hirschi, K. M., Reynolds, P. R., & Arroyo, J. A. (2017). Inhibition of the receptor for advanced glycation end-products (RAGE) protects from secondhand smoke (SHS)-induced intrauterine growth restriction IUGR in mice. *Cell and Tissue Research*, *370*(3), 513–521. https://doi.org/10.1007/s00441-017-2691-z

Maltepe, E., & Fisher, S. J. (2015). Placenta: The Forgotten Organ. *Annual Review of Cell and Developmental Biology*, *31*, 523–552. https://doi.org/10.1146/annurev-cellbio-100814-125620

Marie Schmidt, A., Du Yan, S., Fang Yan, S., & Stern aY, D. M. (n.d.). *The biology of the receptor for advanced glycation end products and its ligands*. www.elsevier.com/locate/bba

Mulrennan, S., Baltic, S., Aggarwal, S., Wood, J., Miranda, A., Frost, F., Kaye, J., & Thompson, P. J. (2015). The role of receptor for advanced glycation end products in airway inflammation in CF and CF related diabetes. *Scientific Reports*, *5*. https://doi.org/10.1038/srep08931

Nardozza, L. M. M., Caetano, A. C. R., Zamarian, A. C. P., Mazzola, J. B., Silva, C. P., Marçal, V. M. G., Lobo, T. F., Peixoto, A. B., & Araujo Júnior, E. (2017). Fetal growth restriction: current knowledge. In *Archives of Gynecology and Obstetrics* (Vol. 295, Issue 5, pp. 1061–1077). Springer Verlag. https://doi.org/10.1007/s00404-017-4341-9

Negishi, Y., Shima, Y., Takeshita, T., & Morita, R. (2020). Harmful and beneficial effects of inflammatory response on reproduction: sterile and pathogen-associated inflammation. In *Immunological Medicine*. Taylor and Francis Ltd. https://doi.org/10.1080/25785826.2020.1809951

Nguyen-Ngo, C., Jayabalan, N., Salomon, C., & Lappas, M. (2019). Molecular pathways disrupted by gestational diabetes mellitus. In *Journal of Molecular Endocrinology* (Vol. 63, Issue 3, pp. R51–R72). BioScientifica Ltd. https://doi.org/10.1530/JME-18-0274

Noguchi, T., Sado, T., Naruse, K., Shigetomi, H., Onogi, A., Haruta, S., Kawaguchi, R., Nagai, A., Tanase, Y., Yoshida, S., Kitanaka, T., Oi, H., & Kobayashi, H. (2010). Evidence for activation of toll-like receptor and receptor for advanced glycation end products in preterm birth. In *Mediators of Inflammation* (Vol. 2010). https://doi.org/10.1155/2010/490406

Oliver, E. A., Buhimschi, C. S., Dulay, A. T., Baumbusch, M. A., Abdel-Razeq, S. S., Lee, S. Y., Zhao, G., Jing, S., Pettker, C. M., & Buhimschi, I. A. (2011). Activation of the receptor for advanced glycation end products system in women with severe preeclampsia. *Journal of Clinical Endocrinology and Metabolism*, *96*(3), 689–698. https://doi.org/10.1210/jc.2010-1418

Osborn, O., & Olefsky, J. M. (2012). The cellular and signaling networks linking the immune system and metabolism in disease. In *Nature Medicine* (Vol. 18, Issue 3, pp. 363–374). https://doi.org/10.1038/nm.2627

Rana, S., Lemoine, E., Granger, J., & Karumanchi, S. A. (2019). Preeclampsia: Pathophysiology, Challenges, and Perspectives. *Circulation Research*, *124*(7), 1094–1112. https://doi.org/10.1161/CIRCRESAHA.118.313276

Rodriguez-Canales, J., Eberle, F. C., Jaffe, E. S., & Emmert-Buck, M. R. (2011). Why is it crucial to reintegrate pathology into cancer research? *BioEssays*, *33*(7), 490–498. https://doi.org/10.1002/bies.201100017

Sabatini, D. M. (2017). Twenty-five years of mTOR: Uncovering the link from nutrients to growth. In *Proceedings of the National Academy of Sciences of the United States of America* (Vol. 114, Issue 45, pp. 11818–11825). National Academy of Sciences. https://doi.org/10.1073/pnas.1716173114

Sanfilippo, F. (2014). Health services research: Opportunities for pathology. In *American Journal of Pathology* (Vol. 184, Issue 9, pp. 2366–2368). Elsevier Inc. https://doi.org/10.1016/j.ajpath.2014.06.007

Sasaki, T., Knyazev, P. G., Clout, N. J., Cheburkin, Y., Göhring, W., Ullrich, A., Timpl, R., & Hohenester, E. (2006). Structural basis for Gas6-Axl signalling. *EMBO Journal*, *25*(1), 80–87. https://doi.org/10.1038/sj.emboj.7600912

Shimizu, I., Yoshida, Y., Suda, M., & Minamino, T. (2014). DNA damage response and metabolic disease. In *Cell Metabolism* (Vol. 20, Issue 6, pp. 967–977). Cell Press. https://doi.org/10.1016/j.cmet.2014.10.008

Stepan, H., Richter, J., Kley, K., Kralisch, S., Jank, A., Schaarschmidt, W., Ebert, T., Lössner, U., Jessnitzer, B., Kratzsch, J., Blüher, M., Stumvoll, M., & Fasshauer, M. (2013). Serum levels of growth arrest specific protein 6 are increased in preeclampsia. *Regulatory Peptides*, *182*(1), 7–11. https://doi.org/10.1016/j.regpep.2012.12.013

Strieder-Barboza, C., Baker, N. A., Flesher, C. G., Karmakar, M., Neeley, C. K., Polsinelli, D., Dimick, J. B., Finks, J. F., Ghaferi, A. A., Varban, O. A., Lumeng, C. N., & O'Rourke, R. W. (2019). Advanced glycation end-products regulate extracellular matrix-adipocyte metabolic crosstalk in diabetes. *Scientific Reports*, *9*(1). https://doi.org/10.1038/s41598-019-56242-z

Sun, Q., Chen, X., Ma, J., Peng, H., Wang, F., Zha, X., Wang, Y., Jing, Y., Yang, H., Chen, R., Chang, L., Zhang, Y., Goto, J., Onda, H., Chen, T., Wang, M. R., Lu, Y., You, H., Kwiatkowski, D., & Zhang, H. (2011). Mammalian target of rapamycin up-regulation of pyruvate kinase isoenzyme type M2 is critical for aerobic glycolysis and tumor growth. *Proceedings of the National Academy of Sciences of the United States of America*, *108*(10), 4129–4134. https://doi.org/10.1073/pnas.1014769108

Tadesse, S., Kidane, D., Guller, S., Luo, T., Norwitz, N. G., Arcuri, F., Toti, P., & Norwitz, E. R. (2014). In vivo and in vitro evidence for placental DNA damage in preeclampsia. *PLoS ONE*, *9*(1). https://doi.org/10.1371/journal.pone.0086791

Tsai, K. Y. F., Hirschi Budge, K. M., Llavina, S., Davis, T., Long, M., Bennett, A., Sitton, B., Arroyo, J. A., & Reynolds, P. R. (2019). RAGE and AXL expression following secondhand smoke (SHS) exposure in mice. *Experimental Lung Research*, *45*(9–10), 297–309. https://doi.org/10.1080/01902148.2019.1684596

Turco, M. Y., & Moffett, A. (2019). Development of the human placenta. In *Development (Cambridge)* (Vol. 146, Issue 22). Company of Biologists Ltd. https://doi.org/10.1242/dev.163428

Vaupel, P., & Harrison, L. (2004). Tumor Hypoxia: Causative Factors, Compensatory Mechanisms, and Cellular Response. *The Oncologist*, *9*(S5), 4–9. https://doi.org/10.1634/theoncologist.9-90005-4

Vince, K., Perković, P., & Matijević, R. (2020). What is known and what remains unresolved regarding gestational diabetes mellitus (GDM). In *Journal of Perinatal Medicine* (Vol. 48, Issue 8, pp. 757–763). De Gruyter Open Ltd. https://doi.org/10.1515/jpm-2020-0254

Wen, H. Y., Abbasi, S., Kellems, R. E., & Xia, Y. (2005). mTOR: A placental growth signaling sensor. *Placenta*, *26*(SUPPL.). https://doi.org/10.1016/j.placenta.2005.02.004

Ye, L., Guan, L., Fan, P., Liu, X., Liu, R., Chen, J., Zhu, Y., Wei, X., Liu, Y., & Bai, H. (2017). Association study between GAS6 gene polymorphisms and risk of preeclampsia in Chinese population. *European Journal of Obstetrics and Gynecology and Reproductive Biology*, *211*, 122–126. https://doi.org/10.1016/j.ejogrb.2017.02.014

CHAPTER 2: A Role for RAGE in DNA Double Strand Breaks (DSBs)
Detected in Pathological Placentas and Trophoblast Cells

Kary Y.F. Tsai, Benton Tullis, Katrina L. Breithaupt, Rylan Fowers, Nelson Jones, Samuel
Grajeda, Paul R. Reynolds and Juan A. Arroyo

Lung and Placenta Research Laboratory, Department of Physiology and Developmental Biology,
Brigham Young University, Provo, UT, USA

Corresponding Author:
Juan A. Arroyo, PhD
Department of Physiology and Developmental Biology
Brigham Young University
3052 LSB
Provo, UT 84602
Phone: (801) 422-3221; Fax: (801) 422-0700
Email: jarroyo@byu.edu

Abstract

Impaired DNA damage responses are associated with several diseases, including pregnancy complications. Recent research identified an ATM-kinase dependent function for the nuclear isoform of the receptor for advanced glycation end-products (RAGE) during double strand break (DSB)-repair. RAGE contributes to end-resectioning of broken DNA sites by binding with the MRE11-Rad50-Nbs1 (MRN) complex. Placental research is limited regarding the impact of genomic instability and the mechanism for potential repair. We tested the hypothesis regarding the involvement of RAGE during the repair of placental DNA-DSBs. We first identified that the pregnancy complications of PE and preterm labor (PTL) experience loss of genomic integrity and an in vitro trophoblast cell model was used to characterize trophoblast DSBs. Colocalized immunofluorescence of γ-H2AX and RAGE support the potential involvement of RAGE in cellular responses to DNA-DSBs. Immunoblotting for both molecules in PE and PTL placenta samples and in trophoblast cells validated a connection. Co-immunoprecipitation studies revealed interactions between RAGE and pATM and MRE11 during DNA-DSBs. Reduced cellular invasion confirmed the role of genomic instability in trophoblastic function. Collectively, these experiments identified genomic instability in pregnancy complications, the impact of defective DNA on trophoblast function, and a possible RAGE-mediated mechanism during DNA-DSB repair.

Keywords: DSB, RAGE, placenta, γ-H2AX, pATM, MRE11

Introduction

        The placenta is a critical organ during pregnancy, serving as the maternal-fetal interface. Throughout pregnancy progression, fetus-derived trophoblasts play key roles in establishing and maintaining placental function and growth (Knöfler et al., 2019). Early in pregnancy, trophoblasts invade the uterine endometrium and myometrium, and convert resident spiral arteries from high to low resistance vessels, in order to increase blood capacity (Knöfler et al., 2019). Besides the importance of invasion, trophoblast cells are also specialized epithelial cells that are responsible for facilitating appropriate exchange of nutrients, and wastes between maternal and fetal compartments (Monson et al., 2017). These unique functions allow embryonic settlement and meets the requirement of enhanced oxygen and nutrient exchange for proper fetal development (Carter et al., 2015). Abnormal placentation is a feature of diverse pregnancy complications including pre-term labor (PTL), intrauterine growth restriction (IUGR) and preeclampsia (PE) (Knuth et al., 2015; Reuvekamp et al., 1999; Zhou et al., 1997). Failures in placental formation result from inappropriate adaptation, shallow trophoblastic invasion, increased trophoblast apoptosis, and insufficient spiral artery modification compromise placental and embryonic growth, and development (Arshad et al., 2014; Bahr et al., 2014). Therefore, trophoblast survival and invasion are essential for successful pregnancies, whereas trophoblast apoptosis and dysfunction correlate with pregnancy complications, and such outcomes may be underpinned with placental genomic instability (Mo et al., 2019).

        DNA damage can be a part of the natural progression of the cell cycle and a means of disposing aberrant cells (Ciccia & Elledge, 2010; Jackson & Bartek, 2009). However, exposure to cytotoxic agents also results in defective DNA accumulation and negatively affects physiological function. The most cytotoxic forms of DNA damage are DNA double-strand

breaks (DNA-DSBs) where both strands of the helix are ruptured. If left unrepaired, these lesions

lead to disorders such as cancer, fibrosis, and neurodegeneration (Aparicio et al., 2014;

O'Driscoll, 2012). A functional repair system is fundamental in maintaining human health when

the harmful effects of DNA-DSBs are manifest. In response to DNA-DSBs, sequential events

involved in the DNA damage response (DDR) will detect, recruit various implicated molecules,

and repair DNA-DSBs via either the error-prone non-homologous end joining (NHEJ) pathway

or the error-free homologous recombination repair (HRR) (Aparicio et al., 2014; Ciccia &

Elledge, 2010; O'Driscoll, 2012). Specifically, during HRR, DSBs activate ataxia-telangiectasia-

mutated (ATM), which functions as the central controller of cellular responses to DNA damage

(Khanna et al., n.d.). ATM subsequently phosphorylates several downstream effectors, including

the activated histone variant γ-H2AX, which marks the locations of DSBs, and the DNA damage

sensor MRE11-Rad50-Nbs1 (MRN) complex, which is essential at damaged DNA sites for end

processing (Smith et al., 2010).

The receptor of advanced glycation end products (RAGE) is a multi-ligand receptor

primarily expressed on cell membranes (Ramasamy et al., 2008). Common ligands for RAGE

include advanced glycation end-products (AGEs) and high mobility group box 1 (HMGB1). The

RAGE-ligand interaction is well-recognized for its modulation of chronic inflammatory diseases,

such as type 2 diabetes, varieties of neurodegeneration, and chronic obstructive pulmonary

disease (Kumar et al., 2017; Lewis, Hirschi, et al., 2017). More recently, our laboratory showed

that increased placental expression of membrane bound RAGE contributes to low trophoblastic

survival and insufficient invasion in a model of IUGR, suggesting a role of RAGE during

placental disease (Lewis, Mejia, et al., 2017). Although membrane bound RAGE is

predominately known for its function in inflammatory signaling, the nuclear isoform of RAGE

(~64 kDa) was recently identified and demonstrated to be a positive regulator during DNA-DSB repair in the lungs via HRR. During HRR events, RAGE is activated by DSB-induced ATM kinase and function with MRN complexes in facilitating end-resectioning at the broken sites of DNA (Kumar et al., 2017).

Although the accumulation of DNA damage has been observed in pathological placentas, knowledge regarding the impact of genomic instability on pregnancy complications is still limited (Furness et al., 2011). The current research sought to, (1) identify pregnancy complications that are associated with genomic instability, (2) understand the effects of DNA damage and its impact on trophoblast invasion, and (3) investigate the functional requirements of RAGE during placental DNA-DSB sensing. Collectively, our study provides novel insights into DNA damage-associated pregnancy complications and identifies the physiological relevance of molecules in the repair process that may foreshadow the development of pregnancy complication treatments.

Materials and Methods

Human Placental Tissues

All placental biopsies and slides from paraffin embedded placental tissues (gestational diabetes (GDM), preterm labor (PTL), preeclampsia (PE) and term control (Cntl) were purchased from the Research Center for Women's and Infant's Health BioBank, Ontario, Canada. In total, there were 6 samples analyzed for each control and disease group. Samples were collected from placentas, delivered in conjunction with delivery of the fetus, either vaginally or by C-section. Sample demographics are shown in Table 2.1.

Cell Culture and Treatments

The first trimester trophoblast cell line, Sw.71, and the choriocarcinoma cell line, Bewo, were used for these studies (n = 10; n = number of experiments performed in triplicate). Both lines were cultured in appropriate cell culture medium (Sw.71, RPMI; Bewo DMEM/F-12) supplemented with 10% fetal bovine serum (FBS) and 1% penicillin and streptomycin. DNA-DSBs were induced by treating cells with 1% cigarette smoke extract (CSE) for 24 h., or 30 μg/mL of Bleomycin (BLM; a commonly used chemotherapy drug for cancer treatment known to induce DSBs.) for 1 h (Robles & Adami, 1998; Tomilin et al., 2011). A neutralizing RAGE antibody (nAb; 2.4 μ/mL), was used in RAGE targeting studies, which blocks functional RAGE via recognition of a 300-residue sequence of the receptor's extracellular domain.

Cigarette Smoke Extract (CSE)

Nicotine is a key component in cigarette smoke that is associated with the development of DBS (Argentin & Cicchetti, 2004). Preliminary studies in our laboratory (data not shown) showed nicotine to be the main component of CSE. CSE was generated, as previously described by Lewis et al. (2017) (Lewis, Mejia, et al., 2017). Briefly, one 2RF4 research cigarette (University of Kentucky, Lexington, KY, USA) was continuously smoked with a vacuum pump into 5 mL of RPMI or DMEM/F-12 medium (Mediatech, Manassas, VA, USA). The smoke-bubbled medium was filtered through a 0.22-μm filter to remove large particles. The resulting medium was defined as 100% CSE and dilutions were made using RPMI or DMEM/F12 medium to a starting stock concentration of 20% CSE. CSE was made fresh for every treatment.

Immunofluorescence (IF)

Table 2.2 lists the antibodies used in these experiments. IF was performed on paraffin embedded placental sections (n = 6; n = number of placental sections per condition) or trophoblast cells (n = 6; n = number of experiments conducted in triplicate) as previously performed in our laboratory (Arroyo et al., 2012). Briefly, serial sections were incubated overnight with rabbit or mouse polyclonal antibodies against phospho-γ-H2AX (Cell Signaling, Danvers, MA, USA) or RAGE (R&D Technologies, Minneapolis, MN, USA). Anti-mouse fluorescein or Texas red-conjugated secondary antibodies were incubated for 1 h; 40,6-diamidino-2-phenylindole dihydrochloride (DAPI) was used for nuclear counterstaining. Slides were viewed on a BX61fluoresce microscope using the appropriate excitation and emission filter (fluorescein or rhodamine filters).

DNA Degradation

Genomic DNA samples were isolated using the genomic DNA mini kit (Thermo Scientific, Rockford, IL, USA, #K182002). Briefly, placental and cell samples (n = 6) were mixed with PBS, proteinase K, RNase A, and genomic lysis/binding buffer and incubated at 55 ⁰C for 10 min for protein digestion. 96–100% ethanol was added to the mixture and the lysates were transferred to a spin column and spun down at 1000xg for 1 min. Spin columns were washed twice with washing buffer and the DNA were eluted by the elution buffer. Sample concentrations were tested using nanodrop and stored at -20 ⁰C prior to applications. Following these steps, samples were electrophoresed on a 70% gel followed by a 1-h EtBr staining. The extent of DNA degradation was quantified using the Image Studio software (LI-COR Biosciences V5.2.5. Lincoln, NE, USA).

18

Cytoplasmic and Nuclear Extraction

Subcellular protein extractions (n = 10; n = number of extractions performed) were done by following the protocol included with the NE-PER Nuclear and Cytoplasmic Extraction Reagents kit (Thermo Scientific, Rockford, IL, USA #78835). Essentially, placental tissues or collected trophoblast cells were combined with CER I in microcentrifuge tubes and incubated on ice for 10 min. CER II was then added to the tubes and vortexed for 5 s, incubated on ice for 1 min, then vortexed again for 5 s. The tubes were then centrifuged at 16,000x g and at 4 °C for 5 min. Supernatants (cytoplasmic fraction) were collected into clean, pre-chilled, pre-labeled microcentrifuge tubes and stored in a -80 °C freezer before applications. The remaining pellets were re-suspended with ice-cold NER supplemented with 50 U/mL of Benzonase and sonicated for 5 times, 5 s each. Microcentrifuge tubes were again centrifuged at 16,000x g and at 4 °C for 10 min. Supernatants (nuclear fraction) were collected into clean, pre-chilled, pre-labeled microcentrifuge tubes and stored in a -80 °C freezer before applications.

Immunoprecipitation

CSE or BLM treated cells were lysed in RIPA buffer, supplemented with 50 U/mL Benzonase, and a cocktail of protease/phosphatase inhibitors. Lysates of 300 μg (n = 10; number of experiments performed) were pre-cleared with A/G- agarose beads and incubated with primary antibodies (phospho-(p)ATM-Cell Signaling Technology, Danvers, MA, USA, mouse#4526 or MRE11-Cell Signaling Technology, Danvers, MA, USA, rabbit#4895) overnight on a shaker at 4 °C. On the following day, 20 μg of A/G-agarose beads (Santa Cruz, CA, USA) were added to the mixture and incubated for 30 min at 4 °C on a shaker. The bead-protein complexes were collected by centrifugation and washed three times using RIPA buffer. 2x Laemmle buffer supplemented with DTT (total volume of 20 μg) were added to the collected

pellets and incubated at 100 ⁰C for 10 min to disassociate the beads and the attached proteins. The supernatant contents were then analyzed using western blotting.

Western Blotting

Placental tissues (n = 6; n = number of placental samples per condition) and cell lysates (n = 10; n = number of experiments performed; 10–20 μg) were separated on a 4–12% Bis-Tris gel and transferred to a nitrocellulose membrane. Membranes were incubated overnight with primary antibodies (phospho-γ-H2AX-Cell Signaling Technology, Danvers, MA, USA, rabbit #9718, RAGE-R&D, Minneapolis, MN, USA, goat #AF1145, p-ATM-Cell Signaling Technology, Danvers, MA, USA, mouse #4526, MRE11-Cell Signaling Technology, Danvers, MA, USA, rabbit #4895, β-Actin-Cell Signaling Technology, Danvers, MA, USA, rabbit #4967 or mouse #3700 and Lamin B1-Cell Signaling Technology, Danvers, MA, USA, rabbit#15068). The membranes were then incubated with fluorescent secondary antibodies for an hour and washed x3 with TBST the next day prior to imaging. Membranes were developed on a Li-COR Odyssey CLx. Fluorescence densities were determined, and comparisons were made between treated and control groups.

Real Time Cell Invasion

Real-time invasion of trophoblast cells (n = 10; n = number of experiments performed) was measured using xCELLigence RTCA DP (Real Time Cell Analysis Dual Plate) instrument from ACEA Biosciences Inc., San Diego, CA, USA on a 16 well CIM-Plate. These plates are composed of an upper and lower chamber, each containing 16 wells. The top wells were coated with Matrigel collagen and incubated for 4 h. Treated trophoblast cells (CSE or BLM) were

plated in the top chamber at a concentration of 20,000 cells/well. The bottom chamber wells were filled with 10% FBS RPMI. The plates were then place in the RTCA DP instrument and invasion readings were taken every 15 min for 24 h.

Statistical Analysis

Endpoints obtained from DNA degradation studies and protein levels of (γ-H2AX, pATM, RAGE and MRN) were statistically compared. Differences in means ± SE were specifically assessed using the Mann-Whitney U-test. Significant differences between the groups were noted at $p < 0.05$.

Results

RAGE and Placental DNA-DSBs

When DNA-DSBs occur, such events are immediately followed by the phosphorylation of the histone octamer H2AX. This newly phosphorylated protein is the first step in the sequential process that leads to the identification of DSBs and activation of DDR, hence, γ-H2AX is a reliable marker for DNA-DSBs (Kuo & Yang, 2008). To determine the expression pattern of γ-H2AX and the functional relevance of RAGE, human placental samples were subjected to immuno-detection of γ-H2AX and RAGE. Qualitative immunofluorescence staining showed increased expression and colocalization of γ-H2AX and RAGE in the PTL and PE placentas when compared to Cntl (Figure 2.1A).

Genomic Instability in Pregnancy Complications

Timely repair of damaged DNA is essential in maintaining a healthy pregnancy, whereas defective DNA accumulation has been observed in pathological placentas (Tadesse et al., 2014).

To confirm the association of DNA damage in pregnancy complications, genomic DNA samples extracted from human placentas complicated by pre-term labor (PTL), preeclampsia (PE) and of normal gestation control (Cntl) were subjected to DNA degradation analysis via gel electrophoresis. Figure 1B depicts characteristic DNA degradation. Quantification of the resulting DNA degradation gel electrophoresis revealed elevated DNA fragmentation in the PE (3.8-fold; $p < 0.01$) and PTL (3.2-fold; $p < 0.01$) samples when compared to controls (Figure 2.1C). These data suggest the presence of DNA damage in pathological PE and PTL placentas.

RAGE and Placental g-H2AX Nuclear Expression

After observing enhanced staining of RAGE and -H2AX in the PE and PTL placental tissues, we next investigated nuclear expression of these proteins in these diseased placentas and controls. A characteristic western blot for placental RAGE and γ-H2AX is shown in Figure 2.2. Immunoblotting of nuclear protein extractions from PE and PTL placental samples revealed increased nuclear RAGE (4.4-fold; $p < 0.0007$ and 1.9-fold; $p < 0.02$) and γ-H2AX (3.7-fold; $p < 0.02$ and 3.9-fold; $p < 0.02$) relative to normal gestation controls (Figure 2.2A,B).

RAGE Interacts with ATM and MRE11 During Placental DNA-DSBs

Previous work showed the recruitment of activated RAGE by p-ATM to the site of DNA damage and RAGE modulation of MRE11 during DNA repair (Kumar et al., 2017). To implicate a similar role for RAGE during placental DNA-DSBs, ATM- or MRE11-RAGE interactions were verified by co-immunoprecipitation. In human placenta samples, immunoprecipitation of pATM showed expression of RAGE in the PE and PTL placentas (1.7-fold; $p < 0.008$ and 1.5-fold; $p < 0.008$; Figure 2.3A). Similarly, MRE11 complexed with RAGE was observed in PTL and PE (2.2-fold; $p < 0.03$ and 3.5-fold; $p < 0.03$; Figure 2.3B).

Role of RAGE in Trophoblast DNA Damage

To better understand RAGE function during DNA-DSBs, in vitro studies were performed with two placental trophoblast cell lines: Sw.71 (cytotrophoblast) and Bewo cells (syncytiotrophoblast). Exposure to tobacco smoke during gestation elicits numerous deleterious outcomes, and in particular, exposure has been linked to trophoblastic apoptosis, DNA damage and increased reactive oxygen species (Slatter et al., 2014). To understand the impact of cigarette smoke on DNA integrity of placental cell types, Sw.71 and Bewo were treated with cigarette smoke extract (CSE) or bleomycin (BLM; a known inducer of DSB) prior to assessing DNA damage. CSE and BLM treatment increased DNA degradation in both Sw.71 (2.0-fold; $p < 0.05$ and 3.6-fold; $p < 0.05$) and Bewo (1.6-fold; $p < 0.003$ and 5.0-fold; $p < 0.05$) cells when compared to the no treatment control cells (Figure 2.4A–D). To further elucidate the relevance of RAGE during DNA damage, a neutralizing RAGE antibody (nAb), which blocks functional RAGE, was used to treat cells in combination with CSE or BLM. When neutralizing RAGE was used in tandem with CSE or BLM, DNA degradation was further increased in Sw.71 (55%; $p < 0.02$ and 50%; $p < 0.03$) and Bewo (49%; $p < 0.0004$ and 44%; $p < 0.006$) cells as compared to cells treated with CSE or BLM alone (Figure 2.4A–D). In agreement with this DNA-DSB scenario, in vitro induction of DSBs using CSE or BLM in trophoblast cells led to increased co-expression of γ-H2AX and RAGE for both Sw.71 and Bewo cells as demonstrated by IF staining (Figure 2.5).

Trophoblast RAGE and γ-H2AX Nuclear Expression

To confirm RAGE and γ-H2AX nuclear expression, western blot was performed on nuclear fractions from trophoblast cells. CSE and BLM treatment of Sw.71 cells increased nuclear expression of RAGE (1.4-fold; $p < 0.02$ and 13.8-fold; $p < 0.02$; Figure 2.6A,C,

respectively) and γ-H2AX (1.8-fold; p < 0.02 and 22.0-fold; p < 0.02; Figure 2.6B,D, respectively). Similarly, CSE and BLM treatment of Bewo cells increased both RAGE (2.6-fold; p < 0.02 and 3.6-fold; p < 0.02; Figure 2.7A,C, respectively) and γ-H2AX (4.7-fold; p < 0.03 and 54.8; p < 0.02; Figure 2.7B,D, respectively).

RAGE Interacts with ATM and MRE11 During CSE and BLM Induced DNA-DSBs

DNA-DSBs induced in Sw.71 cells by CSE orchestrated the recruitment of RAGE by pATM (2.8-fold; p < 0.03; Figure 2.8A) and MRE11 (2.8-fold; p < 0.03; Figure 2.8B) to the site of DNA damage. CSE exposure also led to the recruitment of RAGE in Bewo cells by pATM (27.8-fold; p < 0.04; Figure 2.8C) and MRE11 (3.0-fold; p < 0.03; Figure 2.8D). These data identified RAGE as a probable substrate during the activation of placental DNA-DSBs repair programs.

Trophoblast Dysfunction as a Consequence of Genomic Instability

The crucial invading function of trophoblasts is essential for successful placental development. To determine the effects of DNA damage on trophoblast invasion, cell invasion assays were performed using the Sw.71 cell line treated with CSE or BLM and invasion was compared with the no treatment controls. Trophoblast invasiveness was decreased with CSE or BLM treatment (Figure 2.9A,B: 2.4-fold; p < 0.0007 and 2.9-fold; p < 0.006). Tellingly, RAGE nAbs administered with CSE or BLM further decreased invasiveness (Figure 2.9A,B: 4.9-fold; p < 0.0004 and 3.7-fold; p < 0.006). These results suggest that DNA instability compromises trophoblast invasion and contributes to anomalous pregnancy progression.

Discussion

DNA double strand-breaks (DNA-DSBs) are known as one of the most damaging forms of DNA complications as they can significantly compromise DNA integrity. Recently, a new role for RAGE was established during DNA-DSB recognition, as well as repair programs (Kumar et al., 2017). Previous reports showed increased DSBs in the PE placenta, but only scant reporting on such DNA defects exist for pregnancies complicated with PTL or GDM (Arroyo et al., 2012). In the current research, we assessed the qualitative expression of γ-H2AX as a key marker of DNA-DSBs (Smith et al., 2010). Detectable staining for γ-H2AX was observed in the PE and PTL placentas. This staining pattern correlated with RAGE localization in these pathological placentas as well. To our knowledge, this is the first report demonstrating DNA-DSBs in the PTL placenta, and the finding of a correlation of γ-H2AX and RAGE during PE and PTL obstetric complications. We further confirmed that both proteins were increased in the nucleus of trophoblast cells in both PE and PTL placentas. This is of interest as RAGE has classically been thought to be a membrane receptor and in our experiments, we observed potential tangential effects of RAGE in the nucleus and co-association with elevated nuclear expression of the DNA-DSB marker γ-H2AX (Mah et al., 2010; Sharma et al., 2012; Siddiqui et al., 2015). To further confirm specific interactions of RAGE with DSB-associated complexes, immunoprecipitation was performed for pATM or MRE11, followed by RAGE protein detection. MRE11 and ATM are integral components of complexes that function in both the recognition of DNA DSBs and repair programs, such as the preferred pathway involving homologous end joining. MRE11 assembles into the MRN complex by binding with RAD50 and NBS1 proteins. MRN complexes rapidly recognize and localize to DNA-DSB foci where it then recruits and assists in ATM phosphorylation and similarly activated downstream DNA damage-

induced proteins (Lamarche et al., 2010; Lavin et al., 2015; Uziel et al., 2003). Our results demonstrate RAGE as a member of these complexes, suggesting the recruitment of RAGE to the DNA-DSBs in the PE and PTL placentas and a novel role for RAGE in maintaining DNA integrity. To further identify potential molecular interplay between RAGE and DNA-DSB related proteins, DNA-DSBs were induced by CSE or BLM treatment of trophoblast cell lines representing the syncytiotrophoblast (Bewo) and the invasive cytotrophoblast (Sw.71). The induction of DNA-DSBs was confirmed by increased nuclear γ-H2AX in the treated cell lines. More interestingly, DNA damage was further augmented when RAGE neutralizing antibody was added in conjunction with the DNA-DSB inducing treatments. Although the exact mechanisms that control nuclear RAGE expression and its nuclear functions are not known, the RAGE neutralizing antibody studies suggests that perhaps membrane bound activation of RAGE is necessary for subsequent nuclear RAGE-mediated protection from DNA-DSBs. These results portend a possible role for RAGE in genomic protection when DNA damaging stimuli encounter trophoblast cells. Concomitantly, nuclear RAGE protein was also increased in the treated cells as compared to controls. This suggests a possible role for this receptor in maintaining genomic integrity in cell lines in a fashion similar to what was observed in the diseased placentas. Support for a possible role of RAGE in pathways downstream of damage recognition, and at stages when repair is initiated, was further verified in trophoblast cells where RAGE-associated with pATM and MRE11 during CSE or BLM, induced DNA-DSBs.

Collectively, our results demonstrated the importance of DNA stability in the regulation of placental/trophoblast behavior and invasion. More importantly, we have initiated a line of research that expands the scope of RAGE biology to include nuclear effects that are necessary for identifying DNA-DSBs and preventing notable loss of DNA integrity in the placenta. Further

studies are needed to demonstrate specific roles for RAGE when placental cells experience DNA-DSBs. For instance, a natural extension of the current work is to perform a series of analyses that aim to characterize DNA-DSB incidence, recognition, and repair when RAGE expression is targeted. Such in vitro and in vivo research should include the knocking out of the RAGE gene in order to confirm a potential vital role in protecting genomic integrity in the event damaging agents are encountered. This critical research would also confirm to what extent RAGE utilization enhances DNA-DSB repair, in order to slow disease progression.

Conclusions

The results summarized in the present investigation provide an important initial step in understanding DNA-DSBs and roles for RAGE that could foreshadow new avenues of study with possible therapeutic utility.

Declarations

Figure 2.1: Genomic Instability in Pregnancy Complications.

(A) Increased staining and co-localization of DNA-DSBs (Green, γ-H2AX), and RAGE (Red) was observed during PE and PTL conditions. DAPI (Blue) was used for nuclear staining. (B) Gel electrophoresis tail length revealed the degree of DNA damage. From left to right: Cntl, PE, and PTL). (C) Quantifications of the fragmented DNA tail length from DNA electrophoresis (n = 6). Images (20x magnification) are representative of experiments involving at least 6 placental sections from each group.
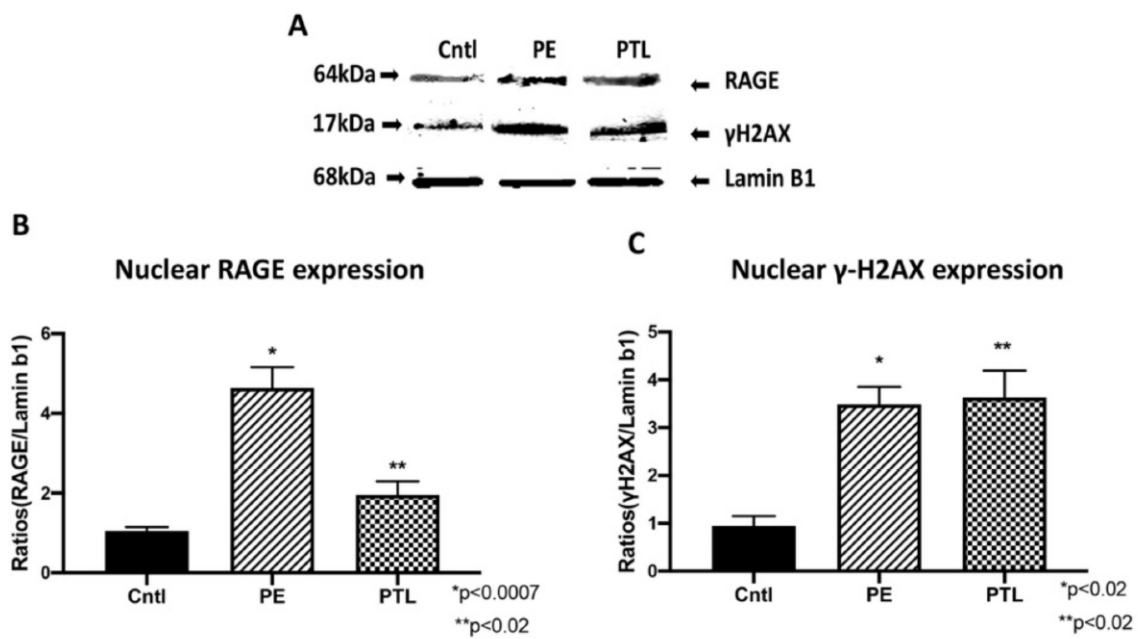
Figure 2.2: RAGE and Placental γ-H2AX Nuclear Expression.

(A) Characteristic western blot for these experiments. (B,C) Elevated -H2AX and RAGE protein expression through western blot on PE and PTL samples when compared to controls.
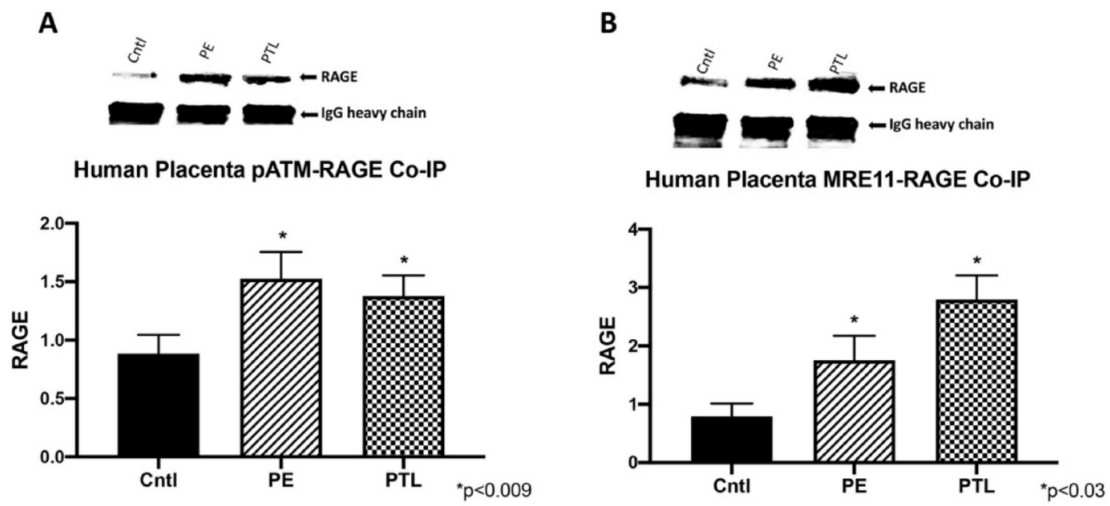
Figure 2.3: RAGE Interacts with ATM and MRE11 During Placental DNA-DSBs.

(A) Increased pATM-RAGE complex in PE and PTL samples when compared to controls. (B) Increased MRE11-RAGE complex in PE and PTL samples when compared to controls.
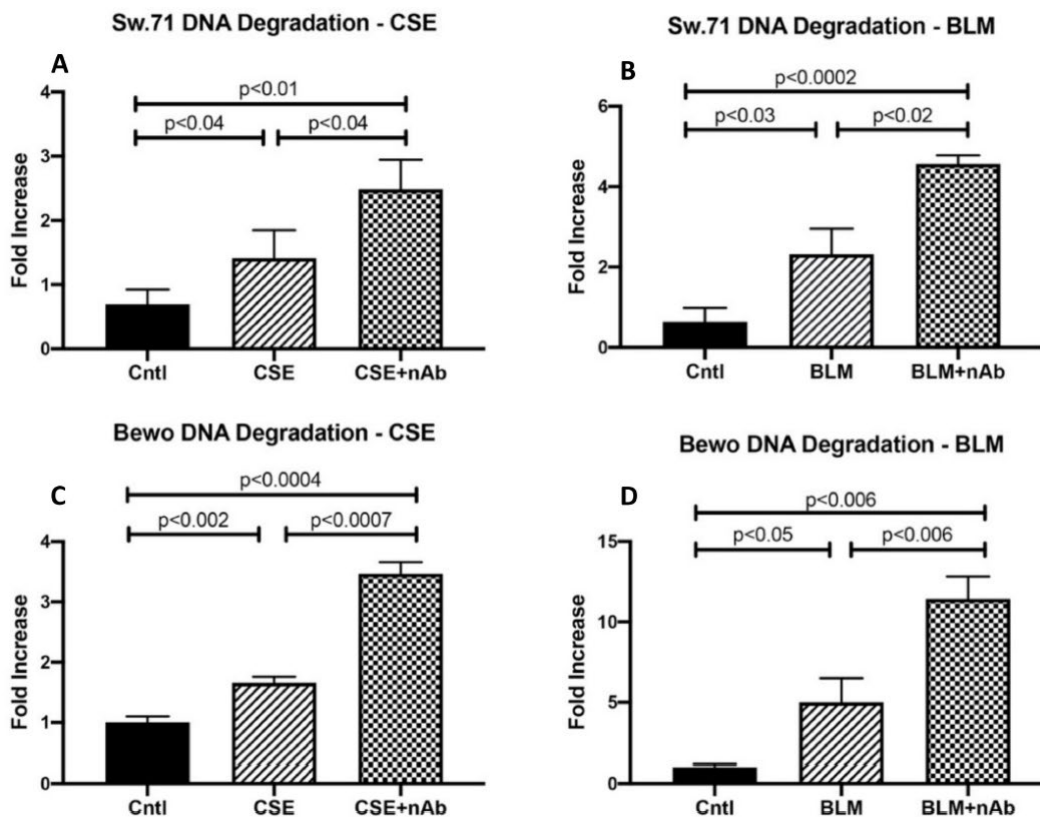
Figure 2.4: Role of RAGE in Trophoblast DNA Damage.

(A) Increased DNA degradation in CSE treated Sw.71 cells. (B) Increased DNA degradation in BLM treated Sw.71 cells. (C) Increased DNA degradation in CSE treated Bewo cells. (B) Increased DNA degradation in BLM treated Bewo cells. (A–D), worsened DNA damage was present with the addition of neutralizing RAGE antibody in both cell types.
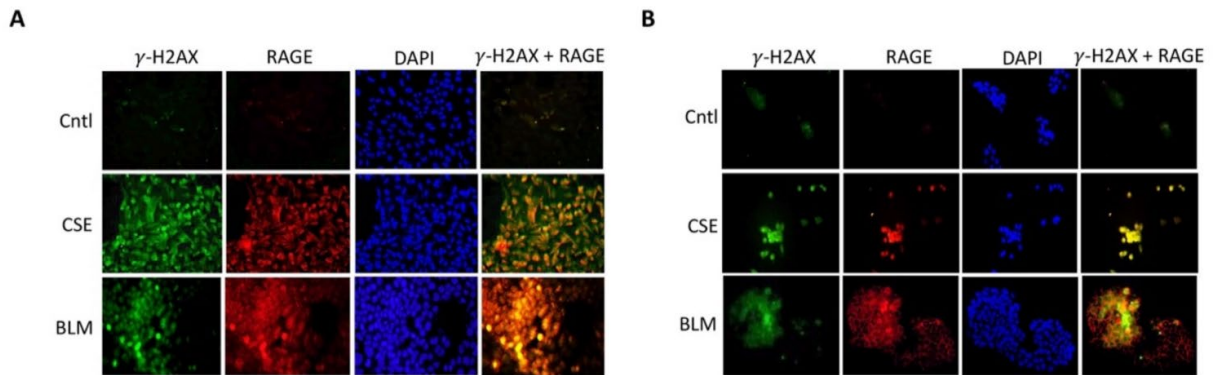
Figure 2.5: Trophoblastic DNA-DSBs and RAGE (IF).

(A,B) Increased staining and co-localization of DNA-DSBs (green, γ-H2AX), and RAGE (Red) was observed from CSE or BLM treated Sw.71 (A) and Bewo (B). Images (40_ magnification) are representative of experiments involving at least 6 different trophoblast experiments from each group.
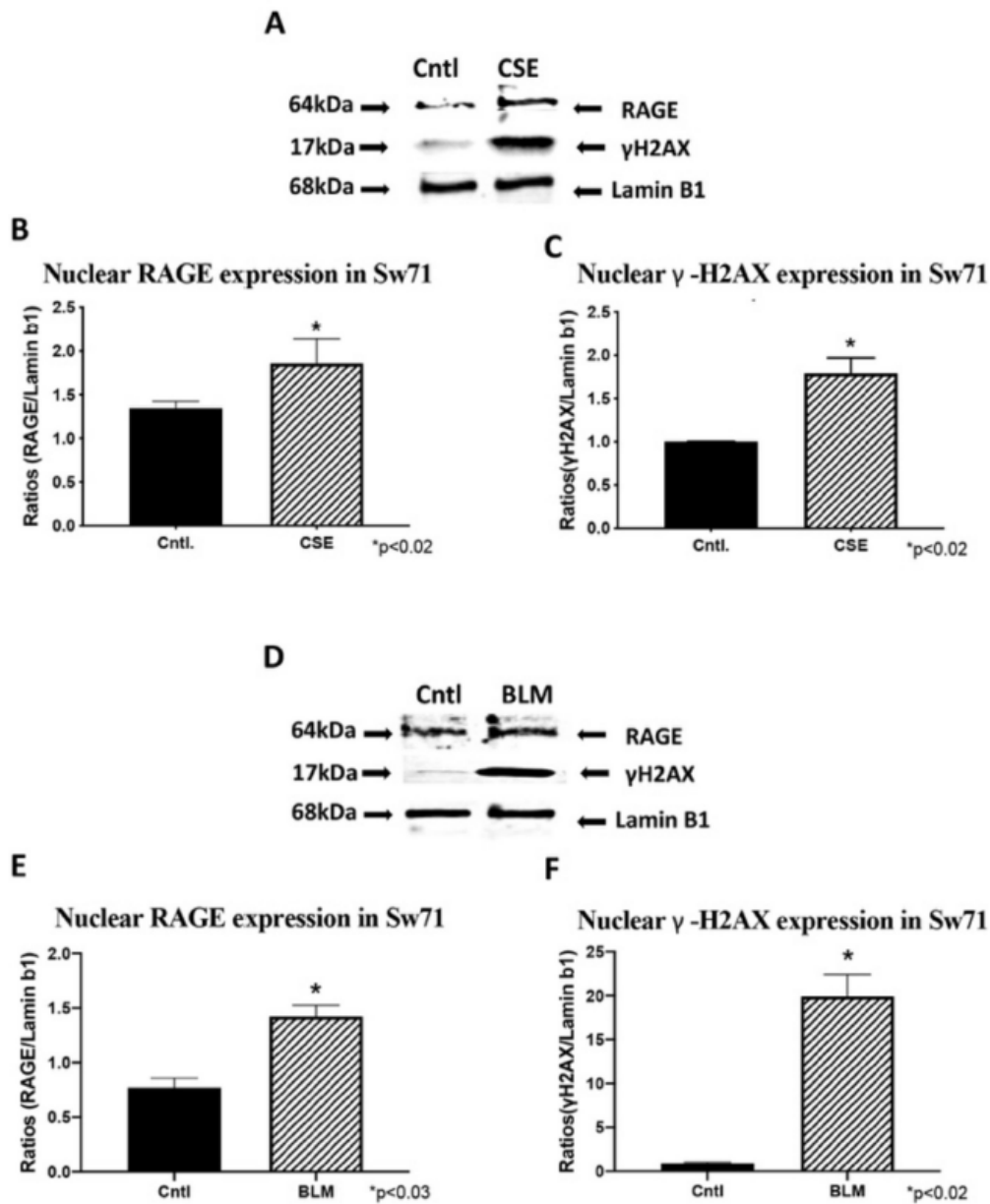
Figure 2.6: Trophoblast Cell, Sw.71, DNA-DSBs and RAGE (WB).

(A) Characteristic western blot for -H2AX and RAGE in CSE treated Sw.71 cells. (B,C) Elevated γ-H2AX and RAGE protein expression in CSE treated cell samples when compared to controls. (D) Characteristic western blot for γ-H2AX and RAGE proteins in BLM treated Sw.71 cells. (E,F), Elevated γ-H2AX and RAGE protein expression in BLM treated cell samples when compared to controls.

Figure 2.7: Trophoblast Cell, Bewo, DNA-DSBs and RAGE (WB).

(A) Characteristic western blot for -H2AX and RAGE in CSE treated Bewo cells. (B,C) Elevated γ-H2AX and RAGE protein expression in CSE treated cell samples when compared to controls. (D) Characteristic western blot for -H2AX and RAGE proteins in BLM treated Bewo cells. (E,F) Elevated γ-H2AX and RAGE protein expression in BLM treated cell samples when compared to controls.
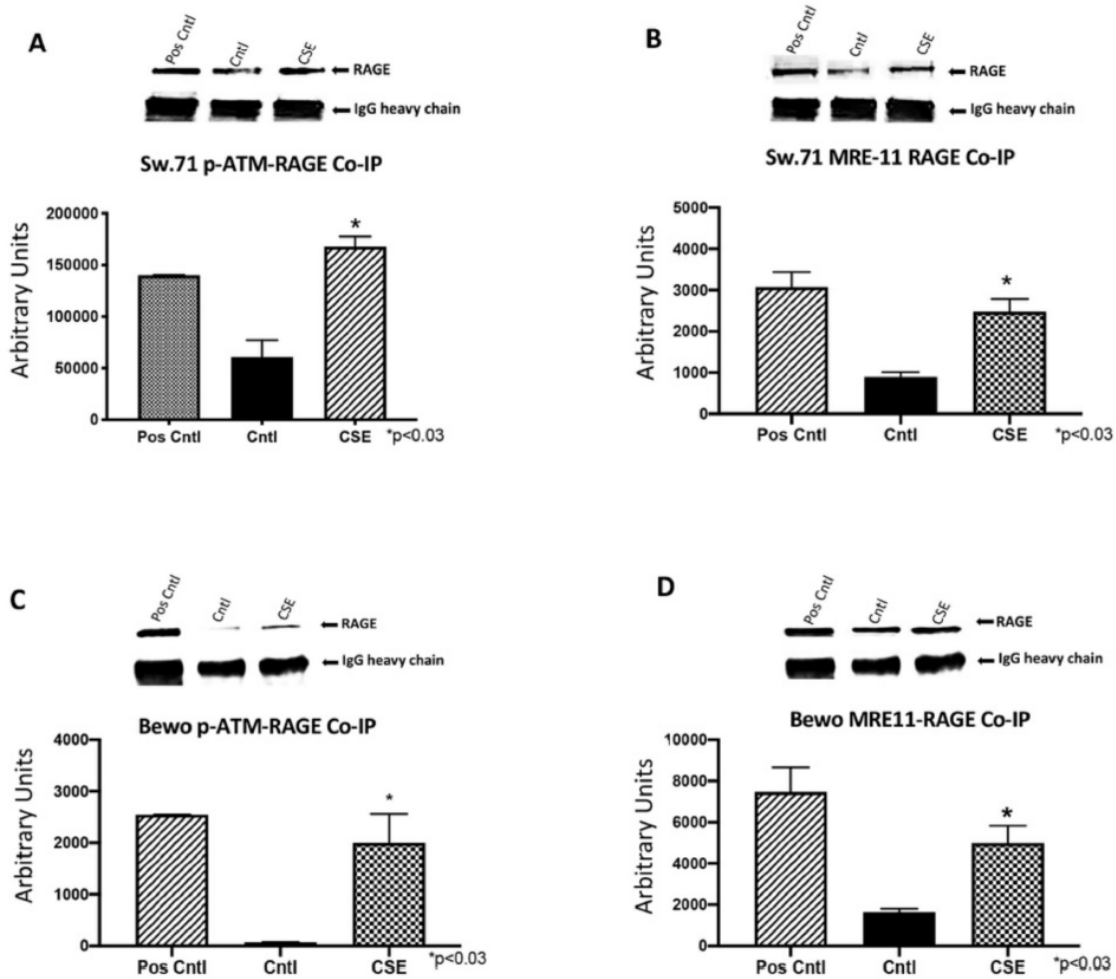
Figure 2.8: RAGE Interacts with ATM and MRE11 During CSE and BLM Induced DNA-DSBs.

Increased pATM-RAGE (A) or MRE11-RAGE (B) complexes in CSE treated Sw.71 when compared to controls. Increased pATM-RAGE (C) or MRE11-RAGE (D) complexes in CSE treated Bewo cells when compared to controls.
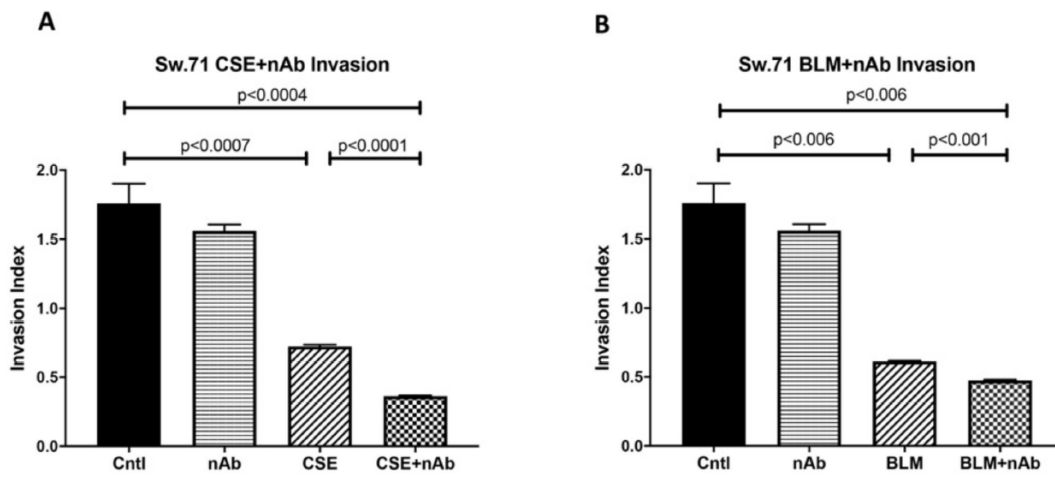
Figure 2.9: Trophoblastic Dysfunction as a Consequence of Genomic Instability.

(A) Decreased invasion in CSE treated Sw.71 cells and further hindrance in invasion when nAb was co-treated with CSE. (B) Decreased invasion in BLM treated Sw.71 cells, the invasion further diminished when nAb was co-treated with BLM.

Table 2.1: Demographical Data from Collected Placental Samples.

Parameters between control and disease placental groups (n = 6) were analyzed for statistical significance (p<0.05) using the Kruskal-Wallis test.

	Control	GDM	PTL	PE	P Value
Maternal Age	34 ± 2.96	35 ± 2.8	29 ± 1.6	36 ± 2.2	0.494
Gestational Age (wks)	38 ± 0.02	39 ± 1.6	32 ± 0.5	32 ± 2.3	0.002
Fetal Weight (g)	3498 ± 59	3247 ± 172	2025 ± 139	2025 ± 139	0.002

% C-section/Vaginal 90%/10%.

Table 2.2: List of Antibodies used per Application.

Antibody	Species	Supplier	Application
RAGE	Goat	R&D (AF1145)	WB, IF
RAGE	Mouse	Abcam (ab89911)	Neutralizing
Phospho-γ-H2AX	Rabbit	Cell Signaling (9718)	WB, IF
Phospho-pATM	Rabbit	Abcam (ab81292)	IP
MRE11	Rabbit	Cell Signaling (4895)	IP

References

Aparicio, T., Baer, R., & Gautier, J. (2014). DNA double-strand break repair pathway choice and cancer. *DNA Repair*, *19*, 169–175. https://doi.org/10.1016/j.dnarep.2014.03.014

Argentin, G., & Cicchetti, R. (2004). Genotoxic and antiapoptotic effect of nicotine on human gingival fibroblasts. *Toxicological Sciences*, *79*(1), 75–81. https://doi.org/10.1093/toxsci/kfh061

Arroyo, J. A., Pastora, G. J., Graham, A., Teng, C. C., Battaglia, F. C., & Galan, H. L. (2012). Placental TonEBP/NFAT5 osmolyte regulation in an ovine model of intrauterine growth restriction. *Biology of Reproduction*, *86*(3). https://doi.org/10.1095/biolreprod.111.094797

Arshad, R., Karim, N., & Hasan, J. A. (2014). Effects of insulin on placental, fetal and maternal outcomes in gestational diabetes mellitus. *Pakistan Journal of Medical Sciences*, *30*(2), 240–244. https://doi.org/10.12669/pjms.302.4396

Bahr, B. L., Price, M. D., Merrill, D., Mejia, C., Call, L., Bearss, D., & Arroyo, J. (2014). Different expression of placental pyruvate kinase in normal, preeclamptic and intrauterine growth restriction pregnancies. *Placenta*, *35*(11), 883–890. https://doi.org/10.1016/j.placenta.2014.09.005

Carter, A. M., Enders, A. C., & Pijnenborg, R. (2015). The role of invasive trophoblast in implantation and placentation of primates. In *Philosophical Transactions of the Royal Society B: Biological Sciences* (Vol. 370, Issue 1663). Royal Society of London. https://doi.org/10.1098/rstb.2014.0070

Ciccia, A., & Elledge, S. J. (2010). The DNA Damage Response: Making It Safe to Play with Knives. In *Molecular Cell* (Vol. 40, Issue 2, pp. 179–204). https://doi.org/10.1016/j.molcel.2010.09.019

Furness, D. L. F., Dekker, G. A., & Roberts, C. T. (2011). DNA damage and health in pregnancy. *Journal of Reproductive Immunology*, *89*(2), 153–162. https://doi.org/https://doi.org/10.1016/j.jri.2011.02.004

Jackson, S. P., & Bartek, J. (2009). The DNA-damage response in human biology and disease. In *Nature* (Vol. 461, Issue 7267, pp. 1071–1078). https://doi.org/10.1038/nature08467

Khanna, K. K., Lavin, M. F., Jackson, S. P., & Mulhern, T. D. (n.d.). *ATM, a central controller of cellular responses to DNA damage*. www.nature.com/cdd

Knöfler, M., Haider, S., Saleh, L., Pollheimer, J., Gamage, T. K. J. B., & James, J. (2019). Human placenta and trophoblast development: key molecular mechanisms and model systems. In *Cellular and Molecular Life Sciences* (Vol. 76, Issue 18, pp. 3479–3496). Birkhauser Verlag AG. https://doi.org/10.1007/s00018-019-03104-6

Knuth, A., Liu, L., Nielsen, H., Merril, D., Torry, D. S., & Arroyo, J. A. (2015). Placenta growth factor induces invasion and activates p70 during rapamycin treatment in trophoblast cells. *American Journal of Reproductive Immunology*, *73*(4), 330–340. https://doi.org/10.1111/aji.12327

Kumar, V., Fleming, T., Terjung, S., Gorzelanny, C., Gebhardt, C., Agrawal, R., Mall, M. A., Ranzinger, J., Zeier, M., Madhusudhan, T., Ranjan, S., Isermann, B., Liesz, A., Deshpande, D., Häring, H. U., Biswas, S. K., Reynolds, P. R., Hammes, H. P., Peperkok, R., … Nawroth, P. P. (2017). Homeostatic nuclear RAGE-ATM interaction is essential for efficient DNA repair. *Nucleic Acids Research*. https://doi.org/10.1093/nar/gkx705

Kuo, L. J., & Yang, L. (2008). *Phosphorylation of H2AX and its Related Molecules*.

Lamarche, B. J., Orazio, N. I., & Weitzman, M. D. (2010). The MRN complex in double-strand break repair and telomere maintenance. In *FEBS Letters* (Vol. 584, Issue 17, pp. 3682–3695). https://doi.org/10.1016/j.febslet.2010.07.029

Lavin, M. F., Kozlov, S., Gatei, M., & Kijas, A. W. (2015). ATM-dependent phosphorylation of all three members of the MRN complex: From sensor to adaptor. In *Biomolecules* (Vol. 5, Issue 4, pp. 2877–2902). MDPI AG. https://doi.org/10.3390/biom5042877

Lewis, J. B., Hirschi, K. M., Arroyo, J. A., Bikman, B. T., Kooyman, D. L., & Reynolds, P. R. (2017). Plausible roles for RAGE in conditions exacerbated by direct and indirect (secondhand) smoke exposure. In *International Journal of Molecular Sciences* (Vol. 18, Issue 3). MDPI AG. https://doi.org/10.3390/ijms18030652

Lewis, J. B., Mejia, C., Jordan, C., Monson, T. D., Bodine, J. S., Dunaway, T. M., Egbert, K. M., Lewis, A. L., Wright, T. J., Ogden, K. C., Broberg, D. S., Hall, P. D., Nelson, S. M., Hirschi, K. M., Reynolds, P. R., & Arroyo, J. A. (2017). Inhibition of the receptor for advanced glycation end-products (RAGE) protects from secondhand smoke (SHS)-induced intrauterine growth restriction IUGR in mice. *Cell and Tissue Research*, *370*(3), 513–521. https://doi.org/10.1007/s00441-017-2691-z

Mah, L. J., El-Osta, A., & Karagiannis, T. C. (2010). γh2AX: A sensitive molecular marker of DNA damage and repair. In *Leukemia* (Vol. 24, Issue 4, pp. 679–686). Nature Publishing Group. https://doi.org/10.1038/leu.2010.6

Mo, H., Tian, F., Li, X., Zhang, J., Ma, X., Zeng, W., Lin, Y., & Zhang, Y. (2019). <scp>ANXA</scp> 7 regulates trophoblast proliferation and apoptosis in preeclampsia. *American Journal of Reproductive Immunology*, aji.13183. https://doi.org/10.1111/aji.13183

Monson, T., Wright, T., Galan, H. L., Reynolds, P. R., & Arroyo, J. A. (2017). Caspase dependent and independent mechanisms of apoptosis across gestation in a sheep model of placental insufficiency and intrauterine growth restriction. *Apoptosis*, *22*(5), 710–718. https://doi.org/10.1007/s10495-017-1343-9

O'Driscoll, M. (2012). Diseases associated with defective responses to DNA damage. *Cold Spring Harbor Perspectives in Biology*, *4*(12). https://doi.org/10.1101/cshperspect.a012773

Ramasamy, R., Yan, S. F., Herold, K., Clynes, R., & Schmidt, A. M. (2008). *Receptor for Advanced Glycation End Products*. *Annals of the New York Academy of Sciences*, *1126*(1), 7–13. https://doi.org/10.1196/annals.1433.056

Reuvekamp, A., Velsing-Aarts, F. V., Poulina, I. E. J., Capello, J. J., & Duits, A. J. (1999). Selective deficit of angiogenic growth factors characterises pregnancies complicated by pre-eclampsia. *BJOG: An International Journal of Obstetrics and Gynaecology*, *106*(10), 1019–1022. https://doi.org/10.1111/j.1471-0528.1999.tb08107.x

Robles, S. J., & Adami, G. R. (1998). *Agents that cause DNA double strand breaks lead to p16 INK4a enrichment and the premature senescence of normal ®broblasts.*

Sharma, A., Singh, K., & Almasan, A. (2012). Histone H2AX phosphorylation: A marker for DNA damage. *Methods in Molecular Biology*, *920*, 613–626. https://doi.org/10.1007/978-1-61779-998-3_40

Siddiqui, M. S., François, M., Fenech, M. F., & Leifert, W. R. (2015). Persistent γH2AX: A promising molecular marker of DNA damage and aging. In *Mutation Research - Reviews in Mutation Research* (Vol. 766, pp. 1–19). Elsevier B.V. https://doi.org/10.1016/j.mrrev.2015.07.001

Slatter, T. L., Park, L., Anderson, K., Lailai-Tasmania, V., Herbison, P., Clow, W., Royds, J. A., Devenish, C., & Hung, N. A. (2014). Smoking during pregnancy causes double-strand DNA break damage to the placenta. *Human Pathology*, *45*(1), 17–26. https://doi.org/10.1016/j.humpath.2013.07.024

Smith, J., Tho, L. M., Xu, N., & Gillespie, D. A. (2010). Chapter 3 - The ATM-Chk2 and ATR-Chk1 Pathways in DNA Damage Signaling and Cancer. *Advances in Cancer Research*, *108*, 73–112. https://doi.org/10.1016/S0065-230X(10)08002-4

Tadesse, S., Kidane, D., Guller, S., Luo, T., Norwitz, N. G., Arcuri, F., Toti, P., & Norwitz, E. R. (2014). In vivo and in vitro evidence for placental DNA damage in preeclampsia. *PLoS ONE*. https://doi.org/10.1371/journal.pone.0086791

Tomilin, N. V., Solovjeva, L. V., Svetlova, M. P., Pleskach, N. M., Zalenskaya, I. A., Yau, P. M., & Bradbury, E. M. (2011). Visualization of Focal Nuclear Sites of DNA Repair Synthesis Induced by Bleomycin in Human Cells. *Radiat. Res.*, *156*, 357–354. https://doi.org/10.1667/0033

Uziel, T., Lerenthal, T., Lilach Moyal, Andegeko, Y., Mittelman, L., & Shiloh, Y. (2003). Requirement of the MRN complex for ATMactivation by DNA damage. *BMBO Jornal*, 5612–5621.

Zhou, Y., Damsky, C. H., & Fisher, S. J. (1997). Preeclampsia Is Associated with Failure of Human Cytotrophoblasts to Mimic a Vascular Adhesion Phenotype One Cause of Defective Endovascular Invasion in This Syndrome? placenta • endothelium • vascular • uterus • cadherins • inte-grins. In *J. Clin. Invest* (Vol. 99, Issue 9).

CHAPTER 3: Differential Expression of mTOR Related Molecules in the Placenta from Gestational Diabetes Mellitus (GMD), Intrauterine Growth Restriction (IUGR) and Preeclampsia Patients

Kary Tsai, Benton Tullis, Tyler Jensen, Taylor Graff, Paul Reynolds, Juan Arroyo

Lung and Placenta Laboratory, Department of Physiology and Developmental Biology, Brigham Young University, Provo, UT, USA

Corresponding Author:
Juan A Arroyo, Ph.D.
Brigham Young University, Department of Physiology and Developmental Biology
3052 Life Sciences Building
Provo, UT 84602
Phone: (801) 422-3221; Fax: (801) 422-0700
E-mail: jarroyo@byu.edu

Abstract

The mechanistic target of rapamycin (mTOR) pathway is involved in the function and growth of the placenta during pregnancy. The mTOR pathway responds to nutrient availability and growth factors that regulate protein expression and cell growth. Disrupted mTOR signaling is associated with the development of several obstetric complications. The purpose of this study was to identify the differential placental expression of various mTOR-associated proteins in the placenta during normal gestation (Control), gestational diabetes mellitus (GDM), intrauterine growth restriction (IUGR) and preeclampsia (PE). Immunohistochemistry localized activated proteins (phospho; p) mTOR, pp70, p4EBP1, pAKT and pERK. Real-time PCR array was performed to show differing placental expression of additional mTOR- associated genes. Western blot was performed for pAMPK protein. We observed: 1) increased pmTOR during GDM and decreased pmTOR during IUGR and PE, 2) increased pp70 during IUGR and decreased pp70 during GDM and PE, 3) increased p4EBP1 during GDM, IUGR, and PE, 4) increased pAKT during GDM, 5) increased pERK during IUGR, 6) differential placental expression of mTOR pathway associated genes and increased pAMPK during GDM and PE. We conclude that regulation of the mTOR pathway is uniquely involved in the development of these obstetric complications. Insights into this pathway may provide avenues that if modify may help alleviate these diseases.

44

Introduction

During gestation, the placenta is responsible for mediating the interface between mother and fetus and notable functions include the regulation of gas exchange, nutrition availability, and waste removal (Aires, 2015). Trophoblasts are an essential cell population in the placenta that confers benefits during the development of the fetus as normal trophoblast function is necessary in the formation of a functioning placenta. Another pertinent feature of the trophoblast biology is their involvement in nutrient transport, an important step for proper fetal development (Lager & Powell, 2012). Aberrant trophoblast function has been implicated in several pregnancy complications, including preterm delivery (PTL) intrauterine growth restriction (IUGR), preeclampsia (PE) and gestational diabetes mellitus (GDM). PTL is associated with up to 70 % of neonatal death, increased incidence of cerebral palsy, neurological defects and pulmonary disorders in the neonate (Challis et al., n.d.). IUGR is an obstetric complication that affects up to 10 % of all pregnancies and is linked to an increased risk of morbidity and mortality for the fetus, characterized by low birth weight (below the 10th percentile) (B. L. Bahr et al., 2014; Mejia et al., 2017). Other IUGR complications include perinatal hypoxia and asphyxia, cerebral palsy, and persistent pulmonary hypertension of the newborn (Arroyo & Winn, 2008; B. Bahr et al., 2014; Mejia et al., 2017).In addition, several studies reported a long-term sequelae of IUGR complications including adult hypertension, heart disease, stroke, and diabetes (Arroyo et al., 2008). There is a risk of up to 44 % of PTL associated with IUGR complications (Delpisheh et al., 2008). PE pregnancies are characterized by high blood pressure after the 20th week of pregnancy; 140 mm Hg (systolic) or 90 mm Hg (diastolic), production of protein in the urine (300 mg in 24 h) and hypoxic placental tissue (Chaudhari et al., 2003;

Emsley et al., 1998; Nelson & Grether, 1999). In extreme forms, PE is also characterized by cerebral and visual disturbances, pulmonary edema, hemolysis, elevated liver enzymes and even seizures. Interestingly PE accounts for around twenty percent of induced PTL (Chaudhari et al., 2003; Obert et al., 1998). PTL observed during PE is due to the necessity of early delivery of the placenta, and in term the fetus, to alleviate the symptoms associated with this disease (Obert et al., 1998). GDM is a state where the pregnant body has become sufficiently resistant to the glucose lowering effects of insulin that hyperglycemia develops (Magee et al., 2014). This pathology affects up to 12 % of all pregnancies and can lead to higher risk of short- and long-term maternal and fetal complications. The list of maternal and fetal complications associated with GDM is lengthy, including maternal gestational hypertension and PE, shoulder dystocia, caesarian delivery, hyperglycemia in the infant, and the development of type 2 diabetes for both mother and child (Jarmuzek et al., 2015).

The mammalian target of rapamycin (mTOR) protein is a phosphatidylinositol kinase-regulated protein kinase, which functions in the regulation of cell growth and protein transcription in response to nutrient availability (Jansson et al., 2006; Wullschleger et al., 2006). This protein has been localized to syncytiotrophoblast cells (Knuth et al., 2015). This expression profile suggests its role in regulating trophoblast proliferation and invasion by serving as a nutrient sensor during pregnancy. In the scheme of its pathway, mTOR is activated by phosphorylation via the phospha-tidylinositol-3 kinase (Pl3K)/AKT signaling axis (Arroyo et al., 2009; Knuth et al., 2015). Downstream effectors, including the 70-kDa ribosomal protein S6 kinase 1 (p70S6K) and the eukaryotic translation initiation factor 4E-binding protein 1 (4EBP1), are known to regulate translation initiation and protein synthesis (Arroyo et al., 2009; Knuth et al., 2015; Mejia et al., 2017). Under physiologic conditions, p70S6K is also mediated through the

extracellular regulated kinase (ERK) pathway (Bigham et al., 2014; Chaudhari et al., 2003; Zhifang et al., 2005). In concordance with the suggested role of mTOR during pregnancy, studies have shown that the inhibition of mTOR activation results in decreased trophoblast invasion in an in vitro model, and elevated expression of mTOR as compensation of IUGR in ovine near term (Arroyo et al., 2009).

Despite extensive research, relationships between pathological conditions during pregnancy and placental mTOR signaling in the aspect of human gestation remains largely unexplored due to ethical issues. In the current study, an initial critical step is taken to establish the fundamental knowledge on this matter by examining differential expression of mTOR and associated molecules and accessing additional mTOR related genes in patients with IUGR, PE and GDM.

Materials and Methods

Human Placenta Samples

All frozen human term placental samples and slides (IUGR, PE, GDM, and control) were purchased from the Research Center for Women's and Infant's Health BioBank, Ontario, Canada. IUGR diagnosis was confirmed by ultrasound showing placental insufficiency with uterine Doppler and absent end diastolic flow (AEDV) and an estimated fetal weight below the 10th percentile. The diagnosis of gestational diabetes mellitus (GDM) was based on 75 g of oral glucose tolerance test (OGTT). All patients diagnosed with GDM were on special diets to regulate this condition. PE diagnosis was based on elevated blood pressure (systolic blood pressure >160 mm Hg and/or a diastolic blood pressure >110 mm Hg) and proteinuria (≥ 5).

There were 10 samples analyzed for each control or pathologic group. Samples were originally

collected from placentas delivered in conjunction with delivery of the fetus either vaginally or by

C-section. Placental samples demographics are shown in Table 3.1.

Immunofluorescence (IF)

IF was performed on paraffin embedded placental sections as previously

performed in our laboratory [20]. Briefly, serial sections were incubated overnight with

rabbit polyclonal antibodies against phospho (p) AKT, pERK, pmTOR, pp70, p4EBP1 (all

from cell Signaling, Danvers, MA) or cytokeratin 7 (for trophoblast localization; Dako,

Carpinteria, CA). Anti-mouse fluorescein or Texas red-conjugated secondary antibody

was incubated for 1 h; 40,6-diamidino-2-phenylindole dihydrochloride (DAPI) was used

for nuclear counterstaining. Slides were viewed on an BX61 fluoresce microscope using

the appropriate excitation and emission filter (fluorescein or rhodamine filters) and scale

bars are set at 100 mm. Individual images (n = 5 for each sample) were analyzed using

ImageJ software evaluating red or green staining intensity.

mTOR PCR Array

Placental RNA was isolated using the Tri-reagent method (Sigma, Saint Louis,

MO) and in accordance with the instructions suggested by the manufacturer. RNA was

quantified using a Nanodrop and cDNA was produced through reverse transcription using

the RT^2 First Strand Kit. A human mTOR signaling RT^2 Profiler PCR 96-well array

(Quiagen, Germantown, MD) was used to determine expression of mTOR related genes.

Briefly, samples containing RT^2 SYBR green, cDNA and RNase water for a total

volume of 270 mL were prepared as suggested. 25 mL of PCR components was added

to each Profiler plate well, sealed, centrifuge and Quantitative real time PCR was completed. PCR array contains 5 housekeeping reference genes (Beta-actin, Beta-2-microglobulin, GAPDH, Hypoxanthine phosphoribosyltransferase 1, and Ribosomal protein, large, P0) and a panel of proprietary controls to monitor genomic DNA contamination (GDC) as well as real-time PCR efficiency (PPC). Experiments were run in triplicate and analyzed using software provided by Qiagen.

Cell Culture

We utilized an immortalized first trimester trophoblast Swan71 cell line (SW71; a generous gift from Dr. Gil Mor at Yale University) for these studies [21]. Cells were cultured in RPMI medium (Mediatech, Manassas, VA) supplemented with 10 % fetal bovineserum (FBS) and 1% penicillin and streptomycin. Cells were treated in 6 well plates and used for protein analysis.

Cell Treatments

Control cells were incubated in media alone (n = 10); the first group of experimental cells were passaged 6 times in media supplemented with 16 mM glucose prior to incubation, or in hypoxic conditions (2% O_2; n = 10). Treatments were conducted for 24 h. Cells were then detached using Trypsin EDTA (0.05 %; ThermoFisher, Waltham, Massachusetts) and lysed using RIPA buffer (Thermo Fisher, Waltham, Massachusetts) for immunoblotting studies.

Immunoblotting

Western blot analysis was used to determine the expression level of pAMPK and pmTOR in control, GDM, IUGR and PE placental samples or in lysates of control and

treated cells as previously described (n = 10) (Arroyo et al., 2009). Cell lysates (50 mg) were separated on a 10% SDS-Page gel and transferred onto nitrocellulose membranes. The membrane was blocked and incubated with antibodies against pAMPK (Cell Signaling Technology, Danvers, MA), pmTOR (Cell Signaling Technology, Danvers, MA) or β actin (1:400; Santa Cruz Biotechnology, Dallas, Texas). Membranes were then incubated with secondary IRDye antibodies (680RD donkey-anti goat and 680RD donkey-anti rabbit; LICOR Lincoln, NE) at room temperature for an hour. Membranes were developed on a Li-COR Odyssey CLx. All results were normalized to β actin as our loading control. Fluorescence densities comparisons were made between treated and control groups.

Statistical Analysis

Comparisons between mTOR gene array differences and pAMPK and pmTOR protein levels were evaluated. Data were analyzed for normality and differences using the Mann–Whitney test with $P < 0.05$ designating significantly different values. Table 1 was analyzed by Kruskal–Wallis test for statistical significance with $P < 0.05$ as statistically significant. All results represent the mean S.E.M.

Results

Placental Samples

Demographics of human placental sample donors were analyzed for significant differences between control GDM, IUGR and PE patients. There were no significant differences in maternal age while there were differences in gestational age and fetal weights from control and disease pregnancies (Table 3.1).

Placental p-mTOR, p-p70 and p-4EBP1

mTOR signaling proteins are expressed in the placenta and are known to be differentially regulated during pregnancy complications (Arroyo et al., 2009). We first wanted to determine expression and localization of mTOR and secondary molecules. We observed that immunofluorescence of pmTOR was qualitatively increased in the GDM placentas compared to controls (Figure 3.1A). In contrast, this protein was decreased in the PE placenta and reductions in expression were much more pronounced in the IUGR placenta (Figure 3.1A). For immunofluorescence protein quantifications, we measured fluorescent emission from 6 different fields using ImageJ. This was repeated in 5 different pictures from each placental condition. pmTOR immunofluorescence intensity quantification confirmed the previous stated results (Figure 3.1B). In terms of localization, p-mTOR was observed in the syncytiotrophoblast layer for all placentas studied, while it was observed in the cytotrophoblast layer predominantly in the control and GDM placenta. Interestingly, p-p70 was increased and localized to both layers of trophoblast cells in the IUGR placenta (Figure 3.2A). There was markedly less p-p70 observed in the control, GDM and PE placentas as compares to IUGR patients. Quantification of pp70 immunofluorescence intensity confirmed these results (Figure 3.2B). p4EBP1 immunofluorescence revealed elevated staining in all the disease placentas studied (GDM, IUGR and PE) compared to controls (Figure 3.3). Quantification of p4EBP1 immunofluorescence intensity confirmed these results (Figure 3.3B)

Placental p-ERK and p-AKT

Regulation of mTOR and p70S6K activity is mediated by phosphatidylinositol-3 kinase/AKT signaling or by the activation of the extracellular regulated kinase (ERK) pathway. Therefore, we next assessed the activation of these molecules in the various placentas. We

observed that ERK protein was only increased in the IUGR placenta with no visible differences in GDM and PE placenta compared to controls (Figure 3.4). Quantification of pERK immunofluorescence intensity confirmed these results (Figure 3.4B). Extremes in p-AKT expression among the groups appeared in placentas from IUGR and PE where detectible increases were apparent in the PE placenta and lessened expression in the IUGR placenta when compared to controls (Figure 3.5). Quantification of pAKT immunofluorescence intensity confirmed these results (Figure 3.2B)

mTOR Associated Gene Activation

We examined gene activation of several mTOR associated molecules to further determine the differences in mTOR signaling between control, GDM, IUGR and PE placentas. We first considered upstream regulators of mTOR signaling. AKT1S1 and AKT3 are known regulators of mTOR activity (Zhifang et al., 2005). While AKT1S1 is negative regulator, AKT 3 positively regulates activation of this molecule. We observed that AKT1S1(1.7-fold, $p < 0.05$) and AKT3 (2.4-fold, $p < 0.05$) were increased in the GDM placenta (Figure 3.6A). In contrast, AKS1S1 was only decreased (1.4-fold, $p < 0.05$) in the IUGR placenta compared to controls (Figure 3.5A). CAB39 and CAB39 L are negative upstream regulators of mTOR signaling. CAB39 was increased in both GDM (1.7-fold, $p < 0.05$) and PE (1.7-fold, $p < 0.05$) placenta compared to controls (Figure 3.6B). Increased CAB39 L gene activation (2.4-fold, $p < 0.05$) was only observed in the GDM placenta (Figure 3.6B) (Bigham et al., 2014). We observed that both PAKAA1 (8.6-fold, $p < 0.02$) and PRKAA2 (8.6-fold, $p < 0.02$), molecules know to (function), were upregulated in the GDM placenta compared to controls (Figure 3.6C). PTEN is an mTOR negative regulator involved in the control of cell growth and division (Milella et al., 2017). GDM placenta was the only tissue that differentially regulated the gene (increase; 5.3- fold; $p < 0.009$)

compared to controls (Figure 3.6D). DEPTOR inhibits kinase activity of mTOR signaling (Mparmpakas et al., 2012). This gene was altered only in the GDM placenta as compared to controls (increased; 2.3-fold; $p < 0.004$), Figure 3.6E). STK11 is a tumor suppressor that regulates cell growth and behavior (Lai et al., 2013). STK11 was only affected in the GDM patients (increased; 1.8-fold; $p < 0.03$) compared to controls (Figure 3.6F). Placental apoptosis and metabolism are important for proper placental function and pregnancy success. The STRADB gene is associated with the regulation of both apoptosis and metabolism (Mahoney et al., 2009) and is known to be a negative regulator of mTOR. We observed decreased STRADB (1.9-fold; $p < 0.0008$) in the GDM placenta while no changes were observed in the other diseased tissues compared to controls (Figure 3.6G).

We next investigated some key genes that downregulate mTOR signaling. HIF1A functions as a hypoxia responsive regulator that activates transcription of many genes involved in energy metabolism, angiogenesis, and others (Harada et al., 2009). Interestingly, increased expression of this gene was only observed in the GDM placenta (1.3-fold; $p < 0.03$) when compared to controls (Figure 3.6H). ULK1 is a kinase involved in autophagy (Kim et al., 2011). Similarly, this gene was significantly increased (5.7-fold; $p < 0.03$) only in the GDM placenta compared to controls (Figure 3.7A). The RPS6 gene encodes a cytoplasmic ribosomal protein that is a component of the 40S ribosomal subunit involved in the regulation of cell growth and proliferation (Magnuson et al., 2012). GDM and PE placenta had increased RSP6 gene activation (each at 1.7-fold; $p < 0.02$) while it was decreased in the IUGR placenta (>25.0-fold; $p < 0.02$) compared to controls (Figure 3.7B). The PPP2CA gene encodes a protein implicated in the negative control of cell growth and division (Li et al., 2013). Interestingly, this gene was only altered in the GDM placenta. When comparing to control, we observed a 2.8-fold ($p < 0.003$)

increase in the GDM placenta (Figure 3.7C). The EIF4E family of genes are involved in the initiation of protein synthesis. The EIF4E gene was increased (3.1- fold; $p < 0.003$) in the placenta from GDM patients compared to controls (Figure 3.7D). In contrast, placental EIF4EBP1 gene expression was decreased (1.4-fold; $p < 0.003$) in the GDM patients compared to controls (Figure 3.7D).

Lastly, we evaluated some mTOR signaling associated genes that are involved in diverse processes of cell signaling and behavior. The PRKAA family of genes include the PRKAA1 and PRKAA32 genes. These genes code for the catalytic subunit of the 5'-prime-AMP-activated protein kinase (AMPK). AMK regulates metabolic enzymes that monitor cell energy status and it is also associated with insulin sensitivity (Bigham et al., 2014). Both PRKAA1 (60-fold; $p < 0.02$) and PRKAA2 (10-fold; $p < 0.02$) were significantly increased in the GDM patients compared to controls (Figure 3.7E). The PIK3 family of proteins are involved in the regulation of several cellular functions such as cell growth, proliferation and survival. The PIK3C3 gene was upregulated in both GDM (4.0-fold; $p < 0.05$) and IUGR placentas (5.2-fold; $p < 0.05$) with no differences observed in the PE tissues (Figure 3.7F). In contrast PIK3CA gene expression was increased in the GDM (61-fold; $p < 0.05$), IUGR (39-fold; $p < 0.05$) and PE (47-fold; $p < 0.05$) patients compared to controls (Figure 3.7F). Similarly, PIK3CB gene was increased in the GDM (93.0-fold; $p < 0.05$), IUGR (4-fold; $p < 0.05$) an PE placenta (2-fold; $p < 0.05$) when compared to controls (Figure 3.7F). Both PIK3CB (1.2-fold; $p < 0.05$) and PIK3CB (4.4-fold; $p < 0.05$) were increased only in the GDM when compared to control tissues (Figure 3.7F). MAPK1 (ERK2) is involved in multiple biochemical signals, and in a wide variety of cellular processes. In the pathological placentas, we observed a significant decrease (1.2-fold; $p < 0.05$) of MAPK1 gene expression only in the GDM placenta when compared to controls (Figure 3.7G). CDC42

gene encodes a small GTPase of the Rho-subfamily protein involve in of control diverse cellular functions and cell cycle progression (Endo et al., 2009). We observed a decreased (2.0-fold; $p < 0.0009$) in the activation of the CDC42 gene only in the GDM tissues compared to controls (Figure 3.7H).

AMPK and mTOR

Together with mTOR, AMPK is one of the major nutrient dependent pathways associated with the regulation of homeostasis (Inoki et al., 2012). We next investigated activated (phospho) AMPK in control and pathological placental samples. We observed increased pAMPK in the GDM, and PE samples (28-fold; 26-fold; $p < 0.05$) while there were no differences in the IUGR placentas as compared to controls (Figure 3.8A-C). To further characterized AMPK and mTOR correlation, trophoblast cells were treated with glucose (to mimic GDM) or hypoxia (to mimic IUGR). We observed increased pAMPK and pmTOR (15-fold and 3.5-fold; $p < 005$) when cells were treated with 16 mM glucose compared to control (Figure 3.9A-B). In cells treated with hypoxia, we observed increased pAMPK (10-fold; $p < 0.05$) while mTOR was decreased (1.4-fold; $p < 0.05$) when compared to controls (Figure 3.9C-D).

Discussion

Proper placental function is essential for fetal health and development. For a successful pregnancy, the placenta must efficiently deliver nutrients and oxygen to the fetus to meet growth demands (Kimball et al., 2015). This process becomes compromised during complicated pregnancies such as preeclampsia and intrauterine growth restriction and each such impairment likely affects fetal development. Interestingly, insights into the mechanistic pathways that contribute to these pathologies are incomplete. Studies examining the processes and mediators

that influence trophoblast invasiveness may be instrumental in providing novel targets for future therapies that combat these obstetric complications. In the present study we assessed the mammalian target of Rapamycin (mTOR) and related signaling molecules in the placenta of mothers affected by GDM, IUGR or PE. mTOR is a kinase that regulates cellular growth when activated by phosphorylation in response to growth factors and nutrients (Knuth et al., 2015). This protein is expressed in the trophoblast of the human placenta and it has been shown to have an important role during placental development (Arroyo et al., 2009). Placental staining confirmed the presence of mTOR and related proteins (p70 and 4EBP1) in the trophoblast villi of the human placenta. When comparing the activated mTOR related proteins between control and the diseases pregnancies, we observed that active mTOR protein was increased during GDM, while decreased in the IUGR and PE placentas. These results are expected as activity of mTOR is considered nutrient dependent and has been shown to be increased during GDM while decreased nutrient availability and diminished expression of mTOR family members are observed during the development of IUGR and PE (Jansson et al., 2006; Mejia et al., 2017; Roos et al., 2007). In terms of pp70 we observed decreased in the GDM placenta and increased during IUGR when compared to controls. In contrast with our results, Sati et al. observed increased pp70 in the GDM placenta as compared to controls (Sati et al., 2016). Perhaps this discordance could be explained by the fact that the placental samples in our studies were obtained from GDM patients in which diabetes was control with dies while the GDM samples use by Sati et al., patients were treated with and on oral insulin-sensitizing antidiabetic medication. Active 4EBP-1was increased in diseased placentas compared to control. This observation suggests that perhaps an alternative mechanism of regelation could be responsible

for 4EBP-1activation in placentas affected by GDM, IUGR or PE (Arroyo et al., 2009; Dreyer et al., 2008; Jansson et al., 2006)

AKT activation has been correlated with mTOR activation, so we also investigated active placental AKT in complicated pregnancies and controls (Knuth et al., 2015). Interestingly we did not observe appreciable differences in activated AKT between the placentas of pregnancies complicated by GDM, IUGR, PE and control. This discordance between AKT activation and mTOR has been previously observed in our lab suggesting that perhaps regulation of placental mTOR activation may be regulated differently between GDM and IUGR or PE and that these differences are independent of AKT (Knuth et al., 2015; Hirschi et al., 2020). Because reports have shown a correlation between activation of p70 and ERK, we investigated ERK activation in diseased placentas and controls. There were similar levels of ERK activation in GDM or PE samples, while higher activation was observed during IUGR when compared to controls. These findings suggest a direct correlation between placental ERK and p70 during IUGR that is not present in the GDM and PE placentas. All these data suggest that regulation of the mTOR pathway is uniquely involved in the development of obstetric complications.

To better understand mTOR function, we investigated mTOR related gene activation in diseased and control placentas. Interestingly, the majority of genes were only affected in the GDM placental samples when compared to controls. The genes differentially impacted in GDM conditions (AKT1S1, AKT3, PRKAA1, PRKAA2, PTEN, DEPTOR, STRADB, PPP2CA, HIF1A, PPP2CA, MAPK1 and CDC42) were mostly associated with negative regulation of mTOR activity. This thematic outcome suggests a possible mechanistic attempt by the placenta to maintain homeostasis in the presence of high glucose levels in maternal circulation. The PI3KC genes are mTOR positive regulators that had increased expression in the GDM placentas

(PIK3C3, PIK3CA, PIK3CB, PIK3Cd and PIK3CG). These genes are responsible for making the

catalytic portion of PI3K. PI3K are enzymes involved in cellular functions and are positive

regulators of mTOR. Our results suggest that activation of this gene could be important in the

increased mTOR activity observed in the GDM placenta (Liu et al., 2009; Hirschi et al., 2019).

Interestingly, RPS6 (involved in the initiation of protein synthesis) gene expression

was upregulated in the GDM and PE placentas and decreased in the IUGR placenta when

compared to controls (K M Hirschi et al., 2019). In contrast, active p70 protein was decreased

during GDM and PE while increased during IUGR. This paradigm was unexpected as p70

protein is often correlated with the activation of RPS6, suggesting that perhaps a different

regulatory program manages RPS6 expression independent of p70 (Ruvinsky et al., 2005). A

similarly functioning regulator, EIF4E, also influences the initiation of protein synthesis and it is

known to be regulated by 4EBP-1 (Siddiqui & Sonenberg, 2015). We observed increased EIF4E

gene expression while EIF4EBP1 (4EBP-1) was decreased during GDM with no changes for

IUGR and PE when compared to controls. This combined observation was unexpected because

EIF4EBP1phosphorylation releases EIF4E and initiates protein synthesis (Truitt et al., 2015).

Furthermore, we observed increased active placental EIF4EBP1staining in all the disease

placentas when compared to controls. This suggests that post transcriptional regulation of these

proteins is possible in the diseased placentas when compared to controls.

AMPK is a regulator of cell homeostasis that regulates the mTOR pathway (Xu et al.,

2012). This AMPK pathway is known to block mTOR activation and is involved in trophoblast

differentiation (Drewlo et al., 2020). Interestingly, there were several genes associated with the

AMPK and mTOR pathways that were changed in the pathological placentas when compared to

controls. The PRKAA family (PRKAA1 and PRKAA32) of genes are genes associated with

AMPK activation. We observed that two members of this family were both increased in the

GDM placentas with no differences detected in the IUGR and PE placentas. These two

molecules are negative regulators of mTOR, suggesting again that an alternative mechanism

elicits increased mTOR in response to high nutrient availability. At the same time, we detected

increased expression of the STK11 gene in the GDM placentas when compared to controls. This

STK11 activation supports increased PRKAA1 and PRKAA32 observed during this condition.

CAB39 and CAB39 L are genes associated with the activation of STK11 (Shackelford & Shaw,

2009). Concurrent with the increased expression of this gene, we observed increases of both

CAB39 and CAB39 L during GDM. Altogether, these results implicate a likely role for AMPK

in the development of placental pathologies. The role of activated AMPK was further confirmed

by protein levels in the pathological placentas and control. As expected, AMPK protein

activation was increased in the GDM placenta. There were no differences in APMK activation

between the IUGR and control tissues. Surprisingly, we also observed activation of AMPK

protein in the PE placenta. Because of these AMPK results, we investigated the correlation

between glucose (mimics GDM environments) or hypoxia (mimics PE environment). We

detected significantly increased protein activation of both mTOR and AMPK. These findings

suggest that glucose is a major factor in increasing these two proteins in GDM pregnancies.

AMPK was also increased during hypoxia. The correlation between aberrant oxygen tension and

AMPK has been previously established and suggest that hypoxia may be responsible for the

regulation of mTOR activity in the villi trophoblast during PE. Taken together, the current

research opens the door to the possibility that these important signaling molecules could be

targeted as a means of effectively ameliorating obstetrics complications including GDM, PE and

IUGR.

Abbreviations

GDM	Gestational Diabetes Mellitus (GDM)
IUGR	Intrauterine Growth Restriction (IUGR)
PE	Preeclampsia
PTL	Preterm delivery
mTOR	The mammalian target of rapamycin
p70S6K	Ribosomal protein S6 kinase beta 1
4EBP1	Eukaryotic translation initiation factor 4E-binding protein 1
AKT	Protein kinase B
ERK	Extracellular regulated kinase
AMPK	5' AMP-activated protein kinase
SW71	Swan 71 first trimester trophoblast cells
CAB39	Calcium-binding protein 39
PAKAA1	Protein Kinase AMP-Activated Catalytic Subunit Alpha 1
PRKAA2	Protein Kinase AMP-Activated Catalytic Subunit Alpha 2
PTEN	Phosphatase and tensin homolog
DEPTOR	DEP domain-containing mTOR-interacting protein
STK11	Serine/threonine kinase 11
STRADB	STE20 Related Adaptor Beta
HIF1A	Hypoxia Inducible Factor 1 Subunit Alpha
ULK1	Unc-51 Like Autophagy Activating Kinase 1

RSP6   Ribosomal Protein S6

PPP2CA   Protein Phosphatase 2 Catalytic Subunit Alpha

EIF4E   Eukaryotic Translation Initiation Factor 4E

PRKAA   5'-AMP-activated protein kinase catalytic subunit alpha-2

PIK3   Phosphatidylino-sitol-4,5-Bisphosphate 3-Kinase Catalytic Subunit Alpha

MAPK1   Mitogen-activated protein kinase 1

CDC42   Cell division control protein 42.

Declarations

Competing interests: The authors report no declarations of interest.
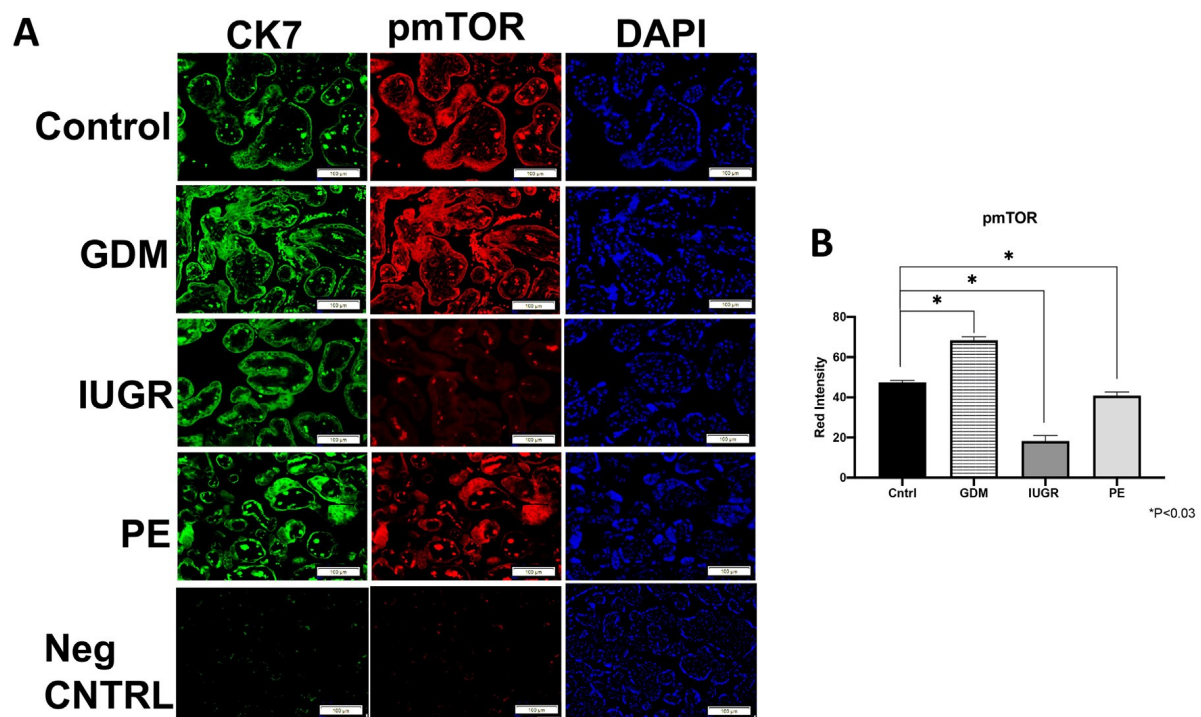
Figure 3.1: Placental phosphor (p) mTOR Staining.

Immunofluorescence (IF) staining showed increased pmTOR expression during GDM but decreased in the IUGR and PE placentas. 60 x scale bars are 50mm (A). Quantification of mTOR staining is shown in B.
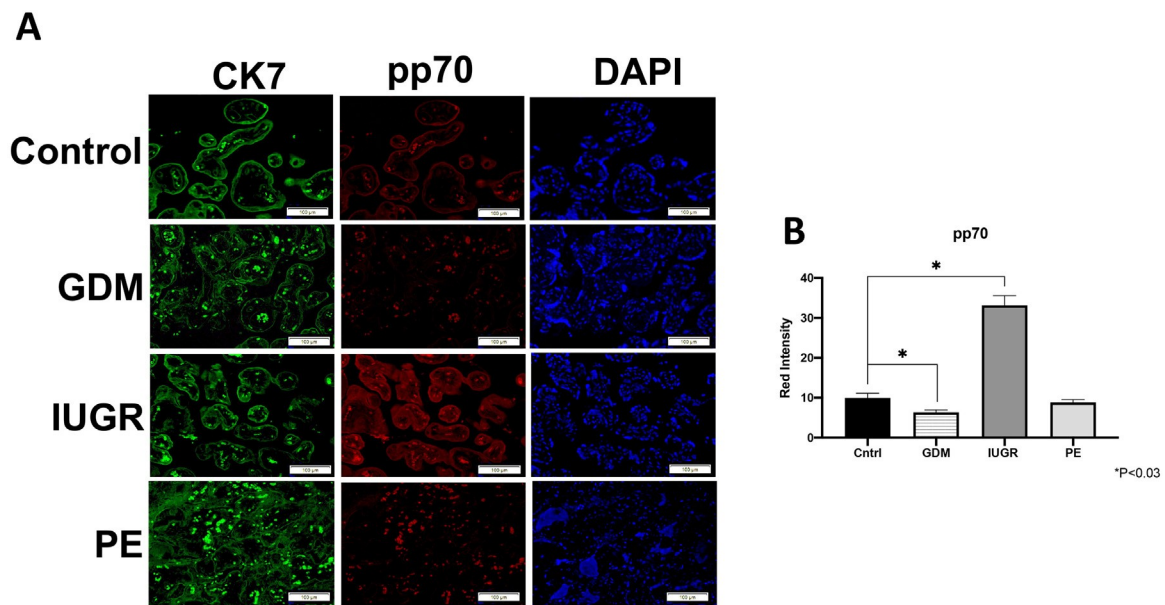
Figure 3.2: Placental phospho (p) p70.

Immunofluorescence (IF) staining showed increased pp70 expression during IUGR but decreased in the GDM and PE placentas. 60 x scale bars are 50 mm (A). Quantification of pp70 staining is shown in B.

A

B
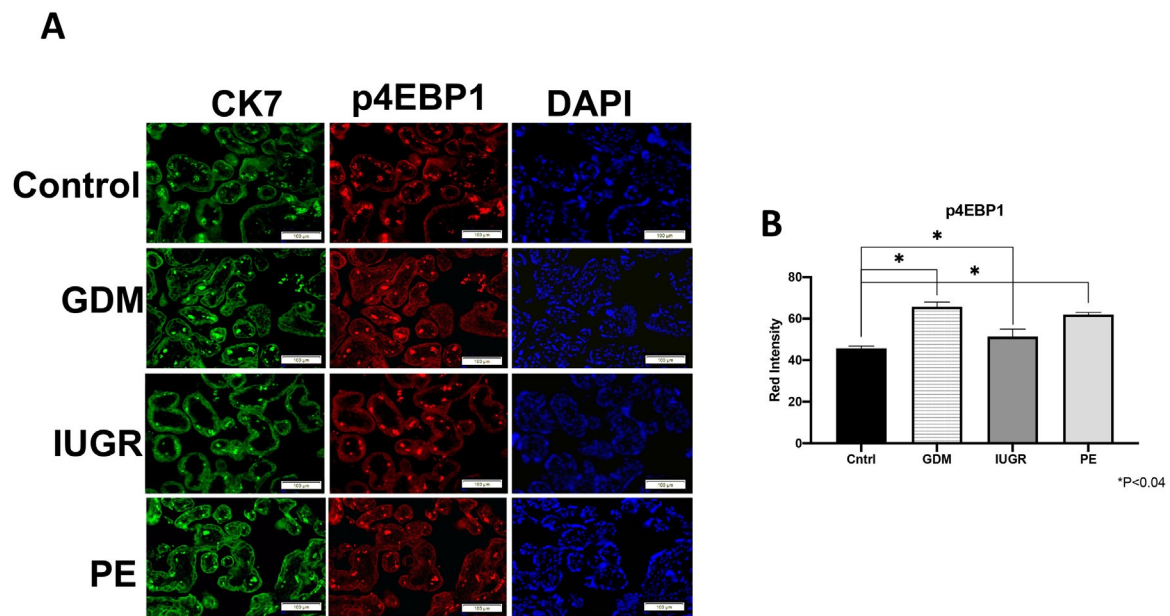
Figure 3.3: Placental phospho (p) 4EBP1.

Immunofluorescence (IF) staining showed increased p4EBP1 expression during in the GDM, IUGR and PE placenta as compared to controls. 60 x scale bars are 50 mm (A). Quantification of p4EBP1 staining is shown in B.
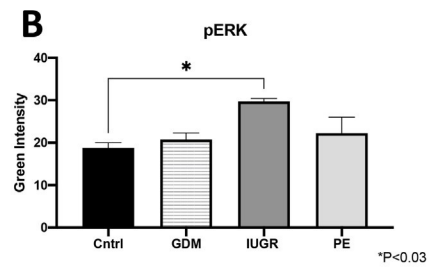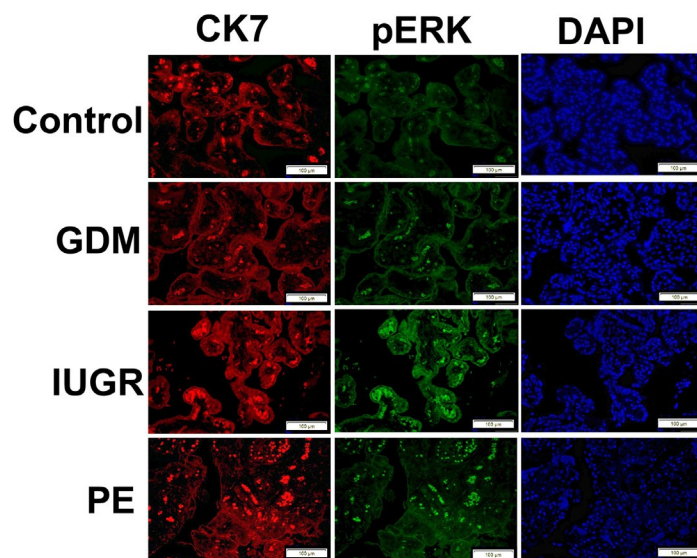
Figure 3.4: Placenta ERK Activation.

Immunofluorescence (IF) staining showed increased pERK expression in the IUGR placenta. 60 x scale bars are 50 mm (A). Quantification of pERK staining is shown in B.
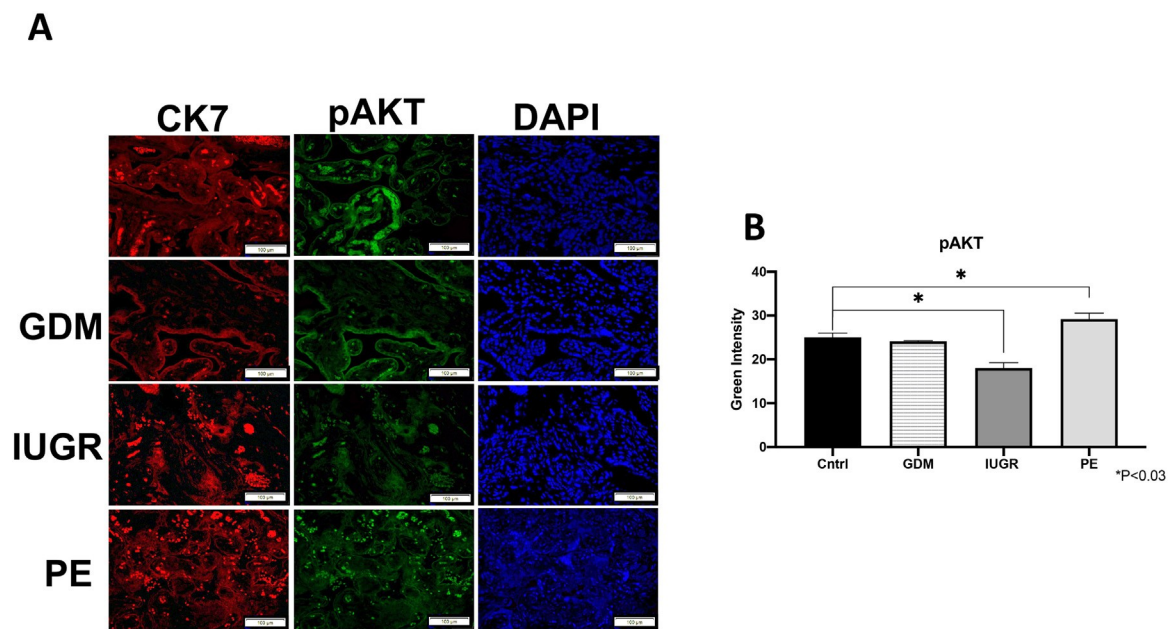
Figure 3.5: Active AKT.

Immunofluorescence (IF) staining showed that pAKT was increased in GDM but decreased in the IUGR placenta. 60 x scale bars are 50 mm (A). Quantification of pAKT staining is shown in B.
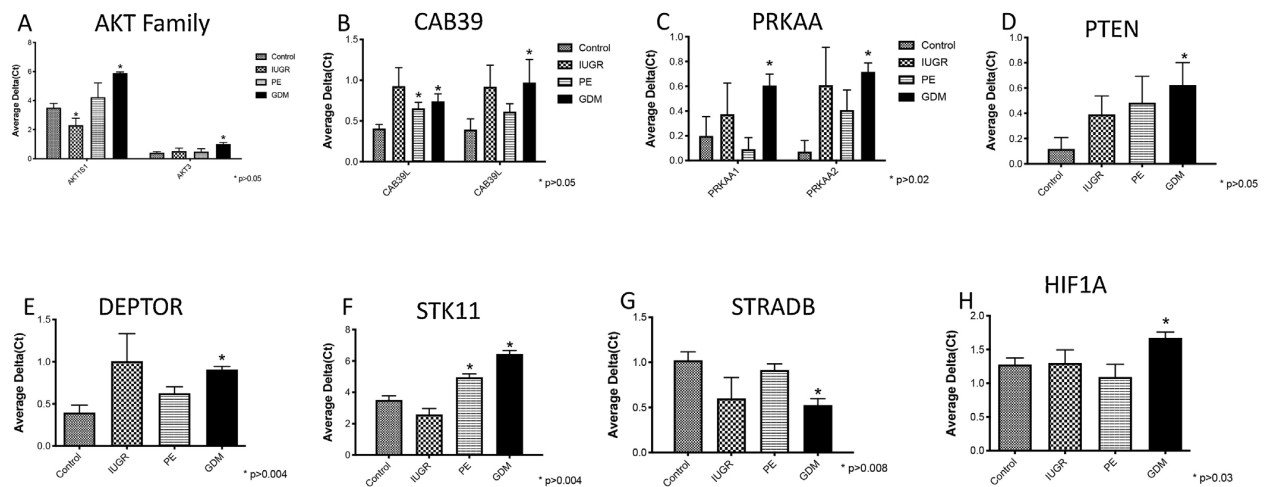
Figure 3.6: AKT, EIF4E, PRKAA, PTEN, DEPTOR, STK11, STRADB and HIF1A Gene Activation.

A human mTOR signaling RT2 Profiler PCR 96-well array demonstrated a differential gene activation between control, IUGR, PE and GDM placental tissues (n = 10). Representative data are shown with *P ≤ 0.05 compared to controls.
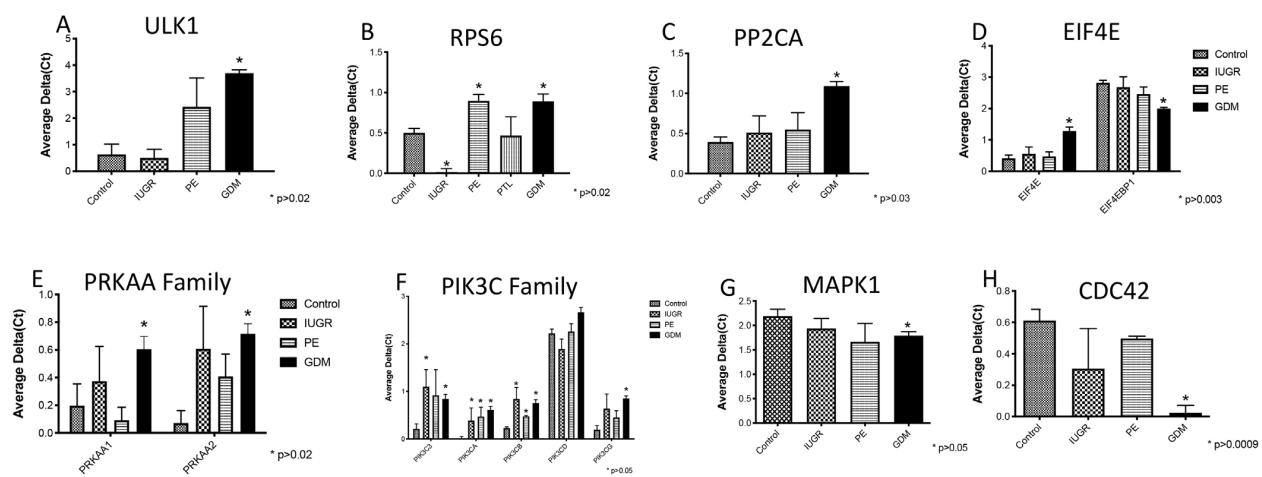
Figure 3.7: ULK1, RPS6, PP2CA, EIF4E, PRKAA, PIK3C, MAPK1, and CDC42 Gene Activation.

A human mTOR signaling RT2 Profiler PCR 96-well array demonstrated a Differential gene activation between control, IUGR, PE and GDM placental tissues (n = 10). Representative data are shown with *$P \leq$ 0.05 compared to controls.
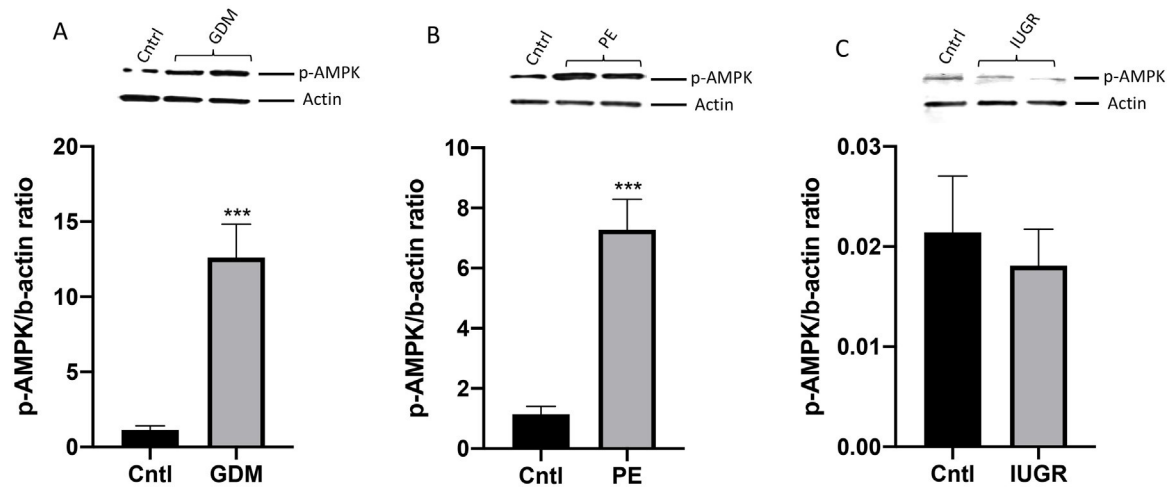
Figure 3.8: Activated Placental AMPK in IUGR, PE and GDM Patients.

Immunoblot was performed for p-AMPK protein determination. AKT was activated in the GDM and PE placentas (n = 10). Representative data are shown with *P ≤ 0.05 when compared to controls.
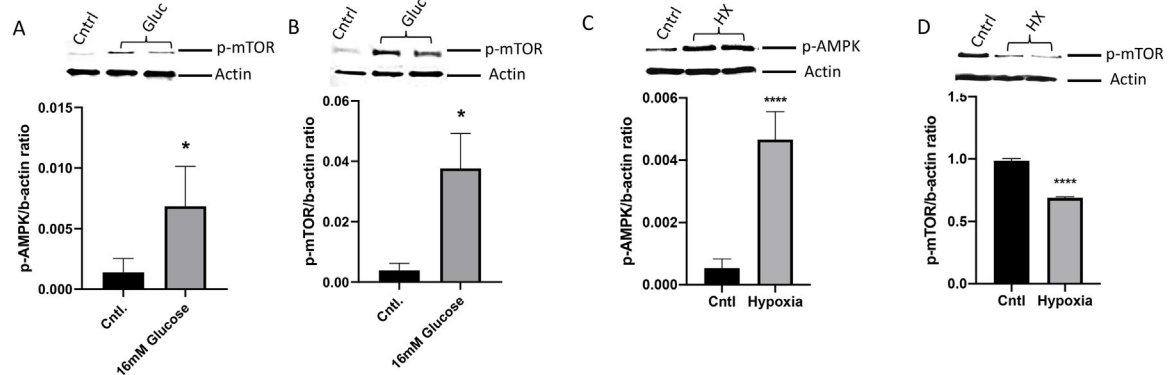
Figure 3.9: Activated Trophoblast AMPK During Glucose and Hypoxia Treatment.

Immunoblot was performed for p-AMPK protein determination. p-AMPK protein was activated in trophoblast cells exposed to either 16 mM glucose or hypoxia. Representative data are shown with *P ≤ 0.05 when compared to controls.

Table 3.1: Demographical Data from Collected Placental Samples.

Parameters between control and disease placental groups (n = 6) were analyzed for statistical significance (p<0.05) using the Kruskal-Wallis test.

	Control	GDM	PTL	PE	P Value
Maternal Age	34 ± 2.96	35 ± 2.8	29 ± 1.6	36 ± 2.2	0.494
Gestational Age (wks)	38 ± 0.02	39 ± 1.6	32 ± 0.5	32 ± 2.3	0.002
Fetal Weight (g)	3498 ± 59	3247 ± 172	2025 ± 139	2025 ± 139	0.002

% C-section/Vaginal 90%/10%.

References

Aires, M. B. (2015). Effects of maternal diabetes on trophoblast cells. *World Journal of Diabetes*, *6*(2), 338. https://doi.org/10.4239/wjd.v6.i2.338

Arroyo, J. A., Anthony, R. V., & Galan, H. L. (2008). Decreased placental X-linked inhibitor of apoptosis protein in an ovine model of intrauterine growth restriction. *American Journal of Obstetrics and Gynecology*, *199*(1), 80.e1-80.e8. https://doi.org/10.1016/j.ajog.2007.12.017

Arroyo, J. A., Brown, L. D., & Galan, H. L. (2009). Placental mammalian target of rapamycin and related signaling pathways in an ovine model of intrauterine growth restriction. *American Journal of Obstetrics and Gynecology*, *201*(6), 616.e1-616.e7. https://doi.org/10.1016/j.ajog.2009.07.031

Arroyo, J. A., & Winn, V. D. (2008). Vasculogenesis and Angiogenesis in the IUGR Placenta. In *Seminars in Perinatology* (Vol. 32, Issue 3, pp. 172–177). https://doi.org/10.1053/j.semperi.2008.02.006

Bahr, B., Galan, H. L., & Arroyo, J. A. (2014). Decreased expression of phosphorylated placental heat shock protein 27 in human and ovine intrauterine growth restriction (IUGR). *Placenta*, *35*(6), 404–410. https://doi.org/10.1016/j.placenta.2014.03.001

Bahr, B. L., Price, M. D., Merrill, D., Mejia, C., Call, L., Bearss, D., & Arroyo, J. (2014). Different expression of placental pyruvate kinase in normal, preeclamptic and intrauterine growth restriction pregnancies. *Placenta*, *35*(11), 883–890. https://doi.org/10.1016/j.placenta.2014.09.005

Bigham, A. W., Julian, C. G., Wilson, M. J., Vargas, E., Browne, V. A., Shriver, M. D., & Moore, L. G. (2014). Maternal PRKAA1 and EDNRA genotypes are associated with birth weight, and PRKAA1 with uterine artery diameter and metabolic homeostasis at high altitude. *Physiol Genomics*, *46*, 687–697. https://doi.org/10.1152/physiolgenomics.00063.2014.-Low

Challis, J. R. G., Lye, S. J., Gibb, W., Whittle, W., Patel, F., & Alfaidy, N. (n.d.). *Understanding Preterm Labor*.

Chaudhari, S., Otiv, M., Chitale, A., Pandit, A., & Hoge, M. (2003). *Pune Low Birth Weight Study – Cognitive Abilities and EducationalPerformance at Twelve Years*.

Delpisheh, A., Brabin, L., Attia, E., & Brabin, B. J. (2008). Pregnancy late in life: A hospital-based study of birth outcomes. *Journal of Women's Health*, *17*(6), 965–970. https://doi.org/10.1089/jwh.2007.0511

Drewlo, S., Johnson, E., Kilburn, B. A., Kadam, L., Armistead, B., & Kohan-Ghadr, H. R. (2020). Irisin induces trophoblast differentiation via AMPK activation in the human placenta. *Journal of Cellular Physiology*, *235*(10), 7146–7158. https://doi.org/10.1002/jcp.29613

Dreyer, H. C., Glynn, E. L., Lujan, H. L., Fry, C. S., Dicarlo, S. E., & Rasmussen, B. B. (2008). Chronic paraplegia-induced muscle atrophy downregulates the mTOR/S6K1 signaling pathway. *J Appl Physiol*, *104*, 27–33. https://doi.org/10.1152/japplphysiol.00736.2007.-Ribo

Emsley, H. C. A., Wardle, S. P., Sims, D. G., Chiswick, M. L., & D'Souza, S. W. (1998). Increased survival and deteriorating developmental outcome in 23 to 25 week old gestation infants, 1990-4 compared with 1984-9. *Archives of Disease in Childhood: Fetal and Neonatal Edition*, *78*(2). https://doi.org/10.1136/fn.78.2.F99

Endo, M., Antonyak, M. A., & Cerione, R. A. (2009). Cdc42-mTOR signaling pathway controls Hes5 and Pax6 expression in retinoic acid-dependent neural differentiation. *Journal of Biological Chemistry*, *284*(8), 5107–5118. https://doi.org/10.1074/jbc.M807745200

Harada, H., Itasaka, S., Kizaka-Kondoh, S., Shibuya, K., Morinibu, A., Shinomiya, K., & Hiraoka, M. (2009). The Akt/mTOR pathway assures the synthesis of HIF-1α protein in a glucose- and reoxygenation-dependent manner in irradiated tumors. *Journal of Biological Chemistry*, *284*(8), 5332–5342. https://doi.org/10.1074/jbc.M806653200

Hirschi, K M, Tsai, K. Y. F., Davis, T., Clark, J. C., Knowlton, M. N., Bikman, B. T., Reynolds, P. R., & Arroyo, J. A. (2019). Growth Arrest Specific Protein (Gas)-6/AXL Signaling Induces Preeclampsia (PE) in Rats. *Biology of Reproduction*. https://doi.org/10.1093/biolre/ioz140

Hirschi, Kelsey M., Tsai, K. Y. F., Davis, T., Clark, J. C., Knowlton, M. N., Bikman, B. T., Reynolds, P. R., & Arroyo, J. A. (2020). Growth arrest-specific protein-6/AXL signaling induces preeclampsia in rats. *Biology of Reproduction*, *102*(1), 199–210. https://doi.org/10.1093/biolre/ioz140

Hirschi, Kelsey M, Fang Tsai, K. Y., Edwards, M. M., Hall, P., Mejia, J. F., Mejia, C. A., Reynolds, P. R., & Arroyo, J. A. (2019). The mTOR Family of Proteins and the Regulation of Trophoblast Invasion by Gas6. *Journal of Cell Signaling*, *04*(02). https://doi.org/10.35248/2576-1471.19.4.203

Inoki, K., Kim, J., & Guan, K. L. (2012). AMPK and mTOR in cellular energy homeostasis and drug targets. *Annual Review of Pharmacology and Toxicology*, *52*, 381–400. https://doi.org/10.1146/annurev-pharmtox-010611-134537

Jansson, N., Pettersson, J., Haafiz, A., Ericsson, A., Palmberg, I., Tranberg, M., Ganapathy, V., Powell, T. L., & Jansson Thomas. (2006). Down-regulation of placental transport of amino acids precedes the development of intrauterine growth restriction in rats fed a low protein diet. *Journal of Physiology*, *576*(2), 519–531. https://doi.org/10.1113/jphysiol.2006.109561

Jarmuzek, P., Wielgos, M., Bomba-Opon, D. A., Dorota, A., & Bomba-Opon, A. (2015). Placental pathologic changes in gestational diabetes mellitus. *Neuroendocrinol Lett*, *36*(2), 101–105. www.nel.edu

Kim, J., Kundu, M., Viollet, B., & Guan, K. L. (2011). AMPK and mTOR regulate autophagy through direct phosphorylation of Ulk1. *Nature Cell Biology*, *13*(2), 132–141. https://doi.org/10.1038/ncb2152

Kimball, R., Wayment, M., Merrill, D., Wahlquist, T., Reynolds, P. R., & Arroyo, J. A. (2015). Hypoxia reduces placental mTOR activation in a hypoxia-induced model of intrauterine growth restriction (IUGR). *Physiological Reports*, *3*(12). https://doi.org/10.14814/phy2.12651

Knuth, A., Liu, L., Nielsen, H., Merril, D., Torry, D. S., & Arroyo, J. A. (2015). Placenta growth factor induces invasion and activates p70 during rapamycin treatment in trophoblast cells. *American Journal of Reproductive Immunology*, *73*(4), 330–340. https://doi.org/10.1111/aji.12327

Lager, S., & Powell, T. L. (2012). Regulation of nutrient transport across the placenta. In *Journal of Pregnancy* (Vol. 2012). https://doi.org/10.1155/2012/179827

Lai, L. P., Lilley, B. N., Sanes, J. R., & McMahon, A. P. (2013). Lkb1/Stk11 regulation of mTOR signaling controls the transition of chondrocyte fates and suppresses skeletal tumor formation. *Proceedings of the National Academy of Sciences of the United States of America*, *110*(48), 19450–19455. https://doi.org/10.1073/pnas.1309001110

Li, Y., Wang, X., Yue, P., Tao, H., Ramalingam, S. S., Owonikoko, T. K., Deng, X., Wang, Y., Fu, H., Khuri, F. R., & Sun, S. Y. (2013). Protein phosphatase 2A and DNA-dependent protein kinase are involved in mediating rapamycin-induced Akt phosphorylation. *Journal of Biological Chemistry*, *288*(19), 13215–13224. https://doi.org/10.1074/jbc.M113.463679

Liu, P., Cheng, H., Roberts, T. M., & Zhao, J. J. (2009). Targeting the phosphoinositide 3-kinase pathway in cancer. *Nature Reviews Drug Discovery*, *8*(8). https://doi.org/10.1038/nrd2926

Magee, T. R., Ross, M. G., Wedekind, L., Desai, M., Kjos, S., & Belkacemi, L. (2014). Gestational diabetes mellitus alters apoptotic and inflammatory gene expression of trophobasts from human term placenta. *Journal of Diabetes and Its Complications*, *28*(4), 448–459. https://doi.org/10.1016/j.jdiacomp.2014.03.010

Magnuson, B., Ekim, B., & Fingar, D. C. (2012). Regulation and function of ribosomal protein S6 kinase (S6K) within mTOR signalling networks. In *Biochemical Journal* (Vol. 441, Issue 1, pp. 1–21). https://doi.org/10.1042/BJ20110892

Mahoney, C. L., Choudhury, B., Davies, H., Edkins, S., Greenman, C., Haaften, G. V., Mironenko, T., Santarius, T., Stevens, C., Stratton, M. R., & Futreal, P. A. (2009). LKB1/KRAS mutant lung cancers constitute a genetic subset of NSCLC with increased sensitivity to MAPK and mTOR signalling inhibition. *British Journal of Cancer*, *100*(2), 370–375. https://doi.org/10.1038/sj.bjc.6604886

Mejia, C., Lewis, J., Jordan, C., Mejia, J., Ogden, C., Monson, T., Winden, D., Watson, M., Reynolds, P. R., & Arroyo, J. A. (2017). Decreased activation of placental mTOR family members is associated with the induction of intrauterine growth restriction by secondhand smoke in the mouse. *Cell and Tissue Research*, *367*(2), 387–395. https://doi.org/10.1007/s00441-016-2496-5

Milella, M., Falcone, I., Conciatori, F., Matteoni, S., Sacconi, A., De Luca, T., Bazzichetto, C., Corbo, V., Simbolo, M., Sperduti, I., Benfante, A., Del Curatolo, A., Cesta Incani, U., Malusa, F., Eramo, A., Sette, G., Scarpa, A., Konopleva, M., Andreeff, M., … Ciuffreda, L. (2017). PTEN status is a crucial determinant of the functional outcome of combined MEK and mTOR inhibition in cancer. *Scientific Reports*, *7*. https://doi.org/10.1038/srep43013

Mparmpakas, D., Zachariades, E., Goumenou, A., Gidron, Y., & Karteris, E. (2012). Placental DEPTOR as a stress sensor during pregnancy. *Clinical Science*, *122*(7), 349–359. https://doi.org/10.1042/CS20110378

Nelson, B. K., & Grether, K. J. (1999). Causes of cerebral palsy. *Current Opinion in Pediatrics*.

Obert, R., Oldenberg, L. G., Wight, D., & Ouse, J. R. (1998). Prevention of Premature Birth. In *MEDICAL PROGRESS* (Vol. 339).

Roos, S., Jansson, N., Palmberg, I., Säljö, K., Powell, T. L., & Jansson, T. (2007). Mammalian target of rapamycin in the human placenta regulates leucine transport and is down-regulated in restricted fetal growth. *Journal of Physiology*, *582*(1), 449–459. https://doi.org/10.1113/jphysiol.2007.129676

Ruvinsky, I., Sharon, N., Lerer, T., Cohen, H., Stolovich-Rain, M., Nir, T., Dor, Y., Zisman, P., & Meyuhas, O. (2005). Ribosomal protein S6 phosphorylation is a determinant of cell size and glucose homeostasis. *Genes and Development*, *19*(18), 2199–2211. https://doi.org/10.1101/gad.351605

Sati, L., Soygur, B., & Celik-Ozenci, C. (2016). Expression of mammalian target of rapamycin and downstream targets in normal and gestational diabetic human term placenta. *Reproductive Sciences*, *23*(3), 324–332. https://doi.org/10.1177/1933719115602765

Shackelford, D. B., & Shaw, R. J. (2009). The LKB1-AMPK pathway: Metabolism and growth control in tumour suppression. In *Nature Reviews Cancer* (Vol. 9, Issue 8, pp. 563–575). https://doi.org/10.1038/nrc2676

Siddiqui, N., & Sonenberg, N. (2015). Signalling to eIF4E in cancer. *Biochemical Society Transactions*, *43*, 763–772. https://doi.org/10.1042/BST20150126

Truitt, M. L., Conn, C. S., Shi, Z., Pang, X., Tokuyasu, T., Coady, A. M., Seo, Y., Barna, M., & Ruggero, D. (2015). Differential Requirements for eIF4E Dose in Normal Development and Cancer. *Cell*, *162*(1), 59–71. https://doi.org/10.1016/j.cell.2015.05.049

Wullschleger, S., Loewith, R., & Hall, M. N. (2006). TOR signaling in growth and metabolism. In *Cell* (Vol. 124, Issue 3, pp. 471–484). https://doi.org/10.1016/j.cell.2006.01.016

Xu, J., Ji, J., & Yan, X. H. (2012). Cross-Talk between AMPK and mTOR in Regulating Energy Balance. In *Critical Reviews in Food Science and Nutrition* (Vol. 52, Issue 5, pp. 373–381). https://doi.org/10.1080/10408398.2010.500245

Zhifang, Y., Jilin, Y., Xingrui, L., & Wei, L. (2005). *Correlation between Loss of PTEN Expression and PKB/AKT Phosphorylation in Hepatocellular Carcinoma* (Vol. 25, Issue 1).

CHAPTER 4: Regulation of Trophoblast Cell Invasion by
Pyruvate Kinase Isozyme M2 (PKM2)

Kary Ya Fang Tsai, Benton Tullis, Juan Mejia, Paul R. Reynolds, Juan A. Arroyo

Lung and Placenta Laboratory, Department of Physiology and Developmental Biology, Brigham Young University, Provo, UT, USA

Corresponding Author:
Juan A Arroyo, Ph.D.
Brigham Young University, Department of Physiology and Developmental Biology
3052 Life Sciences Building
Provo, UT 84602
Phone: (801) 422-3221; Fax: (801) 422-0700
E-mail: jarroyo@byu.edu

Abstract

The Pyruvate kinase isozymes M2 (PKM2) protein is a metabolic enzyme that regulates the final step of glycolysis. This enzyme is present in highly proliferating cells and is expressed in the placenta. We recently demonstrated upregulated placental PKM2 during human intrauterine growth restriction (IUGR). Our current objective was to determine PKM2 regulation of trophoblast invasion, trophoblast PKM2 localization as well as mTOR protein expression, and to determine effects of activation of PKM2 during IUGR. Human placental tissues were obtained and analyzed by immunohistochemistry and western blot. Trophoblast cells were cultured in normoxic and hypoxic conditions and real time cell invasion and PKM2 protein were determined during activation (Fructose-6-bisphosphate; FBP6) or inhibition (Shikonin) of PKM2. *In vivo* studies determined the effects of PKM2 activation on placental and fetal weights. IUGR samples had elevated levels of p-PKM2. Different trophoblast PKM2 localization and expression was observed during normoxia and hypoxia. Decreased trophoblast invasion and PKM2 expression was observed during mTOR inhibition. Protection from decreased placental and fetal weights was observed by PKM2 activation. We conclude that PKM2 regulates trophoblast cell invasion depending on its subcellular location. Our results suggest that PKM2 regulation in trophoblast cells is more directly affected during hypoxia and its expression is regulated by mTOR activity. Additionally, we conclude that activation of PKM2 could reverse and/or rescue the deceased placental and fetal weights observed during IUGR. These results suggest that PKM2 could be a mediator of trophoblast cell invasion and its abundance influences the development of complicated pregnancies like IUGR.

Keywords: placenta, PKM2, mTOR, trophoblast invasion, hypoxia

Introduction

In order to have a successful pregnancy, proper oxygenation of the placenta and fetus is essential (Huppertz, 2014). Studies have shown that when a fetus experiences hypoxic stress, its cardiac output is redistributed toward the heart and the brain at the expense of other organs. This circulatory effect may lead to metabolic and cardiovascular disturbances later on in adulthood (Ahmed, 2014; Bourque et al., 2012; Denton et al., 2015; Giussani & Davidge, 2013; Iqbal & Ciriello, 2013; Matheson et al., 2016; Myatt, 2006; Rueda-Clausen et al., 2014). Adequate oxygenation is important for metabolic efficiency in placental tissue as the placental trophoblasts mediate processes that require high energy consumption such as nutrient transfer, synthesis of hormones and secretion of molecules (Bahr et al., 2014). Changes in supply of nutrients to the fetus can affect its growth and development leading to obstetric complications such as intrauterine growth restriction (IUGR) (Cetin & Antonazzo, 2009). Local hypoxia has been thought to play an important role during IUGR. Normally, the uterine spiral arteries are characterized as high resistance and low-capacity vessels. During pregnancy, endovascular trophoblasts invade and replace the maternal endothelial cells that line the spiral arteries, modifying these arteries into high capacity and low resistance vessels to meet increased blood flow demands (Knuth et al., 2015; PIJNENBORG et al., 1991). During IUGR, shallow trophoblast invasion fails to convert uterine spiral arteries into high capacity and low resistance vessels, which leads to decreased blood flow and local hypoxia (Knuth et al., 2015; PIJNENBORG et al., 1991). This insufficient modification of the arteries stemming from shallow invasion reduces oxygen levels and nutrient supply and further affects placental metabolism during IUGR. As such, placental metabolic adaptions are particularly important in allowing the cells to meet ATP demands in the face of altered oxygen or substrate supply (Tissot Van Patot et al., 2010). This underscores an important role for placental metabolism in placental

growth and in the onset of obstetric complications such as IUGR.

An important enzyme involved in metabolism is Pyruvate Kinase M2 (PKM2). PKM2 is a metabolic enzyme that transits between a less active dimer and an active tetramer that catalyzes the last and rate-limiting reaction in the glycolytic pathway. These different forms of PKM2 regulate glucose metabolism through either dimeric PKM2 mediated aerobic glycolysis or tetrameric mediated oxidative phosphorylation. The balance between the two forms is achieved through the allosteric PKM2 regulation by fructose-1, 6-bisphosphate (FBP). Essentially, FBP, an early glycolytic intermediate, binds to PKM2 and converts it from the less active dimeric form with lower affinity for its substrate(s) to an active tetrameric form with higher substrate affinity (Mazurek, 2011; Mazurek et al., 1997). When glucose is abundant, FBP levels increase and PKM2 is activated, leading to TCA cycle progression. The disassociation of FBP converts PKM2 to the dimeric form which promotes aerobic glycolysis, converting pyruvate to lactate for energy production (Bahr et al., 2014). The PKM2 dimer activity results in the accumulation of glycolytic intermediates that are involved in the synthesis of nucleic acids, amino acids, and lipids (Gupta & Bamezai, 2010). Dimeric PKM2 can also enter the nucleus to regulate gene expression and can play an important role in invasion and cell proliferation by diverting glycolytic intermediates that accumulate in various biosynthetic path-ways (Zhang et al., 2019). The transition between dimeric and tetrameric forms of PKM2 can play an important role in tumor cell energy supply, epithelial–mesenchymal transition (EMT), invasion and metastasis and cell proliferation. Shikonin is a natural product with therapeutic effects ranging from anti-inflammatory, anti-oxidant, and anti-cancer due to inhibition of dimeric PKM2 activity (Zhao et al., 2018). Inhibiting PKM2 by Shikonin suppresses cell glycolysis and invasion while promoting apoptosis.

An important regulator of cell growth is the mammalian target of rapamycin (mTOR) protein (Jansson et al., 2006; Wullschleger et al., 2006). mTOR is a phosphatidylinositol kinase-regulated protein kinase that regulates cell growth in response to the availability of nutrients and growth factors. Previous studies have shown a direct correlation between mTOR activation and trophoblast invasion (Knuth et al., 2015). Furthermore, mTOR is known to regulate the expression of PKM2 protein suggesting a role for PKM2 during placental trophoblast invasion (Sun et al., 2011; Wong et al., 2013).

Based on roles of PKM2 in cell invasion and embryonic tissues, and the association of shallow trophoblast invasion with IUGR pregnancies, we wanted to determine the role of PKM2 and mTOR in the invasion of trophoblast cells (Bahr et al., 2014). This included assessing nuclear and cytosolic extracts of the trophoblast samples and identifying the invasive properties of these cells. Investigating the role of PKM2 and the mTOR pathway in relation to trophoblast invasion will provide valuable insight into IUGR pathology.

Materials and Methods

Human Placental Tissues

All frozen human term placental samples and slices (IUGR and Control) were purchased from the Research Center for Women's and Infant's Health BioBank, Ontario, Canada. In total there were 10 samples analyzed for each control and disease group. Samples were collected from placentas delivered in conjunction with delivery of the fetus either vaginally or by C-section. Sample demographics are shown in Table 1.

Immunohistochemistry

Immunohistochemistry was performed as previously outlined in our lab (Arroyo et al., 2010). Briefly, slides were de-waxed, washed in a 1x Tris buffer solution (TBS), and blocked with Background Sniper (Biocare Medical, #BS966H, Concord, CA) for 1 h. This was followed by incubation overnight with a primary antibody (PKM2-Cell Signaling Technology, Danvers, MA, Cytokeratin 7-Dako, Carpinteria, CA, mouse (for trophoblast localization). Slides were then incubated for 1 h with Mach 2 Universal HRP Polymer Detection (Biocare Medical, Concord, CA), followed by color development with diaminobenzidine (DAB) for 5 min (Biocare Medical, Concord, CA). A 5 s Hematoxylin soak was used for nuclear counterstain. Slides were washed 3x for 5 min in TBS between each step. Slides were mounted using Permount media.

Cell Culture

An immortalized first trimester trophoblast Swan71 cell line (SW71) was used in this study. The SW71 cell line was a generous gift from Dr. Gil Mor at Yale University (Straszewski-Chavez et al., 2009). Cells were trophoblast maintained and cultured in RPMI medium (Mediatech, Manassas, VA) supplemented with 10% fetal bovine serum (FBS) and 1% penicillin and streptomycin. Cells were plated and treated in 6 well plates and used for protein analysis.

Cell Treatments

Control cells were incubated in media alone (n=10); the first group of experimental cells were treated with media supplemented with 100 nM of fructose 1,6-biphosphate (n=10; FBP6, an PKM2 activator; R and D Systems, Minneapolis, MN), a second group of experimental cells were treated with media supplemented with 1 μm of Shikonin (n=10; PKM2 inhibitor;

Selleckcheme, Houston, TX), and a third group of experimental cells were treated with media supplemented with 40 nM of Rapamicin (n 10; mTOR inhibitor; Selleckcheme, Houston, TX. Treatments were conducted for 24 h. Cells were then detached using Trypsin EDTA (0.05%; Thermo Fisher, Waltham, Massachusetts) for invasion analysis or lysed used RIPA buffer (Thermo Fisher) for immunoblotting studies.

Cytoplasmic and Nuclear Extraction

Placental and trophoblast cells were lysed were in a microcentrifuge tube with 500 µL of (ice cold) CER I, and 5 µL of protease inhibitor (Thermo Scientific, Rockford, IL). The rest of the protocol was followed in accordance with the NE-PER Nuclear and Cytoplasmic Extraction Reagents kit (Thermo Scientific, Rockford, IL) using 27.5 µL of (ice cold) CER II and 125 µL of ice-cold NER with1.25 µL of protease inhibitor (Thermo Scientific, Rockford, IL). Supernatants were collected into clean, chilled, pre-labeled microcentrifuge tubes and kept on ice. To determine protein concentrations, cytoplasmic and nuclear supernatants were analyzed with a Pierce BCA Protein Assay Kit (Thermo Scientific, Rockford, IL). Briefly, 2 µL of each sample was combined with 150 µL of Reagent A and B (50:1) in a labeled 96 well plate. The plate was covered and incubated at 37 °C for 20 min, cooled to RT, and read on a SpectraMax 340 PC absorbance microplate reader (Molecular Devices, Sunnyvale, CA). Samples were run in duplicate, averaged, and compared to a bovine serum albumin standard curve. Supernatants, in micro- centrifuge tubes, were stored at 80 °C for future use. Cytosolic and nuclear extract purity was determined by western blot analysis using lamin B 1 and beta actin antibodies.

Western Blotting

Whole tissue lysates (50 μg) or cytoplasmic and nuclear lysates (50 μg) were separated on a 10% SDS-Page gel and transferred onto nitrocellulose membranes. The membranes were blocked for 1 h followed by overnight incubation with primary antibodies (p-PKM2 and PKM2, Cell Signaling Technology, Danvers, MA; mTOR; 1:200; Cell Signaling Technology, Danvers, MA). Membranes were then incubated with secondary IRDye antibodies (1:10,000, 680RD donkey-anti goat and 680RD donkey-anti rabbit; LI-COR Lincoln, NE) at room temperature for an hour. Membranes were finally developed on a Li-COR Odyssey CLx. All results were normalized to Lamin B1 or B actin (Santa Cruz Biotechnology, Dallas). Fluorescence densities were determined, and comparisons were made between treated and control groups.

Real Time Cell Invasion Determination

Real time cell invasion was performed as previously described (Aagaard et al., 2017). Briefly, additional cell cultures were conducted, and invasion was assessed in 16 well-CIM-Plates (n 9; ACEA Biosciences, San Diego, CA). These plates are composed of an upper chamber coated with type IV collagen (1:40; Corning, Corning, NY) and a lower chamber with 10% FBS RPMI. Cells were plated in the top chamber at a concentration of 20, 000 cells/well in 2% FBS RPMI in a total volume of 100 μL in the presence FB6 or Shikonin. The cells were then placed in the RTCA DP instrument and invasion readings were taken every 15 min for 24 h.

Animals and Tissue Preparation

Animal use was approved by the Institutional Animal Care and Use Committee at Brigham Young University. C57 Black 6 (C57BL/6) mice were purchased from Charles River

laboratories, Wilmington, MA. To obtain timed pregnancies, females were caged with males overnight. Placentae and mesometrial compartments were dissected from pregnant mice at 18.5 days of gestation (dGA). Placentae and fetuses were weighed, and tissues were snap frozen in liquid Nitrogen for RNA and protein analysis. Whole conceptuses were frozen in dry ice-cooled heptane for immunohistochemistry analysis. All tissue samples were stored at 80 °C until used. Secondhand Smoke (SHS) and PKM2 activator Treatment. The generation of thane IUGR pregnancy occurred following expo- sure of pregnant mice (n 7) to SHS conditions as previously shown by Winden et al. (Winden et al., 2014) Pregnant mice were placed in the nose-only Scireq *InExpose* cigarette-smoking robot starting at day 14.5 dGA and exposed for four days with necropsy at 18.5 dGA. IUGR was induced following 4 days of exposure wherein a computer-controlled puff of smoke generated every minute resulted in 10 s of SHS exposure (from six cigarettes; 2R1, University of Kentucky, Lexington, KY) followed by 50 s of rom air (fresh air). This procedure was done daily for 10 min during the time of treatment. Control animals (n 7) were place in soft restrains and exposed only to room air daily for 10 min. For PKM2 activation studies the SHS treated animals were treated with 50 mg/kg of TEPP-46 PKM2 activator (Millipore, Saint Louis, MO) from 11dGA through necropsy at 18dGA (Angiari et al., 2020; Le et al., 2020). At this point, placental and fetal weight were recorded for *in vivo* studies.

Statistical Analysis

Control and IUGR placentas and cell protein lysates end points were compared for PKM2. Data was analyzed for normality and differences using the Mann-Whitney test with $p < 0.05$ as significantly different. Table 1 was analyzed with the Kruskal-Wallis test for statistical significance with $p < 0.05$ as statistically significant. All data represent the mean ± SEM.

Results

Placenta Demographics

Human placenta sample demographics were analyzed for significant differences between Control and IUGR groups. There was no difference in maternal age. IUGR groups had statistically lower (p < 0.0003) gestational ages compared to controls. Fetal weights from IUGR patients were also statistically lower (P < 0.0001) compared to the control group.

Placental PKM2 Expression During IUGR

We first wanted to determine PKM2 expression in human placenta tissues of normal gestation and IUGR. IHC did not reveal differences in PKM2 expression in the villi of the trophoblast cell in the IUGR placenta as compared to controls (Figure 4.1). No differences were observed in cytosolic PKM2 protein expression between IUGR and control placentas (Figure 4.1A–B). Elevated nuclear expression of PKM2 was detected in the IUGR placentas (1.4-fold; p < 0.03) as compared to control placentas (Figure 4.1C).

PKM2 and Trophoblast Invasion

To determine PKM2 in SW71 trophoblast invasion, we first determined the localization of PKM2 in these cells. Interestingly, we observed a higher expression of PKM2 in the nucleus as opposed to the cytosol in SW71 cells (Figure 4.2A–B). We next determined cell viability using the already published suggested concentration for Shikonin (1 μm–500 μm) and (100 nm–250nm). We did not observe any differences in cell viability between the treated and control cells (data not shown). To further characterize the role of PKM2 in trophoblast cell invasion, we next investigated the effects of its activation/inhibition during the invasion of these cells. We observed increased in trophoblast invasion (1.8-fold; p < 0.002) when PKM2 was

activated (Figure 4.2C). In contrast, there was a significant decrease in trophoblast invasion (65-fold; $p < 0.002$) when cells were treated with Shikonin (Figure 4.2C). These results confirmed a role for PKM2 in the regulation of trophoblast invasion. Nuclear PKM2 is used as a transcriptional regulator while cytosolic PKM2 predominantly functions as a glycolytic enzyme (Bahr et al., 2014; Park et al., 2019). We next examined the nuclear and cytosolic PKM2 protein levels in the trophoblast cells treated with F1BP6 or Shikonin. We observed that both pPKM2 and PKM2 were decreased in the cytosol (1.9-fold; 1.7-fold; $p < 0.03$) when Shikonin was added to the cells while no differences were observed with F1BP6 treatment (Figure 4.3A–B). In contrast, both pPKM2 (1.7-fold; 2.5-fold; $p < 0.04$) and PKM2 (1.7-fold; 1.8-fold; $p < 0.004$) were increased in the nucleus with treatment of F1BP6 or Shikonin when compared to controls (Figure 4.3C–D). As previously mentioned, IUGR is associated with local hypoxia. Therefore, we decided to examine trophoblast invasion and PKM2 levels in hypoxia treated and normoxic trophoblast cells. Hypoxia treatment decreased trophoblast invasion for both F1BP6 (3.0-fold; $p < 0.005$) and Shikonin (55-fold; $p < 0.005$) treated trophoblast cells (Figure 4.4). Cytosolic pPKM2 protein was only decreased with F1BP6 (2-fold; $p < 0.03$) when the cells were exposed to hypoxia (Figure 4.5A). In contrast, cytosolic PKM2 protein was not changed with either treatment during hypoxia (Figure 4.5B). In comparison, nuclear PKM2 was decreased in both, F1BP6 (1.6-fold; $p < 0.03$) or Shikonin (1.9-fold; $p < 0.03$) treatment with no differences for nuclear pPKM2 in the hypoxia treated trophoblast cells when compared to controls (Figure 4.5C–D).

mTOR, PKM2 and Trophoblast Invasion

A role for mTOR in trophoblast invasion has been previously shown (Knuth et al., 2015). Because PKM2 expression can be regulated by mTOR, we decided to determine if the

impairment of mTOR affects PKM2 expression and leads to altered trophoblast invasion. For these experiments, SW71 trophoblast cells were treated with 40 nm of Rapamycin for 24 h. Activation of mTOR was reduced (1.1-fold; $p < 0.05$) in treated cells as compared to control (Figure 4.6A). Interestingly, PKM2 protein was also reduced in the treated trophoblast compared to controls (Figure 4.6B). These results correlated with a reduction in invasion of treated trophoblast cells (Figure 4.6C). To further confirm a correlation between mTOR and PKM2, we inhibited PKM2 and measured pmTOR in trophoblast cells and observed decreased mTOR activation when PKM2 was inhibited (Figure 4.6D).

PKM2 and IUGR

PKM2 is present in cancer cells and embryonic tissues. To better understand the role of activated PKM2 *in vivo*, we decided to use the SHS induced IUGR model wherein placental and fetal weights are compromised. TEEP46 is a PMK2 inhibitor successfully used *in vivo* (Angiari et al., 2020; Le et al., 2020). We treated mice with both SHS and TEEP46, the PKM2 activator, and assessed the outcomes of placental and fetal weights (Lewis et al., 2017). There was a significant 28% reduction in placental weight ($p < 0.0003$) in SHS exposed mice compared to room air controls. This reduction was improved when animals were treated with SHS and TEEP46 (Figure 4.7A). Similarly, we demonstrated a 49% reduction in fetal weight ($p < 0.0002$) in SHS exposed mice, which was recovered when SHS animals were treated with the PKM2 activator (Figure 4.7B).

Discussion

The Pyruvate Kinase M2 (PKM2) enzyme is regulated by multiple signal pathways and has been shown to have an important role in cancer cell metabolism and growth (Chen et al., 2011; Wu & Le, 2013). Less active PKM2 inhibits overall glycolysis, but promotes aerobic

glycolysis, converting pyruvate to lactate for energy production. The inhibition of glycolysis by the less active dimer form of PKM2 allows redistribution of glycolytic intermediates to support biosynthesis of macromolecules and cancer proliferation (Cairns et al., 2011; Christofk et al., 2008). Although PKM2 in cancer cells has been studied, understanding of PKM2 in the placenta and embryonic tissues is very limited. Previous studies in our laboratory demonstrated increased nu- clear PKM2 in the IUGR placenta (Bahr et al., 2014). To confirm our previous results, we performed IHC and western blot. We observed no differences when staining for PKM2 in the IUGR placenta and control. Interestingly, we detected increased PKM2 protein in the nucleus of the IUGR placenta by blotting. These results suggest that placental PKM2 localization could play a role in IUGR disease progression and that its expression may be involved in the use of alternative glycolytic pathways during this disease.

A hallmark of pregnancies associated with IUGR is shallow invasion of the trophoblast cells and this shallow invasion is associated with local hypoxia and inhibition of trophoblast invasion (Knuth et al., 2015). We first wanted to determine the expression of PKM2 in the invasive trophoblast cells. We observed that PKM2 was mostly expressed in the nucleus of these cells. Previous reports established a role for PKM2 as a nuclear transcription factor (Yang et al., 2011, 2012). Our results suggest that PKM2 in these cells could potentially have a bigger role as a transcription factor in addition to effecting other signaling transduction processes. Because of the high PKM2 expression in these invasive cells, we sought to determine the role of PKM2 activation and the invading properties of these trophoblast cells. Interestingly, our studies showed that trophoblast invasion was regulated by the activation of this enzyme. These results portend that perhaps levels of PKM2 activation could be a factor involved in the regulation of trophoblast invasion during pregnancy. Previous reports showed that phospho PKM2 (pPKM2)

can act as a transcription factor in tumor cells (Hitosugi et al., 2009; Yang et al., 2011, 2012, 2014). We looked at the cytosolic and nuclear expression of PKM2, p-PKM2 in control and treated cells. Trophoblast cells treated with Shikonin experienced decreased cytosolic expression of both pPKM2 and PKM2 while their expression was increased in the nucleus of these cells. This set of observations support the idea that PKM2 dimer inhibition leads to an increased role for PKM2 as a transcription factor, and a shift from the TCA cycle to the less effective aerobic glycolysis under minimum environmental stress may result in decreased cell invasion (Zhang et al., 2019). Interestingly, we observed no differences in cytosolic pPKM2 and PKM2 while there was increased nuclear expression during FBP treatment. This was unexpected as we suspected cytosolic PKM2 to be increased. Although nuclear expression of PKM2 was increased, the increase was higher for PKM2 than for pPKM2. This may mean that PKM2-mediated transcriptional control is lower during PKM2 activation by FBP. Collectively, these results suggest alternative regulation for PKM2 localization during its activation or inhibition.

As previously mentioned, pregnancies complicated by IUGR are characterized by the development of hypoxia and shallow trophoblast invasion. Our results showed decreased trophoblast invasion with either FBP or Shikonin treatment in the hypoxia treated cells. Decreased invasion in the FBP treated samples confirmed the role of FBP in stabilizing tetrameric PKM2 and the oxidation phosphorylation pathway. This paradigm reduces metabolic efficiency under hypoxia conditions leading to the reduction in trophoblast invading ability. Trophoblastic invasion was further potentiated with the dimeric PKM2 mediated aerobic glycolysis inhibition by Shikonin. Interestingly, we detected decreased cytosolic pPKM2 but not PKM2 when trophoblasts were treated with FBP. In contrast, cytosolic PKM2

was only increased with Shikonin treatment of these cells. In the nuclear fractions, only PKM2 was changed (decreased) with either treatment. These results suggest a separate signaling pathway controls PKM2 regulation during hypoxia treatment. Because regulation of PKM2 expression and previous observations that placental mTOR was decreased during IUGR, we wanted to determine if there was a correlation between these molecules in trophoblast cells during IUGR (Arroyo et al., 2009; Kimball et al., 2015; Mejia et al., 2017). Using Rapamycin as an mTOR inhibitor, we detected decreased mTOR activation and that the decrease correlated with diminished PKM2 expression and hindered trophoblast invasion. To further confirm mTOR and PKM2 correlation, we showed that mTOR expression decreases by Shikonin inhibiting action on PKM2 in the trophoblasts. These suggest roles for both molecules in the regulation of trophoblast invasion.

PKM2 is increased in embryonic tissues, and its abundance is likely supportive of the rapid growth and development required during pregnancy (Dombrauckas et al., 2005). To further describe the role of PKM2 activation during pregnancy, we determined the impact of PKM2 activation on compromised placental and fetal weight during IUGR. We observed decreased placental and fetal weight in our model of IUGR that was recovered with co-treatment of a PKM2 activator. These targeting studies suggest an important role for PKM2 activation and foretells avenues that could be beneficial for the development of possible therapies during disease associated with compromised placenta and fetal weights including IUGR.

In conclusion, PKM2 appears to be an excellent candidate of study in understanding metabolic differences and their effects during trophoblast invasion. It is currently unclear if PKM2 activity in human placentas serves as a primary or secondary regulator of placental

metabolism. However, our results suggest that perhaps, similar to what is suggested in cancer cells, PKM2 expression could serve as a secondary effect to hypoxia in the placenta (Tal et al., 2010). Future studies are needed to better understand the role of PKM2 during the development of the placenta throughout gestation.

Declarations

Competing interest: None of the authors have any actual or potential competing financial or other interests with entities possibly interested in the subject matter.
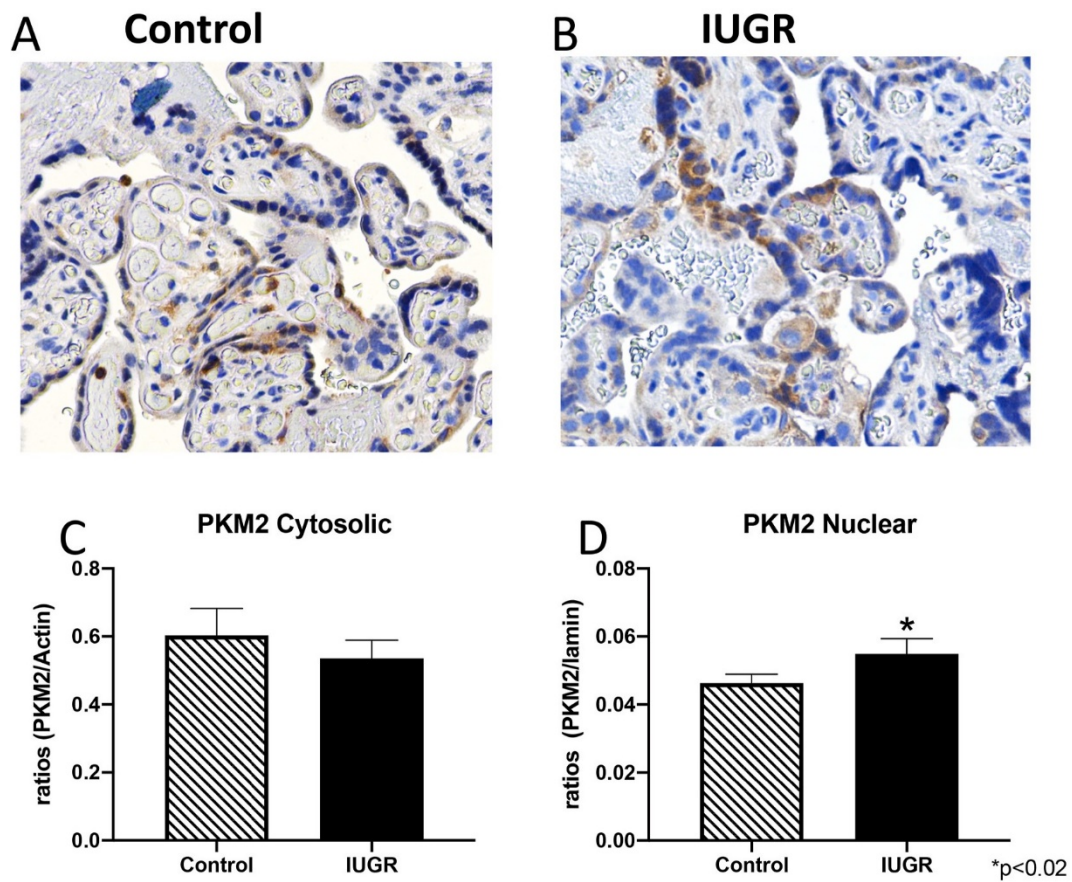
Figure 4.1: Placental PKM2 Expression During IUGR.

IHC staining showed no differences in PKM2 expression (DAB, brown) in the villi of trophoblast cells (Hematoxylin counterstain, blue) between normal gestation control and IUGR (A-B). Subcellular quantification of protein expression showed no difference in the cytosolic expression of PKM2 between IUGR and control samples (C), while elevated nuclear expression was detected in the IUGR placenta compared to controls (D). Data are shown with *P $\leq$ 0.05 compared to controls.
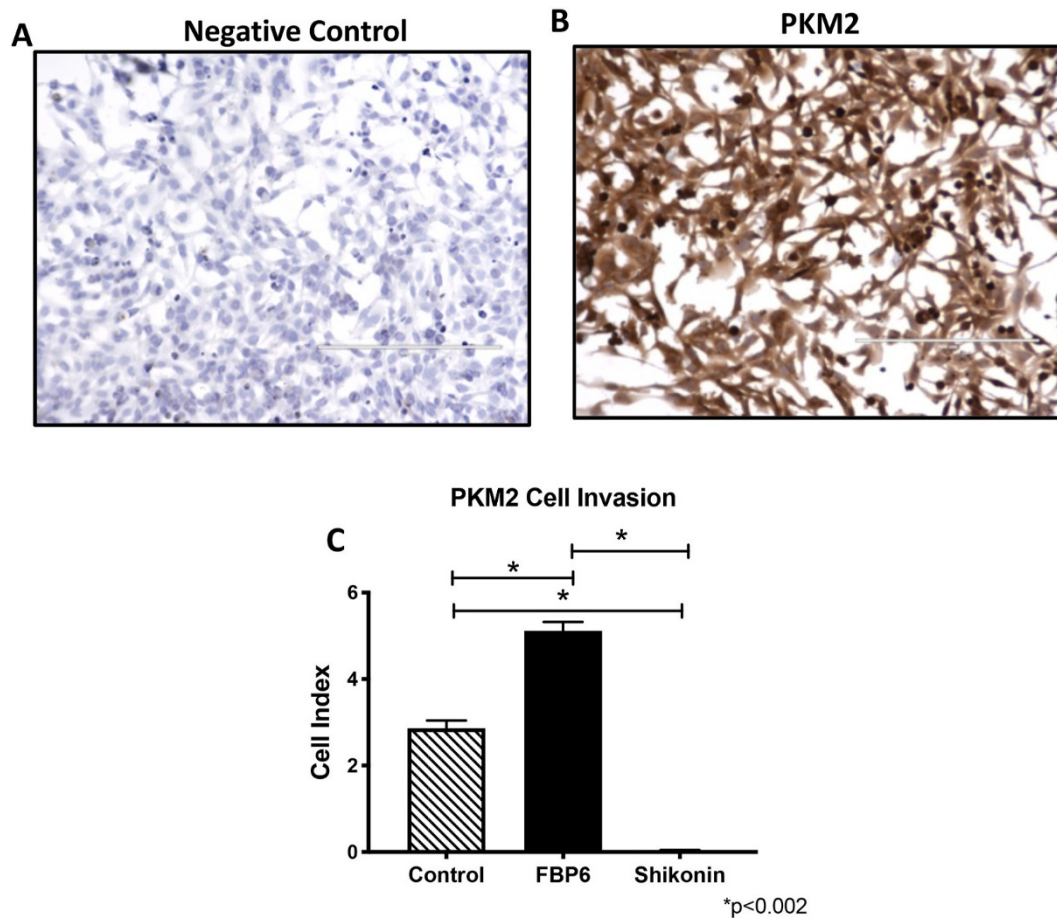
Figure 4.2: PKM2 and Trophoblast Invasion.

PKM2 was predominantly present in the nucleus compared to the cytosol of SW71 trophoblast cells. (A-B). Trophoblast invasion was increased (1.8-fold; $p < 0.002$) during PKM2 activation through FBP6 treatment, while the invading event was decreased (65-fold; $p < 0.002$) during PKM2 inhibition by Shikonin (C). Data are shown with *$P \leq 0.05$ compared to controls.
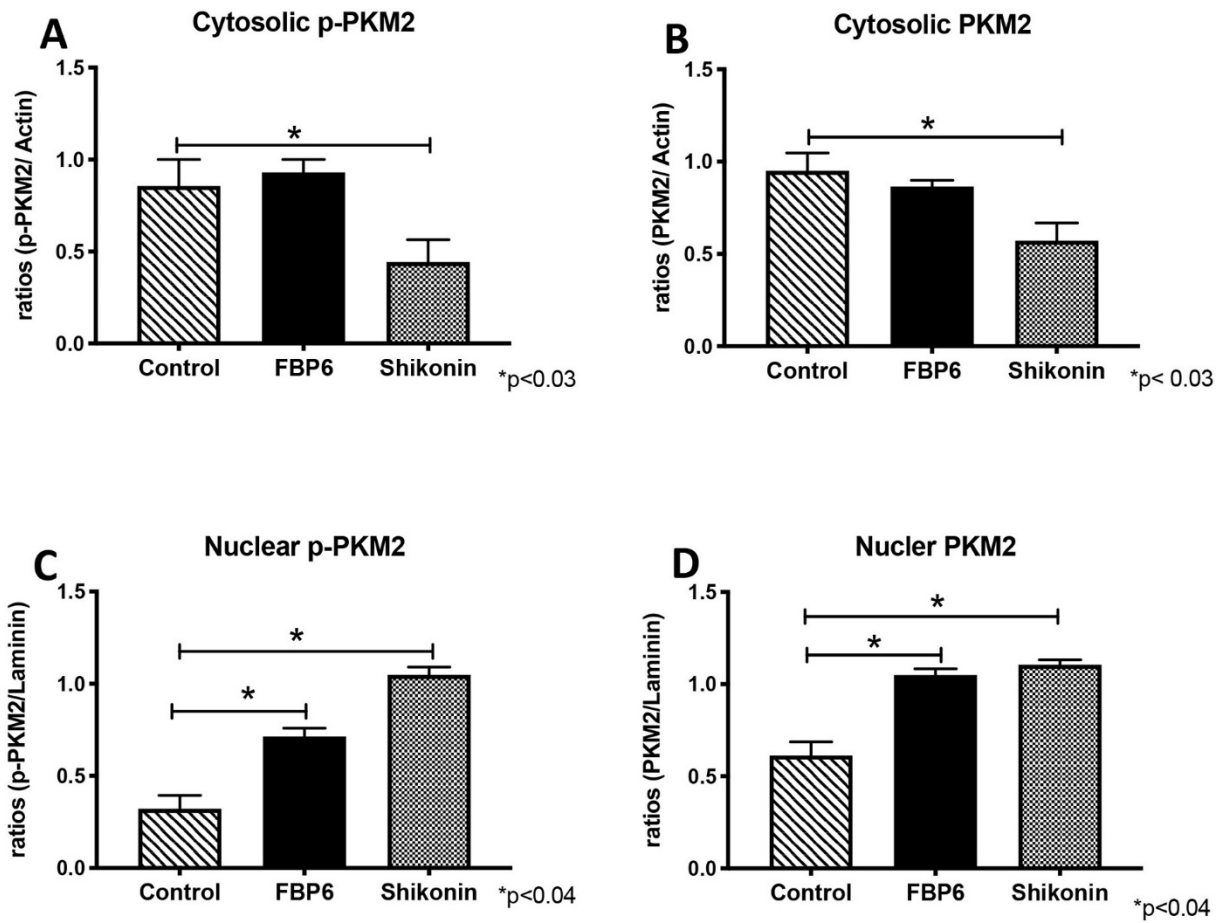
Figure 4.3: Subcellular PKM2 and p-PMK2 Expression.

Cytosolic expression of p-PKM2(A) and PKM2 (B) was decreased (1.9-fold; 1.7-fold; $p < 0.03$) when treated with Shikonin. No significant differences in p-PKM2 or PKM2 were detected when trophoblast cells were treated with FBP6 compared to controls (A-B). p-PKM2 (1.7-fold; 2.5-fold; $p < 0.04$) and PKM2 (1.7-fold; 1.8-fold; $p < 0.004$) nuclear expression were significantly increased with FBP6 or Shikonin treatment compared to controls (C-D). Data are shown with *$P \leq 0.05$ compared to controls.

Hypoxia Cell Invasion
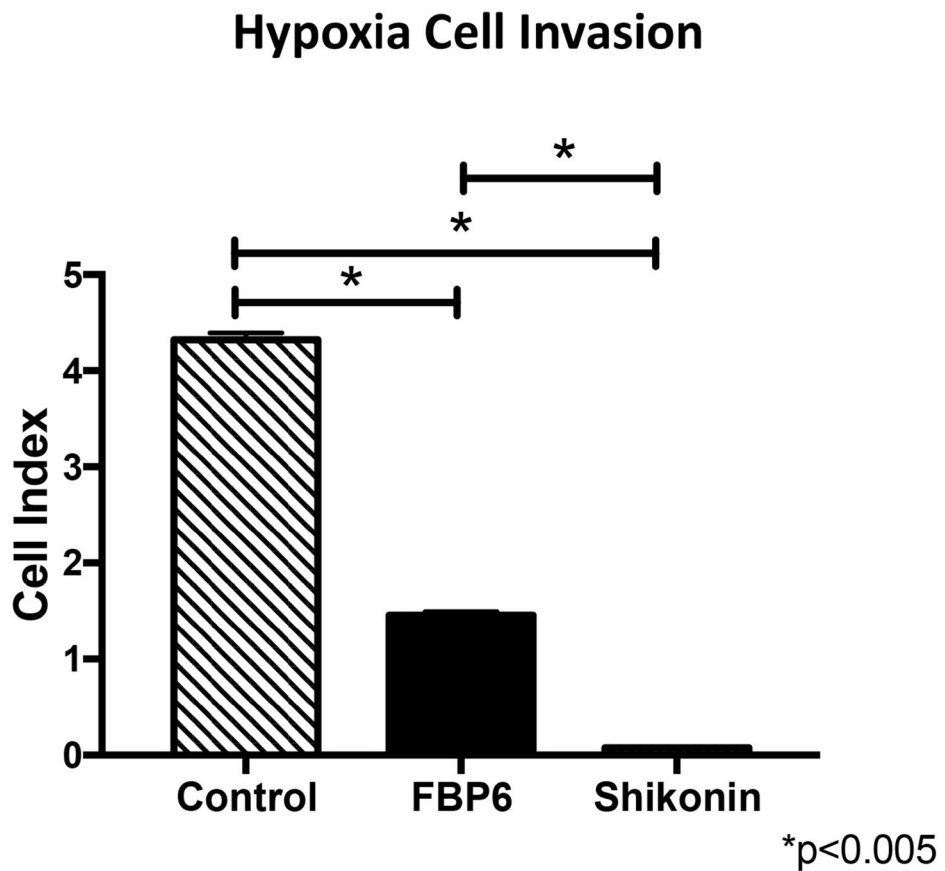
Figure 4.4: PKM2 and Hypoxic Trophoblast Invasion.

Hypoxia treatment decreased trophoblast invasion in both FBP6 (3.0-fold; p < 0.005) or Shikonin (55-fold; p < treated trophoblast cells. Data are shown with *P ≤ 0.05 compared to controls.
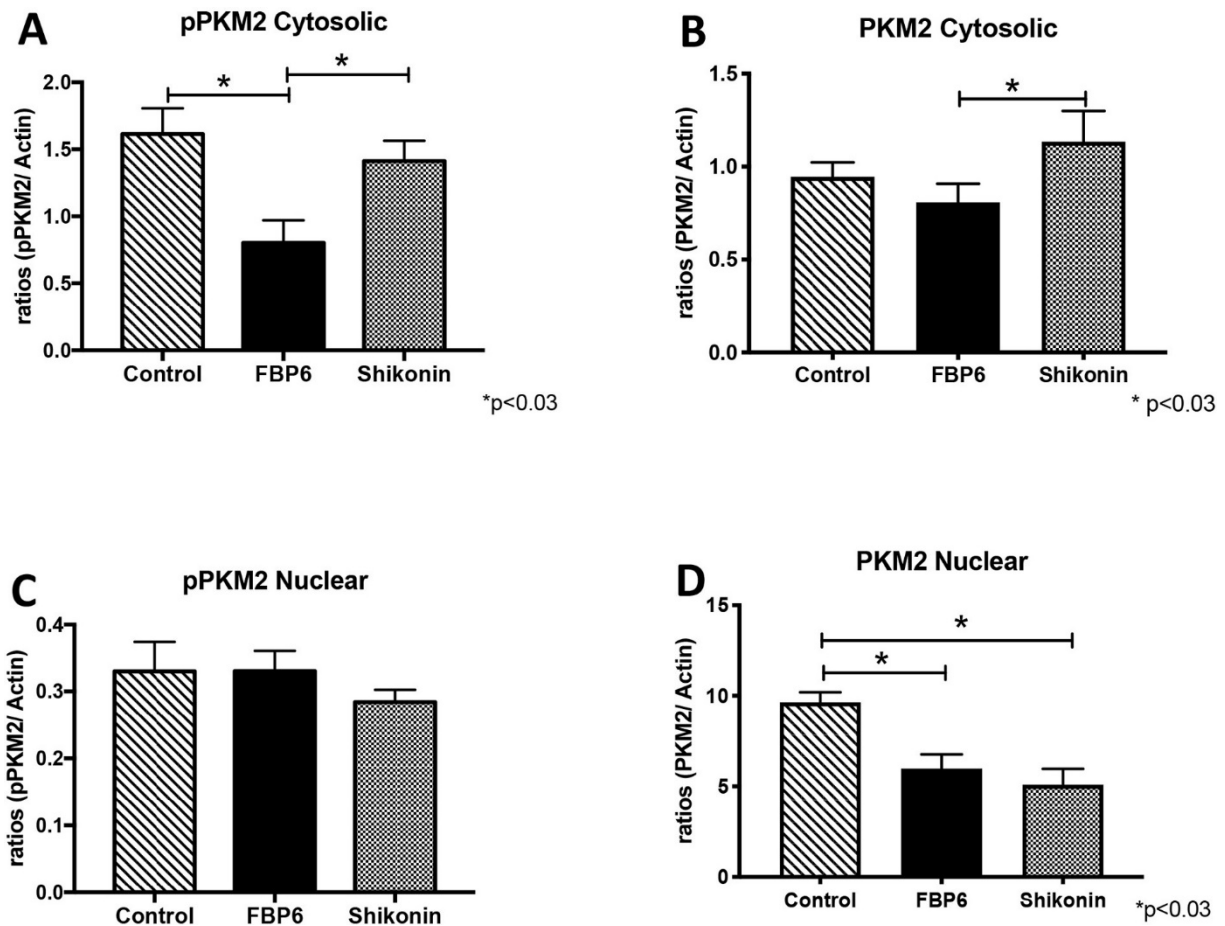
Figure 4.5: Subcellular PKM2 and p-PKM2 Expression

In Hypoxic Trophoblasts. Cytosolic expression of p-PKM2 was decreased (2-fold; $p < 0.03$) in FBP6 treated hypoxic cells (A), while PKM2 showed no significant difference with either treatment relative to controls (B). Nuclear PKM2 was decreased in both, FBP6 (1.6-fold; $p < 0.03$) or Shikonin (1.9-fold; $p < 0.03$) treatment with no differences for nuclear pPKM2 (C) in the hypoxia treated trophoblast when compared to controls (C-D). Data are shown with *$P \leq 0.05$ compared to controls.
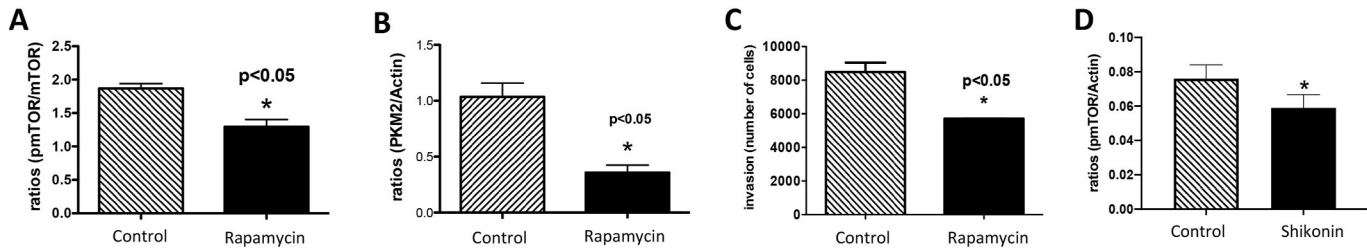
Figure 4.6: mTOR, PKM2 and Trophoblast Invasion.

mTOR inhibition by Rapamycin treatment resulted in reduced mTOR activation (1.1-fold; $p < 0.05$) compared to controls (A). PKM2 protein was reduced ($p < 0.05$) when treated with Rapamycin compared to controls (B). Trophoblast invasion was decreased ($p < 0.05$) when mTOR was inhibited by Rapamycin (C). mTOR activation was reduced when PKM2 was inhibited by Shikonin treatment (D). Data are shown with *P ≤ 0.05 compared to controls.
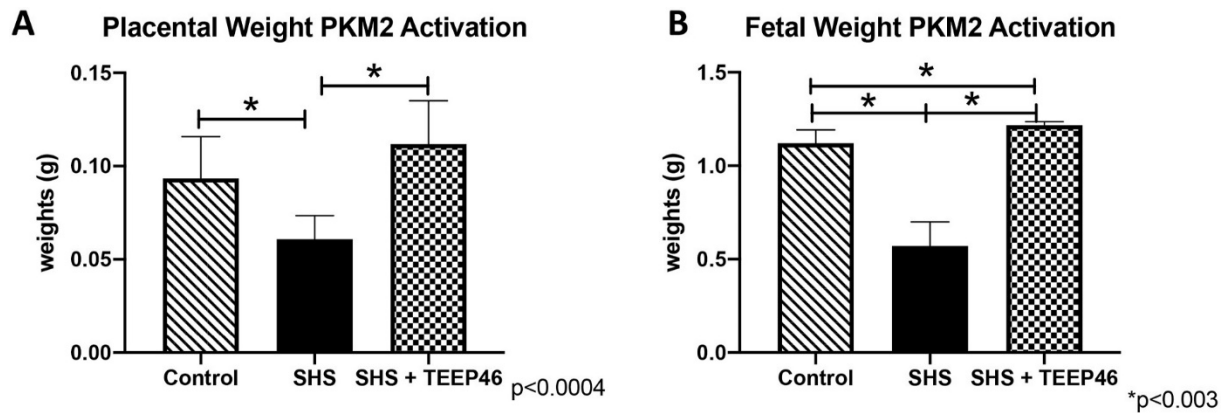
Figure 4.7: PKM2 Effect on Placental and Fetal Weights in a SHS Induced IUGR Model.

A significant 28% reduction in placental weight ($p < 0.0003$) was observed in the SHS mice compared to controls, while the reduction was improved by treatment of TEEP46, a PKM2 activator (A). SHS induced a significant 49% reduction in fetal weight ($p < 0.0002$) that was recovered with TEPP46 treatment during SHS (B). Data are shown with *P ≤ 0.05 compared to controls.

References

Aagaard, K. M., Lahon, A., Suter, M. A., Arya, R. P., Seferovic, M. D., Vogt, M. B., Hu, M., Stossi, F., Mancini, M. A., Harris, R. A., Kahr, M., Eppes, C., Rac, M., Belfort, M. A., Park, C. S., Lacorazza, D., & Rico-Hesse, R. (2017). Primary Human Placental Trophoblasts are Permissive for Zika Virus (ZIKV) Replication. *Scientific Reports*, *7*(1). https://doi.org/10.1038/srep41389

Ahmed, A. (2014). Molecular mechanisms and therapeutic implications of the carbon monoxide/hmox1 and the hydrogen sulfide/CSE pathways in the prevention of pre-eclampsia and fetal growth restriction. *Pregnancy Hypertension: An International Journal of Women's Cardiovascular Health*, *4*(3), 243–244. https://doi.org/10.1016/j.preghy.2014.04.013

Angiari, S., Runtsch, M. C., Sutton, C. E., Palsson-McDermott, E. M., Kelly, B., Rana, N., Kane, H., Papadopoulou, G., Pearce, E. L., Mills, K. H. G., & O'Neill, L. A. J. (2020). Pharmacological Activation of Pyruvate Kinase M2 Inhibits CD4+ T Cell Pathogenicity and Suppresses Autoimmunity. *Cell Metabolism*, *31*(2). https://doi.org/10.1016/j.cmet.2019.10.015

Arroyo, J. A., Brown, L. D., & Galan, H. L. (2009). Placental mammalian target of rapamycin and related signaling pathways in an ovine model of intrauterine growth restriction. *American Journal of Obstetrics and Gynecology*, *201*(6). https://doi.org/10.1016/j.ajog.2009.07.031

Arroyo, J. A., Li, C., Schlabritz-Loutsevitch, N., McDonald, T., Nathanielsz, P., & Galan, H. L. (2010). Increased placental XIAP and caspase 3 is associated with increased placental apoptosis in a baboon model of maternal nutrient reduction. *American Journal of Obstetrics and Gynecology*, *203*(4). https://doi.org/10.1016/j.ajog.2010.05.021

Bahr, B. L., Price, M. D., Merrill, D., Mejia, C., Call, L., Bearss, D., & Arroyo, J. (2014). Different expression of placental pyruvate kinase in normal, preeclamptic and intrauterine growth restriction pregnancies. *Placenta*, *35*(11), 883–890. https://doi.org/10.1016/j.placenta.2014.09.005

Bourque, S. L., Dolinsky, V. W., Dyck, J. R. B., & Davidge, S. T. (2012). Maternal resveratrol treatment during pregnancy improves adverse fetal outcomes in a rat model of severe hypoxia. *Placenta*, *33*(5), 449–452. https://doi.org/10.1016/j.placenta.2012.01.012

Cairns, R. A., Harris, I. S., & Mak, T. W. (2011). Regulation of cancer cell metabolism. *Nature Reviews Cancer*, *11*(2). https://doi.org/10.1038/nrc2981

Cetin, I., & Antonazzo, P. (2009). The Role of the Placenta in Intrauterine Growth Restriction (IUGR). *Zeitschrift Für Geburtshilfe Und Neonatologie*, *213*(03). https://doi.org/10.1055/s-0029-1224143

Chen, J., Xie, J., Jiang, Z., Wang, B., Wang, Y., & Hu, X. (2011). Shikonin and its analogs inhibit cancer cell glycolysis by targeting tumor pyruvate kinase-M2. *Oncogene*, *30*(42). https://doi.org/10.1038/onc.2011.137

Christofk, H. R., Vander Heiden, M. G., Wu, N., Asara, J. M., & Cantley, L. C. (2008). Pyruvate kinase M2 is a phosphotyrosine-binding protein. *Nature*, *452*(7184). https://doi.org/10.1038/nature06667

Denton, K., Phillips, J. K., Goyal, R., Jang, E. A., & Longo, L. D. (2015). Antenatal maternal hypoxia: criterion for fetal growth restriction in rodents. *Frontiers in Physiology | Www.Frontiersin.Org*, *1*, 176. https://doi.org/10.3389/fphys.2015.00176

Dombrauckas, J. D., Santarsiero, B. D., & Mesecar, A. D. (2005). Structural Basis for Tumor Pyruvate Kinase M2 Allosteric Regulation and Catalysis '. *Biochemistry*, *44*(27). https://doi.org/10.1021/bi0474923

Giussani, D. A., & Davidge, S. T. (2013). Developmental programming of cardiovascular disease by prenatal hypoxia. *Journal of Developmental Origins of Health and Disease*, *4*(5), 328–337. https://doi.org/10.1017/S204017441300010X

Gupta, V., & Bamezai, R. N. K. (2010). Human pyruvate kinase M2: A multifunctional protein. In *Protein Science* (Vol. 19, Issue 11, pp. 2031–2044). https://doi.org/10.1002/pro.505

Hitosugi, T., Kang, S., Vander Heiden, M. G., Chung, T.-W., Elf, S., Lythgoe, K., Dong, S., Lonial, S., Wang, X., Chen, G. Z., Xie, J., Gu, T.-L., Polakiewicz, R. D., Roesel, J. L., Boggon, T. J., Khuri, F. R., Gilliland, D. G., Cantley, L. C., Kaufman, J., & Chen, J. (2009). Tyrosine Phosphorylation Inhibits PKM2 to Promote the Warburg Effect and Tumor Growth. *Science Signaling*, *2*(97). https://doi.org/10.1126/scisignal.2000431

Huppertz, B. (2014). Oxygenation of the placenta and its role in pre-eclampsia. *Pregnancy Hypertension: An International Journal of Women's Cardiovascular Health*, *4*(3). https://doi.org/10.1016/j.preghy.2014.04.016

Iqbal, W., & Ciriello, J. (2013). Effect of maternal chronic intermittent hypoxia during gestation on offspring growth in the rat. *American Journal of Obstetrics and Gynecology*, *209*(6), 564.e1-564.e9. https://doi.org/10.1016/j.ajog.2013.08.027

Jansson, N., Pettersson, J., Haafiz, A., Ericsson, A., Palmberg, I., Tranberg, M., Ganapathy, V., Powell, T. L., & Jansson, T. (2006). Down-regulation of placental transport of amino acids precedes the development of intrauterine growth restriction in rats fed a low protein diet. *The Journal of Physiology*, *576*(3). https://doi.org/10.1113/jphysiol.2006.116509

Kimball, R., Wayment, M., Merrill, D., Wahlquist, T., Reynolds, P. R., & Arroyo, J. A. (2015). Hypoxia reduces placental mTOR activation in a hypoxia-induced model of intrauterine growth restriction (IUGR). *Physiological Reports*, *3*(12). https://doi.org/10.14814/phy2.12651

Knuth, A., Liu, L., Nielsen, H., Merril, D., Torry, D. S., & Arroyo, J. A. (2015). Placenta growth factor induces invasion and activates p70 during rapamycin treatment in trophoblast cells. *American Journal of Reproductive Immunology*, *73*(4), 330–340. https://doi.org/10.1111/aji.12327

Le, S., Zhang, H., Huang, X., Chen, S., Wu, J., Chen, S., Ding, X., Chen, S., Zhao, J., Xu, H., Cui, J., Zou, Y., Yu, J., Jiang, L., Wu, J., Ye, P., & Xia, J. (2020). PKM2 Activator TEPP-46 Attenuates Thoracic Aortic Aneurysm and Dissection by Inhibiting NLRP3 Inflammasome-Mediated IL-1β Secretion. *Journal of Cardiovascular Pharmacology and Therapeutics*, *25*(4). https://doi.org/10.1177/1074248420919966

Lewis, J. B., Mejia, C., Jordan, C., Monson, T. D., Bodine, J. S., Dunaway, T. M., Egbert, K. M., Lewis, A. L., Wright, T. J., Ogden, K. C., Broberg, D. S., Hall, P. D., Nelson, S. M., Hirschi, K. M., Reynolds, P. R., & Arroyo, J. A. (2017). Inhibition of the receptor for advanced glycation end-products (RAGE) protects from secondhand smoke (SHS)-induced intrauterine growth restriction IUGR in mice. *Cell and Tissue Research*, *370*(3). https://doi.org/10.1007/s00441-017-2691-z

Matheson, H., W Veerbeek, J. H., Stephen Charnock-Jones, D., Burton, G. J., Wa Yung, H., & Yung, H. W. (2016). Morphological and molecular changes in the murine placenta exposed to normobaric hypoxia throughout pregnancy. *The Authors. The Journal of Physiology*, *594*(5), 1371–1388. https://doi.org/10.1113/JP271073

Mazurek, S. (2011). Pyruvate kinase type M2: A key regulator of the metabolic budget system in tumor cells. *International Journal of Biochemistry and Cell Biology*, *43*(7), 969–980. https://doi.org/10.1016/j.biocel.2010.02.005

Mazurek, S., Michel, A., & Eigenbrodt, E. (1997). *Effect of Extracellular AMP on Cell Proliferation and Metabolism of Breast Cancer Cell Lines with High and Low Glycolytic Rates*. http://www-jbc.stanford.edu/jbc/

Mejia, C., Lewis, J., Jordan, C., Mejia, J., Ogden, C., Monson, T., Winden, D., Watson, M., Reynolds, P. R., & Arroyo, J. A. (2017). Decreased activation of placental mTOR family members is associated with the induction of intrauterine growth restriction by secondhand smoke in the mouse. *Cell and Tissue Research*, *367*(2), 387–395. https://doi.org/10.1007/s00441-016-2496-5

Myatt, L. (2006). Placental adaptive responses and fetal programming. *Journal of Physiology*, *572*(1), 25–30. https://doi.org/10.1113/jphysiol.2006.104968

Park, Y.-J., Kim, J. Y., Lee, D. Y., Zhang, X., Bazarsad, S., Chung, W.-Y., & Kim, J. (2019). PKM2 enhances cancer invasion via ETS-1-dependent induction of matrix metalloproteinase in oral squamous cell carcinoma cells. *PLOS ONE*, *14*(5). https://doi.org/10.1371/journal.pone.0216661

PIJNENBORG, R., ANTHONY, J., DAVEY, D. A., REES, A., TILTMAN, A., VERCRUYSSE, L., & ASSCHE, A. (1991). Placental bed spiral arteries in the hypertensive disorders of pregnancy. *BJOG: An International Journal of Obstetrics and Gynaecology*, *98*(7). https://doi.org/10.1111/j.1471-0528.1991.tb13450.x

Rueda-Clausen, C. F., Stanley, J. L., Thambiraj, D. F., Poudel, R., Davidge, S. T., & Baker, P. N. (2014). Effect of prenatal hypoxia in transgenic mouse models of preeclampsia and fetal growth restriction. *Reproductive Sciences*, *21*(4), 492–502. https://doi.org/10.1177/1933719113503401

Straszewski-Chavez, S. L., Abrahams, V. M., Alvero, A. B., Aldo, P. B., Ma, Y., Guller, S., Romero, R., & Mor, G. (2009). The Isolation and Characterization of a Novel Telomerase Immortalized First Trimester Trophoblast Cell Line, Swan 71. *Placenta*, *30*(11). https://doi.org/10.1016/j.placenta.2009.08.007

Sun, Q., Chen, X., Ma, J., Peng, H., Wang, F., Zha, X., Wang, Y., Jing, Y., Yang, H., Chen, R., Chang, L., Zhang, Y., Goto, J., Onda, H., Chen, T., Wang, M.-R., Lu, Y., You, H., Kwiatkowski, D., & Zhang, H. (2011). Mammalian target of rapamycin up-regulation of pyruvate kinase isoenzyme type M2 is critical for aerobic glycolysis and tumor growth. *Proceedings of the National Academy of Sciences*, *108*(10). https://doi.org/10.1073/pnas.1014769108

Tal, R., Shaish, A., Barshack, I., Polak-Charcon, S., Afek, A., Volkov, A., Feldman, B., Avivi, C., & Harats, D. (2010). Effects of Hypoxia-Inducible Factor-1α Overexpression in Pregnant Mice. *The American Journal of Pathology*, *177*(6). https://doi.org/10.2353/ajpath.2010.090800

Tissot Van Patot, M. C., Murray, A. J., Beckey, V., Cindrova-Davies, T., Johns, J., Zwerdlinger, L., Jauniaux, E., Burton, G. J., & Serkova, N. J. (2010). Human placental metabolic adaptation to chronic hypoxia, high altitude: hypoxic preconditioning. *Am J Physiol Regul Integr Comp Physiol*, *298*, 166–172. https://doi.org/10.1152/ajpregu.00383.2009.-We

Winden, D. R., Barton, D. B., Betteridge, B. C., Bodine, J. S., Jones, C. M., Rogers, G. D., Chavarria, M., Wright, A. J., Jergensen, Z. R., Jimenez, F. R., & Reynolds, P. R. (2014). Antenatal exposure of maternal secondhand smoke (SHS) increases fetal lung expression of RAGE and induces RAGE-mediated pulmonary inflammation. *Respiratory Research*, *15*(1). https://doi.org/10.1186/s12931-014-0129-7

Wong, N., De Melo, J., & Tang, D. (2013). PKM2, a Central Point of Regulation in Cancer Metabolism. *International Journal of Cell Biology*, *2013*. https://doi.org/10.1155/2013/242513

Wu, S., & Le, H. (2013). Dual roles of PKM2 in cancer metabolism. *Acta Biochimica et Biophysica Sinica*, *45*(1). https://doi.org/10.1093/abbs/gms106

Wullschleger, S., Loewith, R., & Hall, M. N. (2006). TOR signaling in growth and metabolism. In *Cell* (Vol. 124, Issue 3, pp. 471–484). https://doi.org/10.1016/j.cell.2006.01.016

Yang, W., Xia, Y., Hawke, D., Li, X., Liang, J., Xing, D., Aldape, K., Hunter, T., Yung, W. K. A., & Lu, Z. (2014). PKM2 Phosphorylates Histone H3 and Promotes Gene Transcription and Tumorigenesis. *Cell*, *158*(5). https://doi.org/10.1016/j.cell.2014.08.003

Yang, W., Xia, Y., Ji, H., Zheng, Y., Liang, J., Huang, W., Gao, X., Aldape, K., & Lu, Z. (2011). Nuclear PKM2 regulates β-catenin transactivation upon EGFR activation. *Nature*, *480*(7375). https://doi.org/10.1038/nature10598

Yang, W., Zheng, Y., Xia, Y., Ji, H., Chen, X., Guo, F., Lyssiotis, C. A., Aldape, K., Cantley, L. C., & Lu, Z. (2012). ERK1/2-dependent phosphorylation and nuclear translocation of PKM2 promotes the Warburg effect. *Nature Cell Biology*, *14*(12). https://doi.org/10.1038/ncb2629

Zhang, Z., Liu, H., Liu, L., Song, W., & Sun, Y. (2019). Effect of Staphylococcus epidermidis on U(VI) sequestration by Al-goethite. *Journal of Hazardous Materials*, *368*, 52–62. https://doi.org/10.1016/j.jhazmat.2019.01.022

Zhao, X., Zhu, Y., Hu, J., Jiang, L., Li, L., Jia, S., & Zen, K. (2018). Shikonin Inhibits Tumor Growth in Mice by Suppressing Pyruvate Kinase M2-mediated Aerobic Glycolysis. *Scientific Reports*, *8*(1). https://doi.org/10.1038/s41598-018-31615-y

CHAPTER 5: General Discussion

Inflammatory Pathologies of Pregnancy Complications

To accommodate the appearance of a foreign body, pregnancy is either a pro-inflammatory or an anti-inflammatory condition. Thus, the regulation of inflammation is directly associated with pregnancy outcomes. RAGE-mediated inflammatory response has been recognized as a significant cause of diseases and can be triggered by infections, trauma, toxins, and genomic instability. Expectedly, RAGE has been shown to mediate pregnancy complications. In concordance with this, previous studies in our laboratory showed increased placental RAGE during obstetric complications.

The other event that links RAGE mediated inflammatory response is DNA damage such as previously reported in neuropathy and pulmonary diseases. Though a pattern of DNA damage has been reported in pathological placentas, its impact on pregnancy is still unknown. However, the newly reported nuclear isoform of RAGE provides a link between inflammation and DNA damage in the placenta. The current work demonstrates the involvement of RAGE during placental DNA-DSB repair. We identified the presence of DSB in preeclampsia and preterm labor and the involvement of RAGE in the DSB repair process through its conjugation with ATM and MRN complex. Similar results were observed when DNA damage was induced in trophoblast cells by cigarette smoke or bleomycin treatment. Additionally, examination of trophoblastic functions revealed the negative impacts of genomic instability on trophoblast invading function which is associated with the development pregnancy complications. These outcomes confirm the implications of RAGE in maintaining genomic integrity in the placenta and suggest a role for genome defect in the pathologies of pregnancy complications.

Altered Signaling in Obstetric Pathologies

Along with inflammation, alterations of other signaling pathway have also been known of its contribution to pregnancy complications example such as mTOR and PKM2 metabolic signaling cascade.

mTOR is also important for regulating energy homeostasis through its interplay with AMPK which exerts opposite actions. Our studies observed elevated levels of mTOR during nutrient abundant GDM placenta and decreased of mTOR during limited nutrient conditions of PE and IUGR. Surprisingly, AMPK was found elevated in both GDM and PE. mTOR also regulates energy availability through mediating PKM2. In our studies, the activation of PKM2 was decreased by inhibiting mTOR through rapamycin treatment. PKM2 positively regulates trophoblast invasion, and this effect was diminished under hypoxia condition which mimics IUGR. Furthermore, the addition of PKM2 activator rescue placental and fetal weight from SHS treatment in rodents. Thus, understanding the metabolic differences of mTOR and PKM2 and their effects during trophoblast invasion allows better insights for placental and fetal developments.

Future Directions

Through exploring the implications of RAGE, mTOR, and PKM2 during pregnancy, we uncovered the fundamental regulations of inflammation and metabolism during placental and fetal developments. Our research primarily focused on the related molecules and the downstream signaling cascades of these pathways. Our research and several lines of study suggest the interplay of the inflammatory and metabolic pathways. Further evaluation of the interplay

between inflammatory and metabolic pathways in individual pregnancy complications will allow better insights for pathologies and disease development and can lead to new avenues that may help alleviate diseases associated with pregnancy complications.

Relevance of Research

Study of pathologies bridges basic research and medicine by enhancing the translational value of the research. This can be beneficial in disease prevention, diagnosis, treatment, and post-treatment care. Though advanced knowledge is constantly uncovered through continuous research, there remains many unexplored pathological pathways especially in the reproductive field. Our work provides understanding in the contribution of inflammatory and the altered signaling pathways and lays a foundation for further investigation on the pathological signaling pathways associate with pregnancy complications. Understanding these mechanisms provide significant insights into broad swaths of biology with far-reaching biomedical relevance in care of patients with obstetric complications.

APPENDIX A: RAGE and AXL Expression Following Secondhand
Smoke (SHS) Exposure in Mice

Kary Ya Fang Tsai, Kelsey M. Hirschi, Sam Llavina, Taylor Davis, Matt Long, Abby
Bennett,Beau Sitton, Juan A. Arroyo, and Paul R. Reynolds

Lung and Placenta Laboratory, Department of Physiology and Developmental Biology,
BrighamYoung University, Provo, UT, USA

Corresponding Author:
Paul R. Reynolds,
Ph.D. Brigham
Young University
Department of Physiology and Developmental
Biology3054 Life Sciences Building
Provo, UT 84602
Phone: (801) 422-1933; Fax: (801) 422-0700
E-mail: paul_reynolds@byu.edu

Abstract

Tobacco exposure is one of the top three global health risks leading to the development of chronic obstructive pulmonary disease (COPD). Although there is extensive research into the effects of cigarette smoke, the effect of secondhand smoke (SHS) in the lung remains limited. SHS induces receptors for advanced glycation end-products (RAGE) and an inflammatory response that leads to COPD characteristics. Semi-synthetic glycosaminoglycan ethers (SAGEs) are sulfated polysaccharides derived from hyaluronic acid that inhibit RAGE signaling. The growth arrest-specific 6 (Gas6) protein is known to induce dynamic cellular responses and is correlated with cell function. Gas6 binds to the AXL tyrosine kinase receptor and AXL-mediated signaling is implicated in proliferation and inflammation. This project's purpose was to study the correlation between RAGE, AXL, and Gas6 during SHS exposure in the lung. C57Bl/6 mice were exposed to SHS alone or SHS + SAGEs for 4 weeks and compared to control animals exposed to room air (RA). Compared to controls we observed: 1) increased RAGE mRNA and protein expression in SHS-exposed lungs which was decreased by SAGEs; 2) decreased expression of total AXL, but elevated pAXL expression; 3) highly elevated Gas6 expression when RAGE was targeted by SAGEs during SHS exposure; 4) SHS-mediated BALF cellularity and inflammatory molecule elaboration; and 5) the induction of both RAGE and AXL by Gas6 in cell culture models. Our results suggest that there is a possible correlation between RAGE and AXL during SHS exposure. Additional research is needed to dissect the molecular interplay between these two important signaling cascades. At this point, studies provide insight into tobacco-mediated effects in the lung and clarify possible avenues for alleviating complications that could arise during SHS exposure such as those observed during COPD exacerbations.

Keywords: RAGE, AXL, tobacco, lung, inflammation

Introduction

        Tobacco smoke contains over 4000 chemical substances (Moritsugu, 2007), and classes

of these entities have been experimentally correlated with adverse health outcomes. The

combustion of tobacco products produces a diversity of compounds observed in both gaseous

and particulate fractions. Many of these compounds are toxic components that induce

inflammation and cause irritation. A common development of prolonged smoke exposure is

chronic obstructive pulmonary disease (COPD), one of the leading causes of mortality and

morbidity and currently estimated to affect roughly 5% of the world's population or about 329

million individuals (World Health Organization, 2011). The data overwhelmingly implicate

active smoking as the greatest risk factor for developing COPD (Hagstad et al., 2014); however,

exposure to secondhand smoke (SHS) is also associated with risk for COPD (Hagstad et al.,

2014). Globally, COPD is projected to be the third leading cause of death by 2020. Economists

have estimated that the economic burden (including both direct and indirect costs) resulting from

COPD was $2.1 trillion in 2010; however, they believe it will rise to $4.3 trillion by 2030

(Lomborg, 2013). Direct costs alone have been estimated to be in the $49.9 billion range,

suggesting a greater need for preventative measures, as well as improvements in earlier diagnosis

and more cost-effective treatment. Critically necessary in developing therapeutics that aid

affected individuals is the need to more fully understand underlying molecular mechanisms that

promulgate inflammatory stress. The current undertaking sought to identify possible interplay

between two smoke-induced progression factors that act as receptors for pro-inflammatory

stimuli: receptors for advanced glycation end-products (RAGE) and AXL receptor tyrosine

kinases (AXL). RAGE is a cell-surface receptor of the immunoglobulin superfamily expressed in

many cell types including endothelial and vascular smooth muscle cells, fibroblasts,

110

macrophages/monocytes, and epithelium (Thornalley, 1998). RAGE is abundantly expressed by well-differentiated pulmonary alveolar type I (ATI) epithelial cells (Schmidt & Stern, 2000). RAGE was first described as a progression factor in cellular responses induced by irreversibly glycated proteins called advanced glycation end-products (AGEs) and cigarette smoke is an important exogenous inducer of AGE formation (Cerami et al., 1997; Nicholl & Bucala, 1998). RAGE has also been distinguished as a pattern recognition receptor that binds S100/calgranulins, amyloid-□peptide, and HMGB-1 to influence gene expression via activated signal transduction pathways (Hofmann et al., 1999; Taguchi, Blood, Del Toro, & Canet, 2000; Yan et al., 1996).

Specifically, a host of pro-inflammatory responses such as those coordinated by MAP kinases, NF-κB, reactive oxygen species (ROS), and other pro-inflammatory mediators such as TNF and IL-1 (Sparvero et al., 2009) result from RAGE-ligand interactions. In contrast to short-lived cellular activation by LPS, engagement of RAGE by its ligands results in prolonged inflammation (Schmidt, Yan, Yan, & Stern, 2001). If left unchecked, such chronic inflammation results in severe tissue injury.

Abrogation of RAGE signaling using *Rage* knockout mice attenuated elastase-induced emphysema (Waseda K, 2015) and significantly protected against smoke-induced airway inflammation and emphysema (Li et al., 2015; Sambamurthy, Leme, Oury, & Shapiro, 2015). Soluble RAGE (sRAGE) was identified as a serum biomarker in tomography assessed emphysema (Carolan BJ, 2014) and its ratio to RAGE ligands was a good predictor of COPD status (Zhang Y, 2014). A link between RAGE and COPD was further supported by data that implicated RAGE polymorphisms in COPD progression (Li Y, 2014). Previous mouse studies in our lab led to discoveries that smoke exposure increased RAGE signaling both *in vitro* and *invivo* (Reynolds et al., 2008; Winden DR, 2014; Wood TT, 2014). Together, these studies demonstrate

that RAGE is a key modulator of inflammation in major lung diseases, and up- regulation in lungs exposed to chronic smoke strongly suggests RAGE may play an importantrole in COPD.

AXL is a receptor tyrosine kinase (RTK) that is documented to function in diverse cellular processes such as proliferation, migration, survival, and metabolism (Brunelleschi, Penengo, Santoro, & Gaudino, 2002). Like family members Tyro3 and Mer, AXL is a transmembrane receptor with two immunoglobulin-like motifs in its extracellular domain that catalyzes kinase reactions (Mark et al., 1994). The vitamin K-dependent protein Gas6 is AXL's most common ligand, and both are widely expressed by lungs, intestine, vascular epithelium, andplacenta (Manfioletti, Brancolini, Avanzi, & Schneider, 1993). Following ligation, AXL signaling results in phosphorylation of cytoplasmic substrates including PI3K, Akt, Src Kinase, ERK, p38, STATE3 and NF-κB (Allen et al., 1999; Fridell et al., 1996; Goruppi, Chiaruttini, Ruaro, Varnum, & Schneider, 2001; Guttridge et al., 2002). It was recently discovered that serum levels of AXL is significantly higher in patients with COPD compared to other patients and that the presence of AXL likely influences COPD prognosis (Berg et al., 2018). Gao et al., recently reported that prenatal tobacco smoke establishes increased risk for asthmatic episodes and other acute exacerbations (Gao, Liu, et al., 2018), supporting other research into the blockade of AXL signaling and resulting amelioration of pulmonary inflammation and airway hyperresponsiveness (Shibata et al., 2014). It is assumed that AXL signaling is a negative regulator of pulmonary epithelial structure and function and that diminished AXL activity correlates with better epithelial barrier integrity, decreased cellular mobility, and less pathological remodeling (Fujino, Kubo, & Maciewicz, 2017).

Due to clearly identified functions of both RAGE and AXL during smoke exposure, a more lucid understanding of their contributions to the inflamed lung is needed. The current

research sought to identify the expression of both receptors during smoke exposure and evaluate potential effects in orchestrating an inflammatory response. We specifically evaluated the expression profile of these receptors in the SHS-exposed mouse lung and related markers of inflammation in an established mouse model of smoke exposure (Joshua B Lewis et al., 2017; Joshua B. Lewis et al., 2017; Reynolds et al., 2008; Robinson, Stogsdill, Lewis, Wood, & Reynolds, 2012; Winden et al., 2014; Wood et al., 2014). We then correlated the inducibility of both receptors in an *in* vitro system involving A-549 cells, an alveolar type II-like epithelial cell line. Future directions should more clearly evaluate the combined functions of both signaling cascades and determine to what extent, if any, they cooperate in the progression of inflammatory disease.

Materials and Methods

Mice and Tissue Preparation

Adult C57Bl/6 mice were exposed to secondhand tobacco smoke (SHS) or room air (RA) for five days a week and over a course of four weeks as already outlined (Winden et al., 2013). Briefly, mice (n=8 per group) were randomly assigned to RA- and SHS-exposure groups and treated using an in-house nose-only smoke exposure system (InExpose System, Scireq, Canada). Treated mice were restrained daily and connected to an exposure tower for 10 minutes where they were nasally exposed to SHS from two standard research cigarettes for five days a week and over a course of four weeks (Wood TT, 2014). The SHS challenge for these studies was chosen according to previously published literature and was associated with a good tolerance of mice to the SHS sessions and an acceptable level of particulate density concentration (Reynolds et al., 2008; Rinaldi et al., 2012). Control animals were similarly handled and restrained but kept in a smoke-free environment. Where indicated, mice were also administered via i.p. injection a bolus

of 30 mg/kg (three days a week for four weeks) of inflammation modulating sulfated polysaccharides derived from hyaluronic acid (HA) called semi-synthetic glycosaminoglycan ethers (SAGEs). SAGEs were a gift from Dr. Glenn D. Prestwich from the University of Utah and they potently prevent RAGE-ligand binding at nanomolar concentrations (Zhang et al., 2011). At the conclusion of the exposure, mice were sacrificed, and lungs were inflation fixed with 4% paraformaldehyde for immunofluorescent studies, lavage to procure bronchoalveolar lavage fluid (BALF) (Stogsdill et al., 2013) or resected prior to the isolation of total protein or RNA (Reynolds, Mucenski, Le Cras, Nichols, & Whitsett, 2004; Stogsdill et al., 2013). The Institutional Animal Care and Use Committee (IACUC) at Brigham Young University approved mice use.

Cell Culture

Human alveolar type II–like pulmonary adenocarcinoma cells (A549; ATCC, Manassas, VA) were maintained in DMEM supplemented with 10% FBS and antibiotics (Mediatech; Manassas, VA). Cells were split into 6-well dishes and grown to 40–50% confluence. A549 cultures were exposed to normal media or media supplemented with Gas6 (R&D, Minneapolis, MN) at a concentration of 600 ng/mL with or without 600 ng/mL R428 (APExBIO, Houston, TX), a commercially available AXL inhibitor. Total protein was isolated after 24 hours. *In vitro* experiments were performed at least twice in triplicate and representative data are shown.

Immunofluorescence

Immunofluorescence (IF) was performed as previously performed in our laboratory (Jimenez et al., 2015). In summary, slides were blocked with Sniper (Biocare Medical, Concord, CA) and incubated overnight with a mouse primary antibody against RAGE (R&D Systems, Minneapolis, MN; Cat# mAb1179, 1:300), AXL (Cell Signaling, Cat#8661S, 1:300), pAXL

114

(Cell Signaling, Cat# 5724S, 1:200), or Gas6 (R&D Systems; Cat# AF885-SP, 1:200). Slides were incubated for an hour with a donkey anti-mouse Texas Red (TX) (Santa Cruz Biotechnology, Santa Cruz, CA). Staining experiments included a no primary control in which sections were treated identically to the others with the exception that slides were incubated with serum that lacked primary antibody Immunofluorescence was detected using a BX6 microscope.

Immunoblotting

Immunoblotting was performed as previously outlined by our laboratory (Winden DR, 2014). Briefly, tissues were homogenized in protein lysis buffer (RIPA, Fisher Scientific, Pittsburg, PA). 20 µg of protein lysates were separated on Mini-PROTEAN® TGX™ Precast gel (Bio-Rad Laboratories, Hercules, CA) and transferred to nitrocellulose membranes. Membranes were blocked and incubated with polyclonal antibodies against RAGE (R&D Systems; Cat# mAb1179 at a dilution of 1:250) or total or phospho AXL (pAXL) (Cell Signaling; Danvers, MA, cat# 5724S, 1:250). Secondary fluorescence tagged antibodies were added for one hour at room temperature. Fluorescence emission was digitally recorded using a C-DiGit® Blot Scanner (LI-COR, Inc., Lincoln, Nebraska). To determine loading consistencies, each membrane was stripped from antibodies and re-probed utilizing an antibody against actin (Cell Signaling; cat# 4967L, 1:500). Immunoblotting was conducted at least twice in triplicate and average band densities were normalized to β-actin densities prior to performing statistical tests.

RNA Isolation and Analysis

RNA was quantified using a Nanodrop and cDNA amplification was performed using Bio-Rad iTaq Universal SYBR® Green One-Step Kit. Data analysis was performed using a Bio-Rad Single Color Real Time PCR detection system (Bio-Rad Laboratories, Hercules, CA). The following primers were synthesized by Invitrogen Life Technologies (Grand Island, NY): RAGE

(For-CCC TTA GCT GGC ACT TAG ATG G and Rev-TGA CCG CAG TGT AAA GAG TCC C), Gas6 (For-GAG TGC CGT GAT TCT GGT C and Rev-CCA CTA AGG AAA CAA TAA CTG) and β-actin (For-ACA GGA TGC AGA AGG AGA TTA C and Rev- CAC AGA GTA CTT GCG CTC AGG A).

Multiplex Cytokine Secretion Assessment

BALF collected at the time of necropsy was used to screen inflammatory mediators. Equal amounts of protein were used for cytokine and chemokine quantification using a LuminexMagpix multiplexing platform (Luminex Corporation, Austin, TX). Quantification of cytokine/chemokine concentrations in the serum samples was specifically performed using a mouse cytokine/chemokine 27-plex bead panel (Millipore Corporation, Billerica, MA). Procedures were performed as suggested by the manufacturer. Briefly, antibody-conjugated magnetic beads were incubated with cell serum samples in a 96-well followed by sequential incubations with biotinylated detection antibody and streptavidin-phycoerythrin. Bead complexes were then read on the Magpix multiplex platform (Luminex Corporation). Standardcurves and data analysis were performed using Milliplex Analyst 5.1 software (Millipore Corporation).

Statistical Analysis

Data are shown as mean ± SE. Differences between groups were determined using Kruskal-Wallis tests, with $P < 0.05$ considered significant.

Results

RAGE Expression Following SHS

Quantitative RT-PCR analysis revealed elevated RAGE expression following SHS exposure when compared to room-air (RA) controls (Figure A.1A). Protein expression was assessed by immunoblotting to confirm correspondence between transcriptional and translational control. There was an equally robust induction of RAGE protein expression observed in SHS-exposed mice compared to controls (Figure A.1B). Qualitatively, immunofluorescent staining showed diffuse RAGE expression in airways and lung parenchyma (Figure A.1C). Administrationof SAGEs significantly inhibited SHS-induced RAGE mRNA (Figure A.1A), total protein (Figure A.1B), and spatial localization of RAGE (Figure A.1C).

AXL and Gas6 Expression Following SHS

Following SHS exposure, total AXL protein was significantly decreased compared to RA exposed animals (Figure A.2A). Interestingly, when SAGEs that ameliorate RAGE signaling were administered, AXL protein expression in SHS-exposed mice was not different than the RA controls (Figure A.2A). These observations were confirmed spatially wherein immunofluorescent staining showed significantly decreased staining for AXL following SHS exposure and a return to diffuse staining when SAGEs were co-administered (Figure A.2B). Despite an observable decrease in total AXL abundance following SHS exposure (Figure A.2B), the activated AXL receptor, pAXL, was significantly increased in the mouse lung following SHS exposure (Figure A.3).

Having confirmed abrogation of total AXL yet markedly increased pAXL following SHS exposure, we next sought to evaluate the expression of Gas6, the key ligand for AXL signaling. Mice subjected to SHS exposure did not significantly alter Gas6 mRNA or protein expression

(Figure A.4A and A.4B); however, when SHS-exposed mice were concomitantly administered SAGEs, Gas6 transcription (Figure A.4A) and protein (Figure A.4B) were significantly enhanced. This intriguing discovery in which RAGE targeting during SHS enhances Gas6 expression thatperpetuates AXL signaling was confirmed qualitatively by immunofluorescent staining (Figure A.4C).

Markers of Inflammation

To assess inflammatory profiles, we conducted a series of experiments to initially evaluate to what extent SHS modulates lung inflammation. Quantification of leukocytic cells in bronchoalveolar lavage fluid (BALF) revealed an expected increase in total cell quantity and PMN abundance following exposure of animals to SHS (Figure A.5A and A.5B). We discovered that total cellular abundance and percentage of PMNs were significantly decreased when SAGEs were co-administered to mice were exposed to SHS (Figure A.5A and A.5B). Evaluation of total protein abundance in BALF samples was undertaken to indirectly assess vascular permeability commonly observed in vessels that are active sites of leukocyte diapedesis. BALF protein was observed to be markedly increased following exposure to SHS but such increases were abrogated in SAGE-treated mice (Figure A.5C).

We next considered specific pro-inflammatory cytokines. Analysis of the mediators secreted into BALF confirmed a marked increase in the expression of IL-1α when mice were exposed to SHS (Figure A.6A). Increased inflammation mediated by IL-2 (Figure A.6B) and TNF-α (Figure A.6C) was also observed following SHS treatment. Analysis of the other inflammatory molecules in the panel resulted in levels that were undetectable or were not significantly different. In each instance, the expression of these SHS-induced mediators was decreased whenmice were co-treated with both SHS and SAGEs (Figures A.6A-C).

RAGE and AXL Expression in an In Vitro Model of Alveolar Epithelium

Due to the discovery that SHS differentially regulated RAGE and AXL expression and that RAGE targeting by SAGEs further impacted the expression of both receptors (Figures A.1 and A.2), we sought to understand the dynamics of both receptors in the context of Gas6. We therefore chose to characterize the two receptors in a cell culture model in which Gas6 was administered. Immunoblotting revealed a significant increase in AXL protein expression following Gas6 treatment and diminished AXL expression when co-cultured with R428 (Figure A.7A). In addition, RAGE was significantly increased by alveolar epithelium following Gas6 treatment andRAGE protein expression was in similar fashion decreased when AXL signaling was inhibited by R428 (Figure A.7B).

Discussion

Consequences of smoke exposure has a long history involving compromise of the respiratory system. Such compromise is underpinned by debilitating, chronic inflammation that hinders respiratory success and lung remodeling. The primary lung disorder that results from tobacco smoke exposure is COPD, a heterogenous inflammatory disorder characterized by airflow obstruction and irreversible tissue loss. It has become increasingly clear that innate immune programs respond to inhaled agents and variable signaling pathways orchestrate basic disease pathogenesis (Brusselle, Joos, & Bracke, 2011). Such inflammatory networks are initiated by mediators that work with the innate immune system to detect inhaled particulates. Through receptor signaling mechanisms, pathways recruit inflammatory modulators in order to attempt the reversal of the dangers of particulates or the endogenous particles released during sustained tissue damage. The current work sought to understand two such signaling initiators: the pattern recognition receptor RAGE and the inflammatory axis controlled by AXL. With

approximately 1 billion people exposed to smoke worldwide, the societal and economic burden of exposure is profound (Courtney, 2015). This excessive burden is primarily driven by the cost of acute exacerbations, which are acute or sub-acute physiologic deterioration in airways function, inflammatory in nature, that lead to more than 1.5 million emergency room visits and 700,000 hospitalizations each year (Ford, 2015; Ford et al., 2013). Recovery from exacerbations can be slow (Seemungal, Donaldson, Bhowmik, Jeffries, & Wedzicha, 2000), with only 75% of patients recovering to baseline lung function at one month (Seemungal et al., 2000).

Exacerbations of COPD are also inducers of bad outcome. The 30-day all-cause risk of readmission and death after hospitalization for a COPD exacerbation are 20% (Sjoding & Cooke, 2014) and 9% (Lindenauer et al., 2013), respectively, but risk is even greater longer term. It is accordingly critical that greater understanding of inflammatory signaling programs be obtained. We discovered enhanced RAGE expression in the lungs of mice after 4 weeks of SHS, which supports previous data obtained by ourselves and others (Carp & Janoff, 1978; Chen L, 2014; Joshua B. Lewis et al., 2017; Reynolds et al., 2008; Reynolds, Stogsdill, Stogsdill, & Heimann, 2011; Robinson et al., 2012). The current undertaking expands the field of smoke exposure research by also demonstrating the abrogation of total AXL in the exposed lung. To date, research involving both AXL and smoking has primarily implicated the receptor in downstream gene regulation programs via methylation (Gao, Liu, et al., 2018; Gao, Urman, et al., 2018). Our discovery that total AXL is diminished in a mouse model of SHS exposure, and subsequent finding that RAGE inhibition via SAGEs leads to increased total AXL expression may shed light into the relatedness of both receptors and the plausibility that AXL may have greater function when RAGE is impaired. There is a clear impetus for expanded research into the biology of pulmonary AXL signaling during SHS exposure as our data intriguingly revealedabundant

activated AXL (pAXL, Figure A.3) following SHS exposure despite lower total AXL expression (Figure A.2). Such an undertaking would also add context to our finding that Gas6 wasmarkedly increased in lungs exposed to SHS while being administered the RAGE blocker SAGEs. Greater Gas6 availability in such a scenario may involve the cooperation of additional receptor tyrosine kinases such as Tyro and Mer, which also bind Gas6 to initiate signaling (Korshunov, 2012; Laurance, Lemarié, & Blostein, 2012). While Gas6 has highest affinity for AXL, all three receptors may have novel functions in the smoke exposed lung that remain unknown. Despite the need for additional detail, it remains clear that RAGE and AXL are not independent, rather a relatedness exists between both signaling receptors (Figures A.1-4).

Our research of BALF revealed characteristics previously observed during inflammatory lung conditions. Elevated BALF protein suggests augmented vascular permeability, which has been associated with airway inflammation (Higaki et al., 2015). Our finding that leukocyte diapedesis was enhanced in SHS-exposed mice, yet significantly diminished in mice that were administered SAGEs, reinforced prior research that demonstrated increased cellular recruitment into the airways of mice and patients exposed to tobacco smoke (Awji, Seagrave, & Tesfaigzi, 2015; Wang et al., 2017). Inflammation modulating molecules were also differentially expressed in the lungs of mice exposed to SHS. Expression of IL-1α, TNF-α and IL-2 were all significantly increased in SHS-exposed mice and returned to basal expression in the animals administered SAGEs. IL-1α is a pro-inflammatory member of the IL-1 family that plays a role in both the innate and adaptive immune responses (Dinarello, 2009). With the precursor and cleaved isoforms both being active, elevated IL-1α has been detected in COPD patients and in mouse models of COPD (Botelho et al., 2011; Pauwels et al., 2011). TNF-α elaboration is associated with down-stream mediators that are released following its secretion including IL-1α,IL-1β, IL-6,

and ROS (Laskin et al., 2010). Secretion of TNF-α is increased in mouse models oftissue injury (Pendino, Shuler, Laskin, & Laskin, 1994) and in several models of lung inflammation (Strzelak, Ratajczak, Adamiec, & Feleszko, 2018). Because TNF-α, IL-1α, and IL-1β cooperate in the modulation of leukocyte migration, the cytokine quantities we've observed may explain the cell counts detected in the exposed mice. We also saw increased SHS-mediatedexpression of IL-2. IL-2 is a key regulator of inflammation in the COPD lung, with known functions in coordinating receptor availability and epithelial cell repair (Crosby & Waters, 2010;Ju, Sharma, Gaskin, & Fu, 2012). Taken together, data obtained from these BALF experiments and prevalent published reports suggest that lung inflammatory responses to SHS are molecularly controlled.

We conducted *in vitro* analyses in order to coordinate RAGE and AXL expression. Given the differential expression programs of RAGE, AXL, and Gas6 during SHS exposure, an understanding of how Gas6 may impact the receptor's expression was contemplated. We found that Gas6, the key ligand for AXL, significantly increased the expression of both RAGE and AXL. Furthermore, cell culture studies involving R428, an inhibitor of AXL signaling, revealed that AXL abrogation diminished Gas6-induced RAGE and AXL expression. While these *in* vitro experiments clearly show inducibility of the receptors in the context of Gas6/AXL, our complete set of data involving inhibitors of RAGE (SAGEs) and AXL (R428) implicates a link between both receptors that was previously unknown. Follow up research should focus on additive and/or compensatory aspects of both RAGE and AXL in the fine tuning of smoke-mediated lung inflammation. Such an undertaking would clarify a possible model in which SHS induces RAGE and pAXL during inflammatory responses (Figure A.8). Exploration of this model with

an emphasis on intervention may ameliorate the acute exacerbations of exposure and in turn, dampen the debilitating effects of acute COPD episodes that require immediate medical intercession.

Abbreviations

ATI (II)	Alveolar type I (or II) cell
AXL	AXL receptor kinase
BALF	Bronchoalveolar lavage fluid
COPD	Chronic obstructive pulmonary disease
CSE	Cigarette smoke extract
FAMRI	Flight Attendant's Medical Research Institute
HMGB-1	High mobility box protein 1
IACUC	Institutional animal care and use committee
IL-1a	Interleukin 1 alpha
IL-2	Interleukin 2
LPS	Lipopolysaccharide
pAXL	Phosphorylated AXL receptor kinase
RA	Room air
RAGE	Receptors for advanced glycation end-products
ROS	Reactive oxygen species
SAGEs	Semi-synthetic glycosaminoglycan ethers
SHS	Secondhand smoke

Declarations
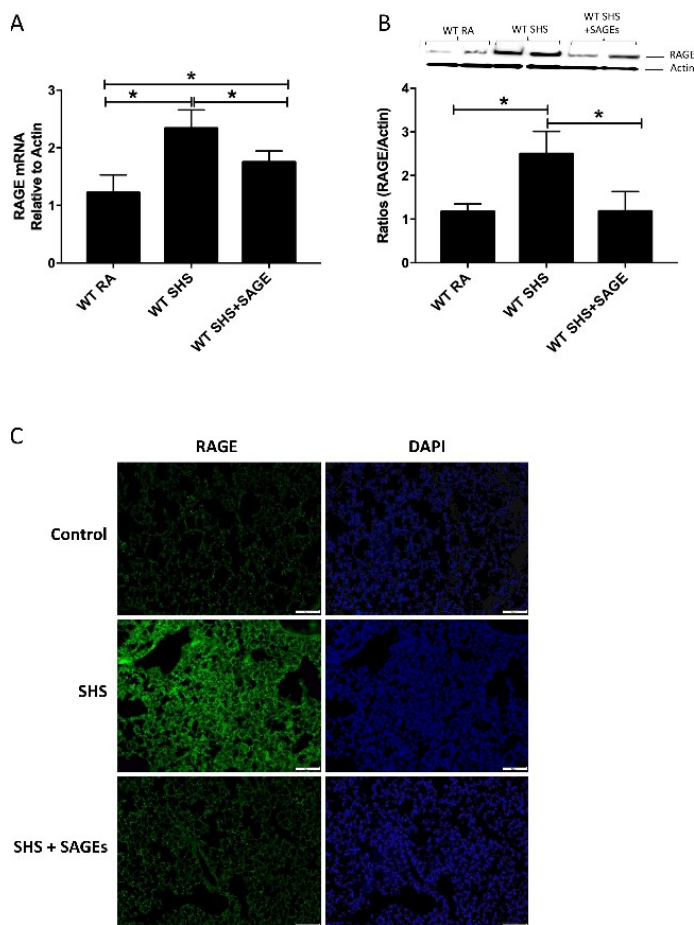
Figure A.1: RAGE mRNA and Protein Expression with SHS Exposure.

A, RAGE mRNA expression was elevated in lungs from mice following exposure to SHS. Exposure of animals to SHS and SAGEs significantly decreased SHS-induced RAGE transcription. The mRNA was normalized to β-actin (n = 6 mice per group) and representative data are shown with *$p \leq 0.05$. B, Analysis of RAGE protein demonstrated that animals exposed to SHS increased RAGE expression while animals co-treated with SAGEs experienced less SHS-induced expression of RAGE. Blots were densitometrically normalized to β-actin and ratios of RAGE/β-actin are presented with *$p \leq 0.05$. C, Immunofluorescence revealed abundant RAGE expression in small airways and lung parenchyma following SHS exposure and markedly less RAGE expression when SAGEs were co-administered with SHS. No primary controls revealed no immunoreactivity. Images (200x magnification) are representative of experiments involving at least four animals from each group.

126
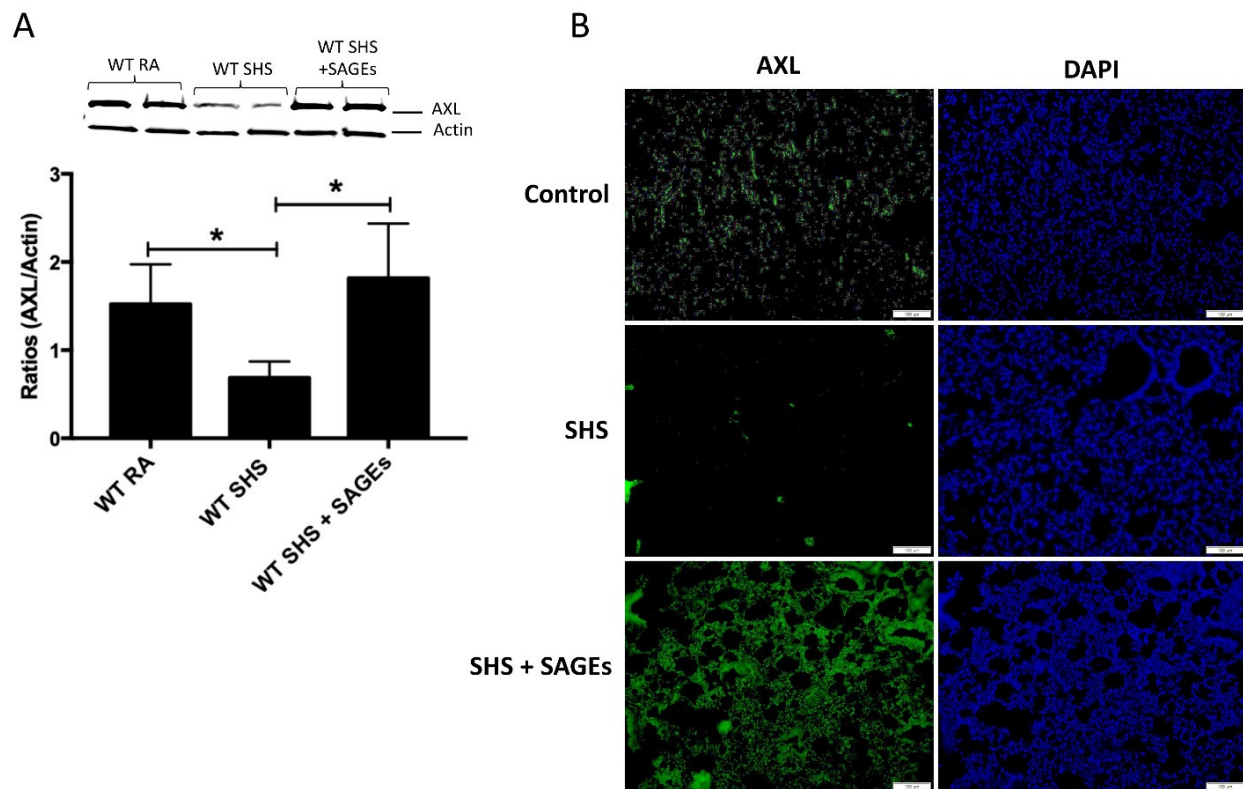
Figure A.2: Total AXL Protein Expression in Response to SHS.

A, AXL expression was decreased in lungs from mice following exposure to SHS. Exposure of animals to SHS and SAGEs significantly increased SHS-mediated AXL back to RA levels. Blots were densitometrically normalized to β-actin and ratios of AXL/β-actin are presented with $*p \leq 0.05$. B, Immunofluorescence revealed notably less AXL expression in the SHS-exposed lung when compared to RA controls and abundant AXL expression when SAGEs were co-administered with SHS. No primary controls revealed no immunoreactivity. Images (200x magnification) are representative of experiments involving at least four animals from each group.

p-AXL　　　　　　　**DAPI**
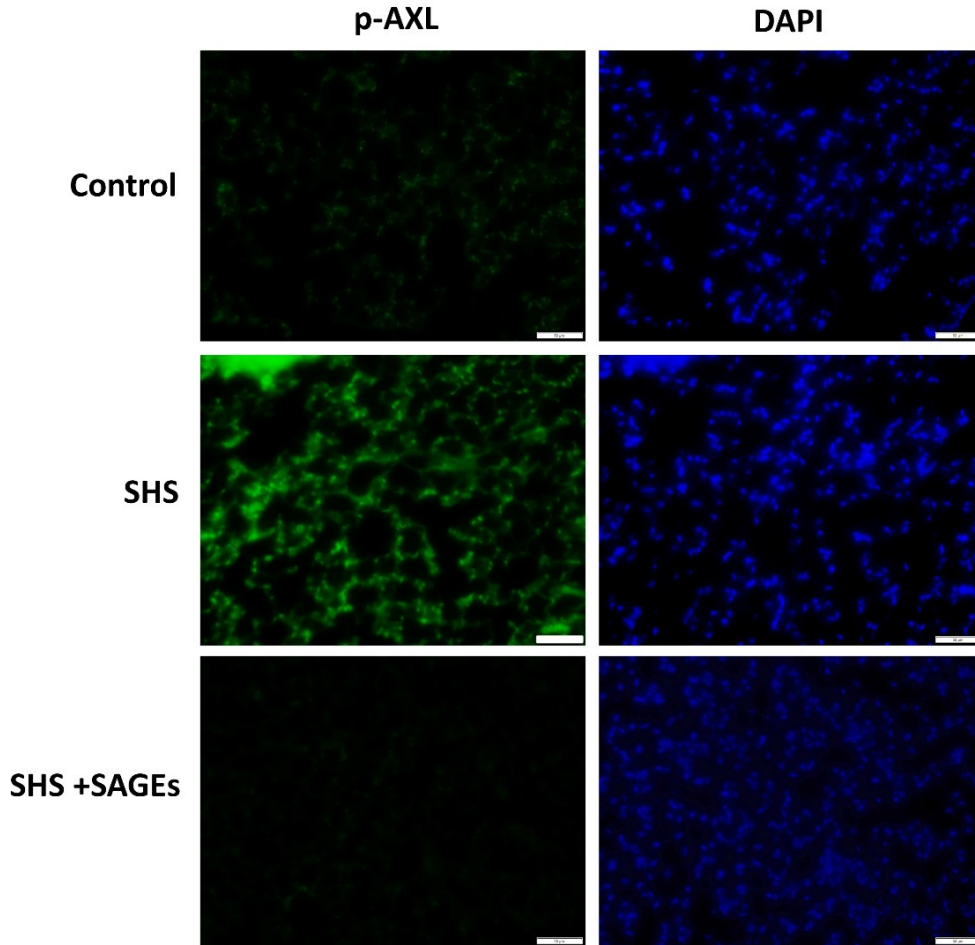
Figure A.3: pAXL Protein Expression in Response to SHS.

Immunofluorescence revealed abundant activated pAXL expression in the SHS-exposed lung compared to undetectable pAXL expression in RA controls. SHS exposure in animals in which RAGE was targeted by SAGEs returned pAXL expression to undetectable levels. No primary controls revealed no immunoreactivity. Images (200x magnification) are representative of experiments involving at least four animals from each group.
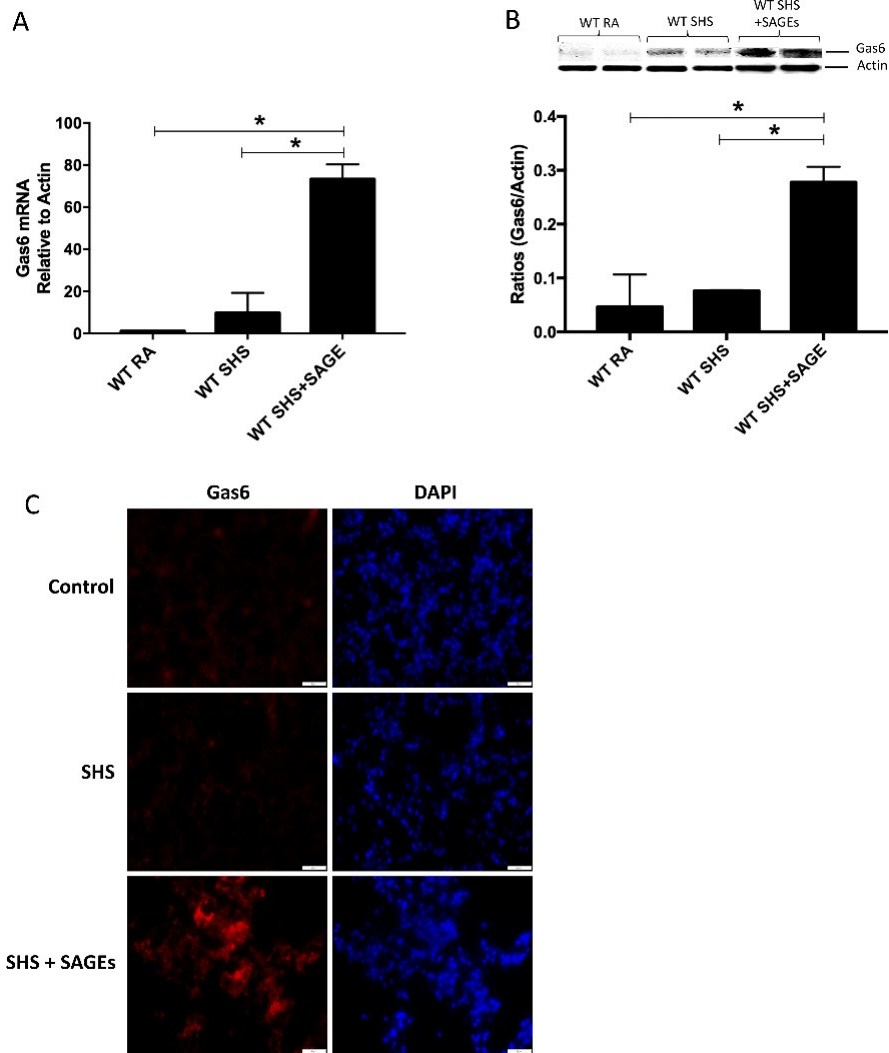
Figure A.4: Gas6 mRNA and Protein Expression in Response to SHS.

A, Gas6 mRNA expression was not significantly different when comparing RA controls and animals exposed to SHS. Exposure of animals to SHS and SAGEs led to a highly significant increase in the transcription of Gas6. The mRNA was normalized to β-actin (n = 6 mice per group) and representative data are shown with *$p \leq 0.05$. B, Immunoblotting for Gas6 revealed significantly Gas6 protein when SHS and SAGEs were used when compared to either RA or SHS alone. C, Immunofluorescence coincided with mRNA analysis in that RA controls and SHS-exposed mice had undetectable Gas6 expression but when RAGE was targeted by SAGEs, highly significant expression patterns for Gas6 were evident. No primary controls revealed no immunoreactivity. Images (200x magnification) are representative of experiments involving at least four animals from each group.
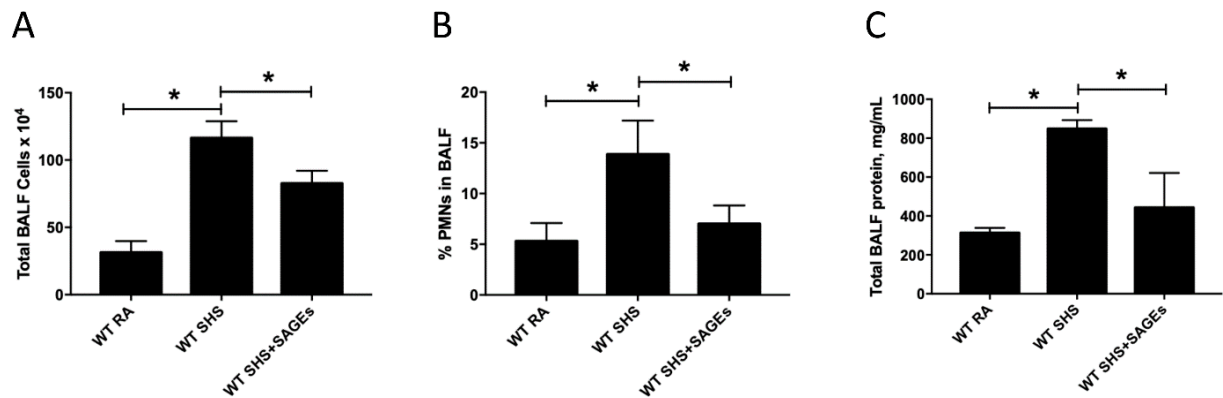
Figure A.5: BALF and Cells with SHS Exposure.

A, Total cells in bronchoalveolar lavage fluid (BALF) were significantly increased in mice exposed to SHS when compared to RA controls (n = 6 mice per group). There was significantly less SHS-induced cellularity in BALF from mice co-administered SHS and SAGEs B, The percentage of polymorphonuclear cells (PMNs) was significantly elevated in mice exposed to SHS compared to room air controls and unchanged in SHS+SAGE exposed mice. C, Total BALF protein was assayed using the BCA technique to demonstrate vascular permeability. Protein was significantly elevated in mice following SHS exposure (n = 6 mice per group) and treatment with SAGEs significantly decreased SHS-induced protein leak. Significant differences are noted as $*p \leq 0.05$.
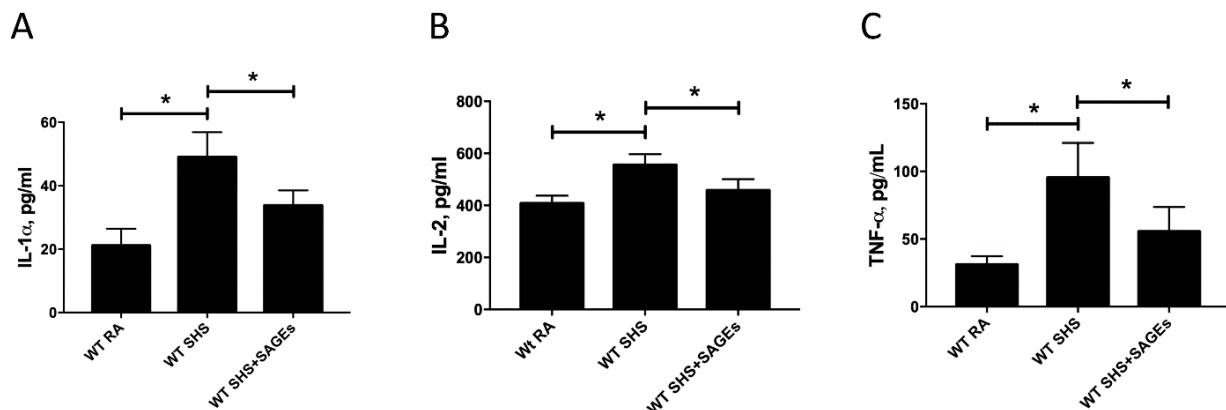
Figure A.6: Inflammatory Cytokines in the Lung Following SHS Exposure.

A, Significantly more IL-1α was secreted into BALF by mice exposed to SHS when compared to RA controls and SAGEs significantly decreased SHS-induced IL-1α secretion (n = 6 mice per group). B, Significant increase of IL-2 secretion into BALF by mice exposed to SHS was observed when compared to controls. SAGEs significantly decreased SHS-induced IL-2 secretion (n = 6 mice per group). C, TNF-α was significantly increased in the BALF by mice exposed to SHS when compared to controls and TNF-α elaboration was diminished when animals were co-administered SAGEs (n = 6 mice per group).
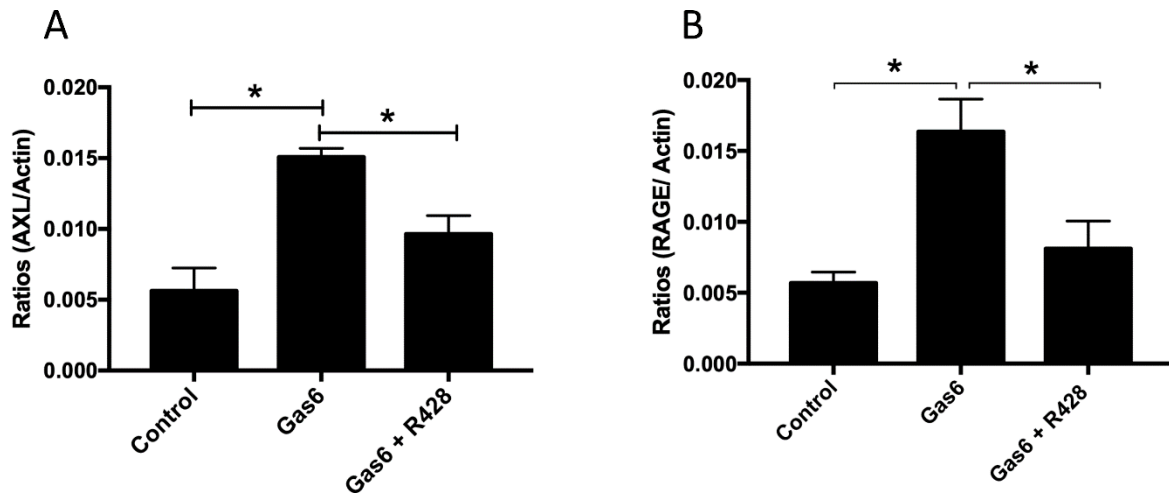
Figure A.7: AXL and RAGE Expression Following Gas6 Administration.

A, Immunoblotting for AXL was conducted in A549 cells following exposure to Gas6 or Gas6 + R428 for 24 hours. A marked increase in AXL protein expression was detected when cells were exposed to Gas6 and AXL and R428 co-treatment decreased Gas6-induced AXL expression. B, Immunoblotting for RAGE was also conducted in A549 cells following exposure to Gas6 or Gas6 + R428 for 24 hours. A marked increase in RAGE protein expression was detected in the presence of Gas6 and AXL targeting by R428 decreased Gas6-induced RAGE expression. Blots performed in triplicate were densitometrically normalized to β-actin and ratios are presented with $*p \leq 0.05$.
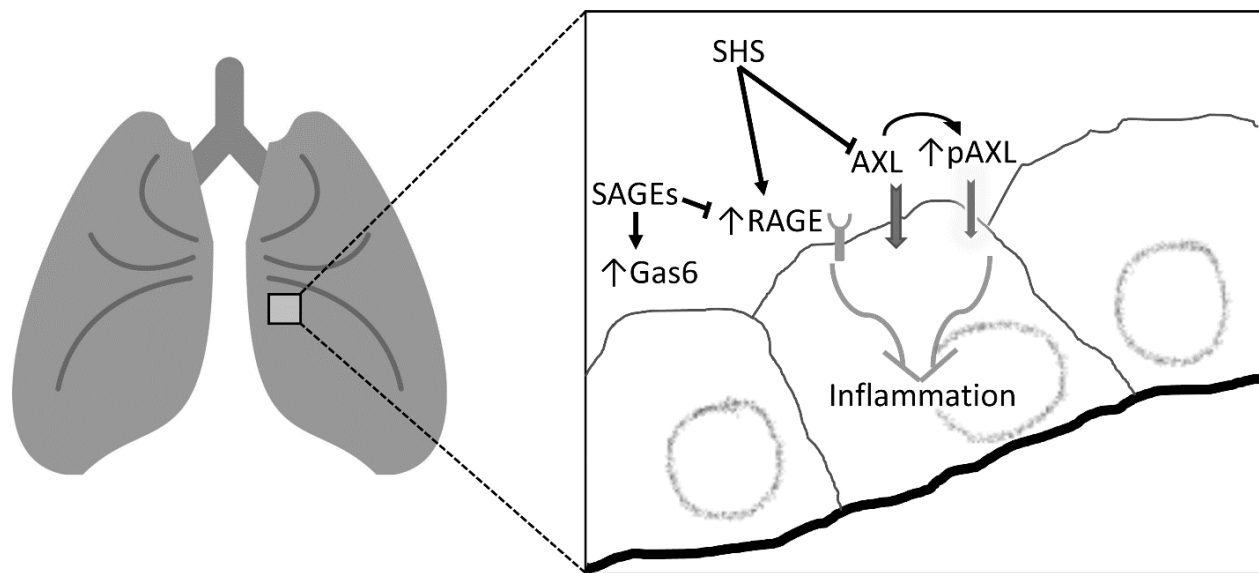
Figure A.8: Proposed Model for SHS Induced Alteration in RAGE and AXL Expression.

Downstream effects of exposure include diminished AXL expression but highly significant pAXL expression and markers of cellular inflammation.

References

Allen, M. P., Zeng, C., Schneider, K., Xiong, X., Meintzer, M. K., Bellosta, P., Wierman, M. E. (1999). Growth arrest-specific gene 6 (Gas6)/adhesion related kinase (Ark) signaling promotes gonadotropin-releasing hormone neuronal survival via extracellular signal-regulated kinase (ERK) and Akt. *Mol Endocrinol, 13*(2), 191-201. doi:10.1210/mend.13.2.0230

Awji, E. G., Seagrave, J. C., & Tesfaigzi, Y. (2015). Correlation of Cigarette Smoke-Induced Pulmonary Inflammation and Emphysema in C3H and C57Bl/6 Mice. *Toxicol Sci, 147*(1), 75-83. doi:10.1093/toxsci/kfv108

Berg, J., Halvorsen, A. R., Bengtson, M. B., Tasken, K. A., Maelandsmo, G. M., Yndestad, A. Helland, A. (2018). Levels and prognostic impact of circulating markers of inflammation, endothelial activation and extracellular matrix remodelling in patients withlung cancer and chronic obstructive pulmonary disease. *BMC Cancer, 18*(1), 739. doi:10.1186/s12885-018-4659-0

Botelho, F. M., Bauer, C. M., Finch, D., Nikota, J. K., Zavitz, C. C., Kelly, A., Stampfli, M. R. (2011). IL-1alpha/IL-1R1 expression in chronic obstructive pulmonary disease and mechanistic relevance to smoke-induced neutrophilia in mice. *PloS one, 6*(12), e28457. doi:10.1371/journal.pone.0028457

Brunelleschi, S., Penengo, L., Santoro, M. M., & Gaudino, G. (2002). Receptor tyrosine kinases as target for anti-cancer therapy. *Curr Pharm Des, 8*(22), 1959-1972. Retrieved from https://www.ncbi.nlm.nih.gov/pubmed/12171522

Brusselle, G. G., Joos, G. F., & Bracke, K. R. (2011). New insights into the immunology of chronic obstructive pulmonary disease. *Lancet, 378*(9795), 1015-1026. doi:10.1016/S0140-6736(11)60988-4

Carolan BJ, H. G., Morrow J, Hersh CP, O'Neal WK, Rennard S, Pillai SG, Belloni P, Cockayne DA, Comellas AP, Han M, Zemans RL, Kechris K, Bowler RP. (2014). The association of plasma biomarkers with computed tomography-assessed emphysema phenotypes. *Respir Res, 15*, 127.

Carp, H., & Janoff, A. (1978). Possible mechanisms of emphysema in smokers. In vitro suppression of serum elastase-inhibitory capacity by fresh cigarette smoke and its prevention by antioxidants. *Am Rev Respir Dis, 118*(3), 617-621. Retrieved from http://www.ncbi.nlm.nih.gov/pubmed/101105

Cerami, C., Founds, H., Nicholl, I., Mitsuhashi, T., Giordano, D., Vanpatten, S., . . . Cerami, A. (1997). Tobacco smoke is a source of toxic reactive glycation products. *Proc Natl AcadSci U S A, 94*(25), 13915-13920.

Chen L, W. T., Guo L, Shen Y, Yang T, Wan C, Liao Z, Xu D, Wen F. (2014). Overexpression of RAGE contributes to cigarette smoke-induced nitric oxide generation in COPD. *Lung, 192*(2), 267-275.

Courtney, R. (2015). The Health Consequences of Smoking—50 Years of Progress: A Report of the Surgeon General, 2014 Us Department of Health and Human Services Atlanta, GA: Department of Health and Human Services, Centers for Disease Control and Prevention, National Center for Chronic Disease Prevention and Health Promotion, Office on Smoking and Health, 2014 1081 pp. Online (grey literature): http://www. surgeongeneral. gov/library/reports/50-years-of-progress. *Drug and Alcohol Review, 34*(6), 694-695.

Crosby, L. M., & Waters, C. M. (2010). Epithelial repair mechanisms in the lung. *Am J Physiol Lung Cell Mol Physiol, 298*(6), L715-731. doi:10.1152/ajplung.00361.2009

Dinarello, C. A. (2009). Immunological and inflammatory functions of the interleukin-1 family. *Annu Rev Immunol, 27*, 519-550. doi:10.1146/annurev.immunol.021908.132612

Ford, E. S. (2015). Hospital discharges, readmissions, and ED visits for COPD or bronchiectasis among US adults: findings from the nationwide inpatient sample 2001-2012 and Nationwide Emergency Department Sample 2006-2011. *Chest, 147*(4), 989-998. doi:10.1378/chest.14-2146

Ford, E. S., Croft, J. B., Mannino, D. M., Wheaton, A. G., Zhang, X., & Giles, W. H. (2013). COPD surveillance--United States, 1999-2011. *Chest, 144*(1), 284-305. doi:10.1378/chest.13-0809

Fridell, Y. W., Jin, Y., Quilliam, L. A., Burchert, A., McCloskey, P., Spizz, G., . . . Liu, E. T. (1996). Differential activation of the Ras/extracellular-signal-regulated protein kinase pathway is responsible for the biological consequences induced by the AXL receptor tyrosine kinase. *Mol Cell Biol, 16*(1), 135-145. doi:10.1128/mcb.16.1.135

Fujino, N., Kubo, H., & Maciewicz, R. A. (2017). Phenotypic screening identifies AXL kinase as a negative regulator of an alveolar epithelial cell phenotype. *Lab Invest, 97*(9), 1047-1062. doi:10.1038/labinvest.2017.52

Gao, L., Liu, X., Millstein, J., Siegmund, K. D., Dubeau, L., Maguire, R. L., . . . Breton, C. V. (2018). Self-reported prenatal tobacco smoke exposure, AXL gene-body methylation, and childhood asthma phenotypes. *Clin Epigenetics, 10*(1), 98. doi:10.1186/s13148-018-0532-x

Gao, L., Urman, R., Millstein, J., Siegmund, K. D., Dubeau, L., & Breton, C. V. (2018). Association between AXL promoter methylation and lung function growth during adolescence. *Epigenetics*, 1-12. doi:10.1080/15592294.2018.1529517

Goruppi, S., Chiaruttini, C., Ruaro, M. E., Varnum, B., & Schneider, C. (2001). Gas6 induces growth, beta-catenin stabilization, and T-cell factor transcriptional activation in contact-inhibited C57 mammary cells. *Mol Cell Biol, 21*(3), 902-915. doi:10.1128/MCB.21.3.902-915.2001

Guttridge, K. L., Luft, J. C., Dawson, T. L., Kozlowska, E., Mahajan, N. P., Varnum, B., & Earp, H. S. (2002). Mer receptor tyrosine kinase signaling: prevention of apoptosis and alteration of cytoskeletal architecture without stimulation or proliferation. *J Biol Chem, 277*(27), 24057-24066. doi:10.1074/jbc.M112086200

Hagstad, S., Bjerg, A., Ekerljung, L., Backman, H., Lindberg, A., Ronmark, E., & Lundback, B. (2014). Passive smoking exposure is associated with increased risk of COPD in never smokers. *Chest, 145*(6), 1298-1304. doi:10.1378/chest.13-1349

Higaki, M., Wada, H., Mikura, S., Yasutake, T., Nakamura, M., Niikura, M., . . . Takizawa, H. (2015). Interleukin-10 modulates pulmonary neutrophilic inflammation induced by cigarette smoke exposure. *Exp Lung Res, 41*(10), 525-534. doi:10.3109/01902148.2015.1096315

Hofmann, M. A., Drury, S., Fu, C., Qu, W., Taguchi, A., Lu, Y., . . . Nawroth, P. (1999). RAGE mediates a novel proinflammatory axis: a central cell surface receptor for S100/calgranulin polypeptides. *Cell, 97*(7), 889-901.

Jimenez, F. R., Belgique, S. T., Lewis, J. B., Albright, S. A., Jones, C. M., Howell, B. M., . . . Reynolds, P. R. (2015). Conditional pulmonary over-expression of Claudin 6 during embryogenesis delays lung morphogenesis. *Int J Dev Biol, 59*(10-12), 479-485. doi:10.1387/ijdb.150086pr

Ju, S. T., Sharma, R., Gaskin, F., & Fu, S. M. (2012). IL-2 controls trafficking receptor gene expression and Th2 response for skin and lung inflammation. *Clin Immunol, 145*(1), 82-88. doi:10.1016/j.clim.2012.07.015

Korshunov, V. A. (2012). AXL-dependent signalling: a clinical update. *Clin Sci (Lond), 122*(8), 361-368. doi:10.1042/CS20110411

Laskin, D. L., Sunil, V. R., Fakhrzadeh, L., Groves, A., Gow, A. J., & Laskin, J. D. (2010). Macrophages, reactive nitrogen species, and lung injury. *Ann N Y Acad Sci, 1203*, 60-65. doi:10.1111/j.1749-6632.2010.05607.x

Laurance, S., Lemarié, C. A., & Blostein, M. D. (2012). Growth arrest-specific gene 6 (gas6) and vascular hemostasis. *Advances in nutrition, 3*(2), 196-203.

Lewis, J. B., Hirschi, K. M., Arroyo, J. A., Bikman, B. T., Kooyman, D. L., & Reynolds, P. R. (2017). Plausible Roles for RAGE in Conditions Exacerbated by Direct and Indirect (Secondhand) Smoke Exposure. *International journal of molecular sciences, 18*(3), 652.

Lewis, J. B., Mejia, C., Jordan, C., Monson, T. D., Bodine, J. S., Dunaway, T. M., Arroyo, J. A. (2017). Inhibition of the receptor for advanced glycation end-products (RAGE) protects from secondhand smoke (SHS)-induced intrauterine growth restriction IUGR in mice. *Cell Tissue Res, 370*(3), 513-521. doi:10.1007/s00441-017-2691-z

Li, D., Lei, C., Zhang, S., Zhang, S., Liu, M., & Wu, B. (2015). Blockade of high mobility group box-1 signaling via the receptor for advanced glycation end-products ameliorates inflammatory damage after acute intracerebral hemorrhage. *Neurosci Lett, 609*, 109-119. doi:10.1016/j.neulet.2015.10.035

Li Y, Y. C., Ma G, Gu X, Chen M, Chen Y, Zhao B, Cui L, Li K. (2014). Association of polymorphisms of the receptor for advanced glycation end products gene with COPD in the Chinese population. *DNA Cell Biol, 33*(4), 251-258.

Lindenauer, P. K., Grosso, L. M., Wang, C., Wang, Y., Krishnan, J. A., Lee, T. A., Drye, E. E. (2013). Development, validation, and results of a risk-standardized measure of hospital 30-day mortality for patients with exacerbation of chronic obstructive pulmonary disease. *J Hosp Med, 8*(8), 428-435. doi:10.1002/jhm.2066

Lomborg, B. (2013). *Global Problems, Smart Solutions: Costs and Benefits*.

Manfioletti, G., Brancolini, C., Avanzi, G., & Schneider, C. (1993). The protein encoded by a growth arrest-specific gene (gas6) is a new member of the vitamin K-dependent proteins related to protein S, a negative coregulator in the blood coagulation cascade. *Mol Cell Biol, 13*(8), 4976-4985. doi:10.1128/mcb.13.8.4976

Mark, M. R., Scadden, D. T., Wang, Z., Gu, Q., Goddard, A., & Godowski, P. J. (1994). rse, a novel receptor-type tyrosine kinase with homology to AXL/Ufo, is expressed at high levels in the brain. *J Biol Chem, 269*(14), 10720-10728. Retrieved from https://www.ncbi.nlm.nih.gov/pubmed/7511603

Moritsugu, K. P. (2007). The 2006 Report of the Surgeon General: the health consequences of involuntary exposure to tobacco smoke. *Am J Prev Med, 32*(6), 542-543. doi:10.1016/j.amepre.2007.02.026

Nicholl, I. D., & Bucala, R. (1998). Advanced glycation endproducts and cigarette smoking. *Cell Mol Biol (Noisy-le-grand), 44*(7), 1025-1033.

Pauwels, N. S., Bracke, K. R., Dupont, L. L., Van Pottelberge, G. R., Provoost, S., Vanden Berghe, T., . . . Brusselle, G. G. (2011). Role of IL-1alpha and the Nlrp3/caspase-1/IL-1beta axis in cigarette smoke-induced pulmonary inflammation and COPD. *Eur Respir J, 38*(5), 1019-1028. doi:10.1183/09031936.00158110

Pendino, K. J., Shuler, R. L., Laskin, J. D., & Laskin, D. L. (1994). Enhanced production of interleukin-1, tumor necrosis factor-alpha, and fibronectin by rat lung phagocytes following inhalation of a pulmonary irritant. *Am J Respir Cell Mol Biol, 11*(3), 279-286. doi:10.1165/ajrcmb.11.3.8086166

Reynolds, P. R., Kasteler, S. D., Cosio, M. G., Sturrock, A., Huecksteadt, T., & Hoidal, J. R. (2008). RAGE: developmental expression and positive feedback regulation by Egr-1 during cigarette smoke exposure in pulmonary epithelial cells. *Am J Physiol Lung Cell Mol Physiol, 294*(6), L1094-1101. doi:10.1152/ajplung.00318.2007

Reynolds, P. R., Mucenski, M. L., Le Cras, T. D., Nichols, W. C., & Whitsett, J. A. (2004). Midkine is regulated by hypoxia and causes pulmonary vascular remodeling. *J BiolChem, 279*(35), 37124-37132. doi:10.1074/jbc.M405254200

Reynolds, P. R., Stogsdill, J. A., Stogsdill, M. P., & Heimann, N. B. (2011). Up-regulation of receptors for advanced glycation end-products by alveolar epithelium influences cytodifferentiation and causes severe lung hypoplasia. *Am J Respir Cell Mol Biol, 45*(6), 1195-1202. doi:10.1165/rcmb.2011-0170OC

Rinaldi, M., Maes, K., De Vleeschauwer, S., Thomas, D., Verbeken, E. K., Decramer, M., . . . Gayan-Ramirez, G. N. (2012). Long-term nose-only cigarette smoke exposure induces emphysema and mild skeletal muscle dysfunction in mice. *Dis Model Mech, 5*(3), 333-341. doi:10.1242/dmm.008508

Robinson, A., Stogsdill, J., Lewis, J., Wood, T., & Reynolds, P. (2012). RAGE and tobacco smoke: insights into modeling chronic obstructive pulmonary disease. *Frontiers in Physiology, 3*(301). doi:10.3389/fphys.2012.00301

Sambamurthy, N., Leme, A. S., Oury, T. D., & Shapiro, S. D. (2015). The receptor for advanced glycation end products (RAGE) contributes to the progression of emphysema in mice. *PloS one, 10*(3), e0118979.

Schmidt, A. M., & Stern, D. M. (2000). RAGE: a new target for the prevention and treatment of the vascular and inflammatory complications of diabetes. *Trends in Endocrinology & Metabolism, 11*(9), 368-375.

Schmidt, A. M., Yan, S. D., Yan, S. F., & Stern, D. M. (2001). The multiligand receptor RAGE as a progression factor amplifying immune and inflammatory responses. *Journal of Clinical Investigation, 108*(7), 949-955. Retrieved from http://www.ncbi.nlm.nih.gov/pmc/articles/PMC200958/

Seemungal, T. A., Donaldson, G. C., Bhowmik, A., Jeffries, D. J., & Wedzicha, J. A. (2000). Time course and recovery of exacerbations in patients with chronic obstructivepulmonary disease. *Am J Respir Crit Care Med, 161*(5), 1608-1613. doi:10.1164/ajrccm.161.5.9908022

Shibata, T., Habiel, D. M., Coelho, A. L., Kunkel, S. L., Lukacs, N. W., & Hogaboam, C. M. (2014). AXL receptor blockade ameliorates pulmonary pathology resulting from primary viral infection and viral exacerbation of asthma. *J Immunol, 192*(8), 3569-3581. doi:10.4049/jimmunol.1302766

Sjoding, M. W., & Cooke, C. R. (2014). Readmission penalties for chronic obstructive pulmonary disease will further stress hospitals caring for vulnerable patient populations. *Am J Respir Crit Care Med, 190*(9), 1072-1074. doi:10.1164/rccm.201407-1345LE

Sparvero, L. J., Asafu-Adjei, D., Kang, R., Tang, D., Amin, N., Im, J., . . . Zeh, H. J. (2009). RAGE (Receptor for Advanced Glycation Endproducts), RAGE ligands, and their role in cancer and inflammation. *Journal of translational medicine, 7*(1), 17.

Stogsdill, M. P., Stogsdill, J. A., Bodine, B. G., Fredrickson, A. C., Sefcik, T. L., Wood, T. T., Reynolds, P. R. (2013). Conditional overexpression of receptors for advanced glycation end-products in the adult murine lung causes airspace enlargement and induces inflammation. *Am J Respir Cell Mol Biol, 49*(1), 128-134. doi:10.1165/rcmb.2013-0013OC

Strzelak, A., Ratajczak, A., Adamiec, A., & Feleszko, W. (2018). Tobacco Smoke Induces and Alters Immune Responses in the Lung Triggering Inflammation, Allergy, Asthma and Other Lung Diseases: A Mechanistic Review. *Int J Environ Res Public Health, 15*(5). doi:10.3390/ijerph15051033

Taguchi, A., Blood, D. C., Del Toro, G., & Canet, A. (2000). Blockade of RAGE-amphoterin signalling suppresses tumour growth and metastases. *Nature, 405*(6784), 354.

Thornalley, P. J. (1998). Cell activation by glycated proteins. AGE receptors, receptor recognition factors and functional classification of AGEs. *Cell Mol Biol (Noisy-le-grand), 44*(7), 1013-1023. Retrieved from http://www.ncbi.nlm.nih.gov/pubmed/9846883

Wang, Y., Jia, M., Yan, X., Cao, L., Barnes, P. J., Adcock, I. M., . . . Yao, X. (2017). Increased neutrophil gelatinase-associated lipocalin (NGAL) promotes airway remodelling in chronic obstructive pulmonary disease. *Clin Sci (Lond), 131*(11), 1147-1159. doi:10.1042/CS20170096

Waseda K, M. N., Taniguchi A, Kurimoto E, Ikeda G, KogaH, Fujii U, Yamamoto Y, Gelfand EW, Yamamoto H, Tanimoto M, and Kanehiro A. (2015). Emphysema requires the receptor for advanced glycation end-products triggering on structural cells. *Am J Respir Cell Mol Biol, 52*(4), 482-491.

Winden, D. R., Barton, D. B., Betteridge, B. C., Bodine, J. S., Jones, C. M., Rogers, G. D., Reynolds, P. R. (2014). Antenatal exposure of maternal secondhand smoke (SHS)increases fetal lung expression of RAGE and induces RAGE-mediated pulmonaryinflammation. *Respir Res, 15*, 129. doi:10.1186/s12931-014-0129-7

Winden DR, B. D., Betteridge BC, Bodine JS, Jones CM, Rogers GD, Chavarria M, Wright AJ, Jergensen ZR, Jimenez FR, and Reynolds PR (2014). Antenatal exposure of maternal secondhand smoke (SHS) increases fetal lung expression of RAGE and induces RAGE-mediated pulmonary inflammation. *Respir Res, 15*(1), 129.

Winden, D. R., Ferguson, N. T., Bukey, B. R., Geyer, A. J., Wright, A. J., Jergensen, Z. R., . . . Reynolds, P. R. (2013). Conditional over-expression of RAGE by embryonic alveolar epithelium compromises the respiratory membrane and impairs endothelial cell differentiation. *Respir Res, 14*, 108. doi:10.1186/1465-9921-14-108

Wood TT, W. D., Marlor DR, Wright AJ, Jones CM, Chavarria M, Rogers GD, and Reynolds PR (2014). Acute secondhand smoke-induced pulmonary inflammation is diminished in RAGE knock out mice. *AJP: Lung Cell Mol Physiol., 307*(10), E919-927.

Wood, T. T., Winden, D. R., Marlor, D. R., Wright, A. J., Jones, C. M., Chavarria, M., Reynolds, P. R. (2014). Acute secondhand smoke-induced pulmonary inflammation is diminished in RAGE knockout mice. *American Journal of Physiology-Lung Cellular and Molecular Physiology, 307*(10), L758-L764.

World Health Organization. (2011). WHO urges more countries to require large, graphic health warnings on tobacco packaging: the WHO report on the global tobacco epidemic, 2011 examines anti-tobacco mass-media campaigns. . *Central European Journal of Public Health*(19), 133, 151.

Yan, S. D., Chen, X., Fu, J., Chen, M., Zhu, H., Roher, A., . . . Schmidt, A. M. (1996). RAGE and amyloid-beta peptide neurotoxicity in Alzheimer's disease. *Nature, 382*(6593), 685-691. doi:10.1038/382685a0

Zhang, J., Xu, X., Rao, N. V., Argyle, B., McCoard, L., Rusho, W. J., . . . Krueger, G. (2011). Novel sulfated polysaccharides disrupt cathelicidins, inhibit RAGE and reduce cutaneous inflammation in a mouse model of rosacea. *PloS one, 6*(2), e16658.

Zhang Y, L. S., Wang G, Han D, Xie X, Wu Y, Xu J, Lu J, Li F, Li M. (2014). Changes of HMGB1 and sRAGE during the recovery of COPD exacerbation. *J Thorac Dis, 6*(6),734-741.

APPENDIX B: Cell Invasion, RAGE Expression and Inflammation
in Oral Squamous Cell Carcinoma (OSCC) Cells
Exposed to E-Cigarette Flavoring

Kary Ya Fang Tsai[1], Kelsey M. Hirschi Budge[1], Anthony P. Lepre[2], Michael S. Rhees[2], Janet Ajdaharian[2], Jordan Geller[2], Daniel G. Epperson[2], Kolten J. Astle[2], Duane R. Winden[2], Juan A. Arroyo[1], and Paul R. Reynolds[1]

[1]Lung and Placenta Research Laboratory, Department of Physiology and Developmental Biology,Brigham Young University, Provo, UT, USA.

[2]College of Dental Medicine, Roseman University of Health Sciences, South Jordan, UT, USA.

Corresponding Author:
Paul R. Reynolds,
Ph.D. Brigham
Young University
Department of Physiology and Developmental
Biology3054 Life Sciences Building
Provo, UT 84602
Phone: (801) 422-1933; Fax: (801) 422-0700
E-mail: paul_reynolds@byu.edu

Abstract

Electronic cigarettes have given rise to a new, largely unregulated market within the smoking industry. While generally supposed to be less harmful than traditional tobacco smoke, awareness of the toxicity of electronic cigarette liquid is still scarce. Our objective was to determine the impact of electronic cigarette flavoring and nicotine on gingival squamous cell carcinoma invasion, RAGE expression and the elaboration of pro-inflammatory molecules.

Gingival and tongue squamous cell carcinoma cells were exposed to Red Hot or Green Apple flavored electronic cigarette flavoring with or without nicotine. Immunofluorescence determined RAGE expression. Real time cellular invasion was assessed using a RTCA DP instrument. Culture medium was assayed for cytokine secretion. Compared to controls we observed: increased cell invasion in gingival cells with Red Hot electronic cigarette flavoring and decreased cell invasion with Green Apple; decreased cell invasion in tongue cells treated with Red Hot electronic cigarette flavoring and no differences in invasion with Green Apple; flavor and nicotine dependent increases in RAGE expression; and differential expression of IL-1α, IL-8, and MMP-13.

We conclude that electronic cigarette flavoring and nicotine orchestrate differential regulation of oral squamous cell carcinoma cell invasion and inflammatory effects. This study provides an important initial step in dissecting RAGE-mediated mechanisms of cancerous invasion and molecular avenues employed by oral squamous cell carcinoma.

141

Introduction

Electronic Cigarette (eCig) use has increased dramatically during the last several years. Numerous reports have sought to establish these products as safer to use than conventional cigarettes.(Pisinger, Godtfredsen, & Bender, 2019; Pisinger & Mackay, 2019) The increased use is further attributed to the notion that eCig prevents the adverse effects of combustible cigarettes and may be pursued as a means that assists smokers in their cessation efforts.(Alzahrani, Pena, Temesgen, & Glantz, 2018) eCigs are hand-held electronic devices that generate vapors or aerosols from e-cigarette liquid (eCig liquid) without combustion.(Chen, Todd, & Fairclough, 2019) eCig liquid usually contains a mixture of propylene glycol, glycerin, nicotine and flavors.(Alzahrani et al., 2018; Uchiyama et al., 2016) Although they are increasing in their popularity, the World Health organization (WHO) regard the use of eCigs as harmful and does not recommend their ongoing use.(Chen et al., 2019; Pisinger et al., 2019; Pisinger & Mackay, 2019) Previous experimental results showed that eCigs with flavorings caused increased oxidative/carbonyl stress, increased inflammatory cytokine release, increase receptor for advanced glycation end products (RAGE) expression, and increased apoptosis in human gingival cells.(Rouabhia et al., 2017; Sundar, Javed, Romanos, & Rahman, 2016)

The receptor for advanced glycation end-products (RAGE) is a pattern-recognition cell-surface receptor that experiences increased expression during exposure to tobacco smoke.(Chapman et al., 2018; Robinson, Stogsdill, Lewis, Wood, & Reynolds, 2012; Winden et al., 2014) Expression of RAGE has been detected in gingival tissues from human subjects with chronic periodontitis and it is overexpressed in gingival tissues from smokers diagnosed with

periodontal diseases.(Chapman et al., 2018) RAGE receptor availability is implicated in the pathogenesis of many inflammatory diseases and more recently, it's been shown to be involved in the invasion of oral squamous cell carcinoma (OSCC) (Bhawal et al., 2005; Chapman et al., 2018).

In the current research endeavor, we examined the effects of two common eCig flavors, sweet apple and cinnamaldehyde, with or without nicotine, on OSCC invasiveness and the effect of exposure on RAGE expression. We also tested the inflammatory profiles of exposure via the assessment of elaborated mediators into cell culture media. OSCC encompasses up to 90% of all oral cancers and affects more than 400 000 individuals yearly (Chapman et al., 2018). OSCC is one of the most prevalent cancers in developing countries with recurrence rates that approach approximately 50%, and its progression is affected by environmental factors including cigarette smoke and alcohol. (Bavle, Venugopal, Konda, Muniswamappa, & Makarla, 2016; Blatt et al., 2017) Tobacco alone is well recognized as one of the major causes of the development of oral cancer (Nagaraj & Zacharias, 2007) and work in our lab demonstrated that secondhand smoke increases OSCC invasion in a RAGE dependent manner.(Chapman et al., 2018) The current project expands the invasive attributes of OSCC by seeking to understand eCig-mediated invasion and inflammation possibly orchestrated by the induction of RAGE.

Materials and Methods

Cell Culture and Treatments

Ca9-22 oral squamous carcinoma cells and CAL-27 human tongue squamous carcinoma cells were used in these experiments (both from ATTC, Manassas, VA). Cells were cultured in RPMI medium (Mediatech, Manassas, VA) supplemented with 10% fetal bovine serum (FBS)

and 1% penicillin and streptomycin. Both cell lines were incubated for 24 hours in medium alone (control), medium supplemented with 2% Cinnamon Red Hots (Red Hot, 8Ohm1, Inc., Ogden, UT) or Reds Apple Juice (Green Apple, Daze Mfg., Los Angeles, CA) eCig liquid in the presence or absence of 6mg of nicotine. A dose curve was pursued and a dose of 2% for both types of eCig liquid exerted changes without affecting cell behavior (data not shown). For invasion studies, cells were detached, and 20,000 cells/mL were incubated in 2% FBS mediumalone, or medium supplemented with 2% eCig liquid in the presence or absence of nicotine.

Real-time Cell Invasion

Real-time cell invasion was determined following the various treatments. An xCELLigence RTCA cell monitoring system was utilized to determine real time invasion of cellsthrough adherence to the protocol suggested by the manufacturer (ACEA Biosciences, Blue Springs, MO, USA). Briefly, invasion was assessed in 16 well CIM-Plates (n= 10 individual cellcultures per treatment; ACEA Biosciences, Blue Springs, MO, USA). The top wells were coatedwith a 1:40 matrigel concentration (Fisher Scientific, Pittsburg, PA) and cells were plated in the top chamber at a concentration of 20,000 cells/well in 2% FBS RPMI with total volume of 100µL in the presence or absence of eCig liquid in the presence or absence of nicotine. The bottom chamber wells were filled with 160 µL of 10% FBS RPMI. The cells were then placed inthe xCELLigence RTCA instrument and invasion readings were completed every 15 minutes for24 hours. Invasive cells were obtained and expressed as cell invasion index.

Immunofluorescence

Immunofluorescence (IF) was performed to determine the localization of RAGE in treated and untreated cells. Slides were incubated overnight with antibody against RAGE (Cell Signaling Technology, Danvers, MA, USA) or an immunoglobulin G1-negative control (JacksonLaboratories, West Grove, PA). Slides were incubated with a Texas red-conjugated secondary

for 1 h and then 4, 6-diamidino-2-phenylindole dihydrochloride (DAPI) for nuclear counterstaining prior to mounting with glass coverslips. Slides were viewed with the appropriateexcitation and emission rhodamine filter.

Periodontal Inflammatory Cytokine Assessment

Medium from treated and control cells were screened using the multiplex Human Cytokine 17-plex Magnetic Bead Kit (EMD Millipore, Billerica, MA). The Milliplex assay was performed as previously described[19]. Beads and the appropriate detection antibodies are includedin the Milliplex Multiplex Assay kit and were added to the control or treated conditioned media. The samples were incubated with antibody-conjugated magnetic beads overnight at 4°C. Bead- complexes were then read on a Magpix multiplex platform (Luminex Corporation, Austin, TX). Median fluorescent values were recorded from a minimum of 80 beads used in the data analysis.Standard curves and data analysis were performed using Milliplex Analyst 5.1 software (Millipore Corporation, Billerica, MA).

Statistical Analysis

Results were checked for normality and data were shown as means ± SE. Differences in cell invasion and cytokine protein expression were determined between

control and treated cells.Mann-Whitney tests were used to compare changes among the cytokines and for differences in invasion indexes. Significant differences between groups were noted at $p < 0.05$. Statistical analysis was completed with GraphPad Prism 7.0 software.

Results

E-Cig Liquid and OSCC Invasion

We first investigated the effects of eCig liquid on OSCC cell invasion. We observed thatthe addition of 2% Green Apple eCig liquid significantly reduced cell invasion (2.7-fold; $p<0.0002$) in Ca9-22 cells (Figure B.1A). The addition of nicotine to the media resulted in some improvement (35%, 1.7-fold; $p<0.0002$) despite the overall decrease in invasion observed in these cells when treated with 2% Green Apple liquid alone (Figure B.1A). In contrast, treatment ofCa9-22cells with 2% Red Hot significantly increased invasion (3.6-fold; $p<0.0002$). Interestingly, increased invasion mediated by Red Hot was decreased (30%, 2.3-fold; $p<0.0002$)with the inclusion of nicotine to the 2% Red Hot eCig liquid (Figure B.1B).

Treatment of CAL-27 tongue squamous cells with 2% Green Apple did not affect cell invasion in either the presence or absence of nicotine (Figure B.2A). Unlike 2% Green Apple, weobserved decreased cell invasion (1.44-fold; $p<0.002$) in the CAL-27 tongue squamous cells when treated with 2% Red Hot eCig liquid (Figure B.2B). Decreased invasion was modestly reduced(7%,1.3-fold; $p<0.002$) when nicotine was added to the 2% Red Hot treatment (Figure B.2B).

RAGE and Cytokine Release

Previous studies by our lab showed a role for RAGE in mediating invasion and inflammation of OSCC cells when exposed to smoke environments (Chapman et al., 2018; Sanders et al., 2017). We therefore investigated the expression of RAGE during eCig liquid treatment of Ca9-22 and CAL-27 carcinoma cells. Immunofluorescence demonstrated increased RAGE staining in Ca9-22 OSCC cells treated with 2% Green Apple or 2% Red Hot (Figure B.3A andB). This increase in RAGE expression was potentiated when nicotine was added to either eCig liquid (Figure B.3A and B). Similarly, RAGE staining was increased following treatment of CAL-27cells that was further potentiated when nicotine was added (Figure B.4A and B).

Prior studies implicate RAGE signaling in the modulation of inflammation via increased cytokine elaboration (Sanders et al., 2017). To determine to what extent cytokine release was regulated by eCig treatment, we performed protein assays that simultaneously screened key inflammatory cytokines observed during periodontal disease. The concentration of IFN-γ, IL-1β,IL-12, IL-4, IL-6, IL-10, IL-12, IL-17, MIP1-α, MMP-9, Osteoprotegerin, Osteopontin, Osteoactivin, RANK, TGFβ1 and TNFα released into cell culture media was below the levels of detection; thus, we were not able to accurately determine their concentrations in the media from either control or treated cells. In the Ca9-22 cells, IL-1α was significantly increased (54- fold; $p<0.02$) when cells were treated with 2% Green Apple when compared to controls (Figure B.5A). The addition of nicotine to Green Apple treatment reduced the expression of this cytokine by 93% (3.4-fold increase; $p<0.02$, Figure B.5A). Treatment of Ca9-22 with 2% Red Hot demonstrated a very significant increase (580-fold; $p<0.02$) of IL-1α when compared to

controls (Figure B.5A). When nicotine was added to the 2% Red Hot media, the increased IL-1α was reduced by 95% (28-fold; p<0.02, Figure B.5A). IL-8 secretion was increased (2.2-fold; p<0.002) by treatingCa9-22 cells with 2% Green Apple alone (Figure B.5B). In contrast, when nicotine was added to the cells in 2% Green Apple, IL-8 was decreased (3.3-fold; p<0.002) when compared to controls (Figure B.5B). Interestingly IL-8 secretion was below detection in the 2% Red Hot treated Ca9-22 cells (Figure B.5B). MMP-13 levels were decreased by 2% Green Apple treatment (1.2-fold increase;p<0.03) in Ca9-22 cells (Figure B.5C). When nicotine was added this small decrease was reversed to basal levels observed in controls (Figure B.5C).

Treatment of the CAL-27 tongue squamous cells with 2% Green Apple showed increased IL-1α (3.6-fold; p<0.02) when compared to controls (Figure B.5D). The addition of nicotine to the 2%Green Apple did not affect IL-1α secretion levels by these cells (3.8-fold; p<0.02). Similarly, treatment of CAL-27 cells with 2% Red Hot alone increased IL-1α (17.8-fold; p<0.02) when compared to controls (Figure B.5D). Interestingly, addition of nicotine reduced IL-1α levels by 52% (8.5-fold increase; p<0.02) compared to the treatment of 2% Red Hot alone (Figure B.5D). IL-8 levelswere mildly increased (1.1-fold; p<0.04) in CAL-27 cells that were treated with 2% Green Apple and this increase was not affected when nicotine was added (Figure B.5E). When CAL-27 cells were treated with 2% Red Hot, IL-8 levels were decreased (1.2-fold; p<0.04) when compared to control cells (Figure B.5E). This decrease was potentiated (3.2-fold; p<0.04) by the addition of nicotine (Figure B.5E). MMP-13 levels were reduced when CAL-27 cells were treated with 2% GreenApple in the absence (2.7-fold;

p<0.0001) or presence (2.9-fold; p< 0.001) of nicotine (Figure B.5F). Interestingly, MMP-13 secretion was below the detection limit in the 2% Red Hot treated CAL-27 cells (Figure B.5F).

Discussion

Although cigarette smoke is already among the top ten contributors to the worldwide health burden, eCigs are a phenomenon that has emerged in the United States during the last decade. Flavored eCig vaping is steadily rising and troubling trends for eCig use suggest an astonishing 1 out of 10 current adolescents regularly vape.(Kong & Krishnan-Sarin, 2017; Singhet al., 2016) While attempts to regulate eCig use are underway (Deeming Tobacco Products To Be Subject to the Federal Food, 2016), the World Health Organization has stated eCig vaping should not be recommended until its true toxicity profile and potential ill health effects have been properly vetted (World Health Organization, 2013). Such adverse health effects associated with eCig use include bronchitis, mouth/throat irritation, headaches, nausea, airway obstruction, bronchospasm, inflammation, and cardiovascular effects (elevated heart rate, blood pressure, andvessel stiffness) (Aberle, Abtin, & Brown, 2013; Etter, 2010; Gennimata SA, 2014; Polosa et al.,2014; Vansickel, Cobb, Weaver, & Eissenberg, 2010; Vardavas et al., 2012; Wang et al., 2018).

To determine the effects of eCig liquid and nicotine in OSCC progression, cell invasion was assessed in commonly studied OSCC cell lines. We measured invasion during exposure to two popular eCig liquids: Cinnamon Red Hots (Red Hot) or Reds Apple Juice (Green Apple) in the presence or absence of nicotine. In the Ca9-22 cells, we observed that invasion was increasedwhen cells were treated with Red Hot alone. In

contrast, cell invasion was decreased when cells were treated with Green Apple alone. These results suggest a flavor dependent effect in the regulation of cell invasion. As many use eCigs as an alternative means of nicotine exposure aside from traditional smoking, an understanding of nicotine related effects is essential. The addition of nicotine in the presence of Red Hot diminished the increased invasion observed in exposed cells. This was unexpected as these results suggest that perhaps the addition of nicotine exerted measurable protection of invasion in Ca9-22 cells treated with Red Hot. When nicotine was added to the Green Apple Ca9-22 treated cells, we observed a near reversal in the invasion index. Although these nicotine results were not capable of reversing invasion to basal levels, these data suggest that nicotine is a key variable of eCig use that must be further explored. Together these data suggest that different molecular means are plausibly involved in the regulation of these cancerous cells that are dependent on flavoring and the presence of nicotine.

In terms of the CAL-27 cells, we did not detect any effect in cell invasion when cells were treated with Green Apple in the presence or absence of nicotine. This was an unexpected difference compared to our observations of the Ca9-22 cells and perhaps this discovery is related to the previous observation that CAL-27 cells are tongue squamous cell carcinoma cells known to have non typical OSCC behaviors (Jiang et al., 2009). This alternative response compared to Ca9-22 cells was also observed when Red Hot was added to the CAL-27 cells. In this instance, invasion was decreased in the presence of eCig liquid alone and significantly recovered when nicotine was added to the cells. Previous studies in our lab has linked RAGE expression to both inflammation and the regulation of invasion during exposure of OSCC to smoke environments (Chapman et al.,

2018; Sanders et al., 2017). We observed detectible RAGE protein expression in both cell types via immunofluorescence staining. Interestingly we observed increased stainingfor RAGE with both eCig liquids in Ca9-22. This increase was further potentiated when nicotinewas added into the treatment. These data suggest the likelihood that RAGE correlates to pathways involved in the regulation of invasion in Ca9-22 cells. Similar results were observed for the CAL-27 tongue cells. These results collectively suggest that in both cell types, RAGE may be involved in alternative cell invasion indexes, dependent on the cell type, during eCig treatment. We anticipate performing follow up studies that target RAGE in order to elucidate to what extent RAGE availability modulates invasiveness. RAGE signaling generally involves the activation of several MAP kinases and the activation of NF-κB (Schmidt & Stern, 2001). To further determine RAGE involvement in these cells, investigations must also be conducted that assess these signaling intermediates as well as nuclear activation of NF-κB in treated cells as well as controls.

We detected increased inflammatory cytokines such as IL-1α and IL-8 when Ca9-22 were treated with either of the eCig liquids. IL-1α and IL-1β are products of distinct genes but are similar in their modulation of inflammation. Both bind the same receptor and are upregulatedduring an inflammatory response. IL-8 is a heparin binding member of the alpha, or CXC family of chemokines. In addition of pro-inflammatory effects, IL-8 oligomerizes and binds G-proteincoupled receptors to enhance angiogenesis during pathologies including cancer. The observed increases in both IL-1α and IL-8 were reduced when nicotine was added in these cells. However, MMP-13 was decreased with Apple Green treatment and not detectable in Red Hot treated Ca9-22 cells. MMPs,

including MMP-13, are zinc and calcium dependent endopeptidasesthat degrade extracellular matrix. MMP-13 specifically has been shown to degrade aggrecans and diverse collagens while functioning during cell-matrix interactions. Cell-matrix interactions are key during invasion. Together with the RAGE immunofluorescence, differential cytokine elaboration suggests that RAGE expression may be involved in the development of inflammationand less so during the regulation of invasion in Ca9-22 cells. Importantly, nicotine treatment seemed to have a marginally protective role for inflammation created by both eCig liquids. This protective role of nicotine has been observed in other diseases and it is suggested to be orchestrated by regulating cytokine expression (Lakhan & Kirchgessner, 2011; Piao et al., 2009).To our knowledge, this protection has not previously been shown during OSCC progression in humans. In the CAL-27 cells, we observed increased IL-1α when cells were treated with both eCig liquids. Interestingly, nicotine did not affect the levels of this cytokine in the Green Apple treated cells. In contrast a significant decrease of IL-1α was observed in cells treated with Red Hot. These results suggest a divergent signaling pathway may be initiated in these cells in a flavor dependent manner; however, RAGE augmentation still suggests RAGE participation. Furthermore, it seems that nicotine protection is also flavor dependent in the CAL-27 cells. IL-8 was mildly increased during Green Apple treatment and was not affected by nicotine addition. Incontrast, Red Hot induced a significant increase of IL-8 that was not reversed by the addition of nicotine. MMP-13 was decreased in these cells treated with Green Apple and below the detectionlimit when cells were treated with Red Hot.

In general, our experiments suggest that different eCig flavors can alternatively affect OSCCs making it difficult to determine specific effects and/or consequences of eCig use. We demonstrate the plausibility that RAGE availability correlates with eCig-mediated invasion and inflammation. Additional studies are critically needed to further identify the relationship betweenRAGE signaling and the pathological behavior of OSCC cells during exposure. Such studies should include RAGE targeting and downstream effects in terms of both signaling intermediates and functional molecule elaboration. Such an undertaking would clarify the molecular underpinning of exposing OSCC cells to vaporized eCig liquids and resulting invasiveness and inflammatory signaling.

Declarations

Conflict of Interest and Ethical Statement: The authors report no conflict of interest. Ethics committee/institute approval was not required because established cell lines were used for these experiments
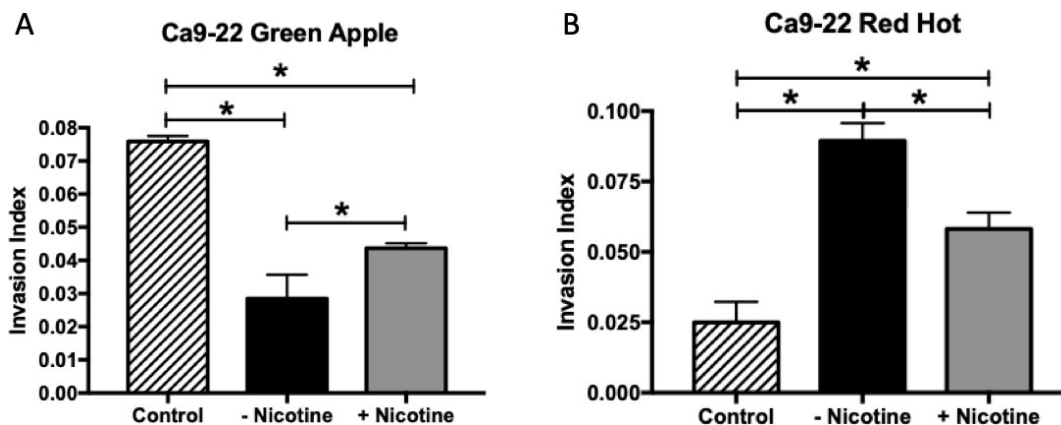
Figure B.1: Ca9-22 Invasion with Exposure to Green Apple or Red Hot eCig Liquid.

The addition of 2% Green Apple eCig liquid (A) significantly reduced cell invasion in the Ca9-22 OSCC cells. This reduction in invasiveness significantly improved with the addition of nicotine. The addition of 2% Red Hot significantly increased invasion of Ca9-22 cells (B). Increased invasion induced by the flavoring alone was improved when nicotine was included in the Red Hot flavoring (B). Invasion experiments were conducted with an n = 10 as outlined in the Methods section and statistically different values are noted as *$P < .05$.

Figure B.2: CAL-27 Invasion with Exposure to Green Apple or Red Hot eCig Liquid.

Green Apple eCig liquid did not affect CAL-27 cell invasion regardless of the presence or absence of nicotine (A). Red Hot eCig liquid reduced CAL-27 invasion which was mildly rescued with the addition nicotine (B). Invasion experiments were conducted in triplicate as outlined in the Methods section and statistically different values are noted as *$P < .05$.
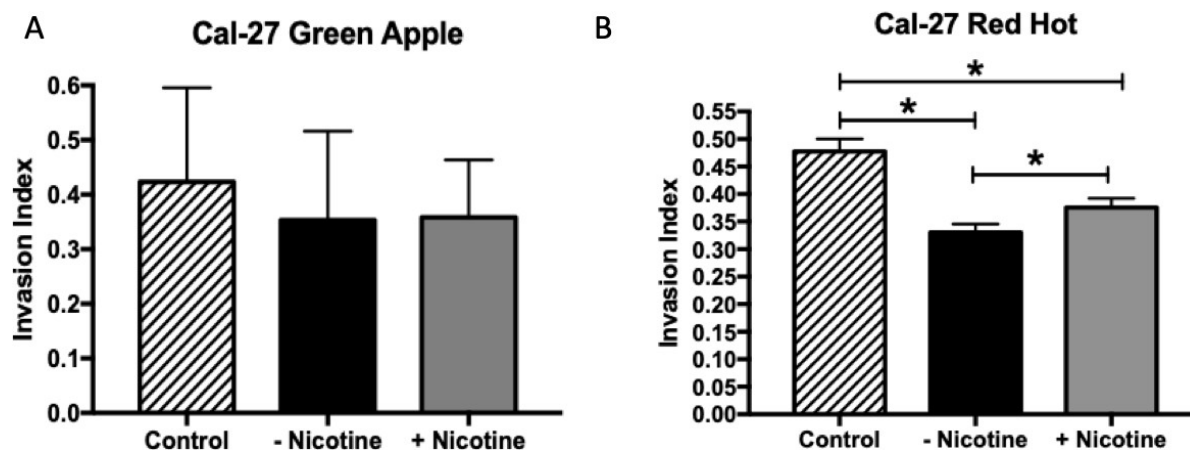
155

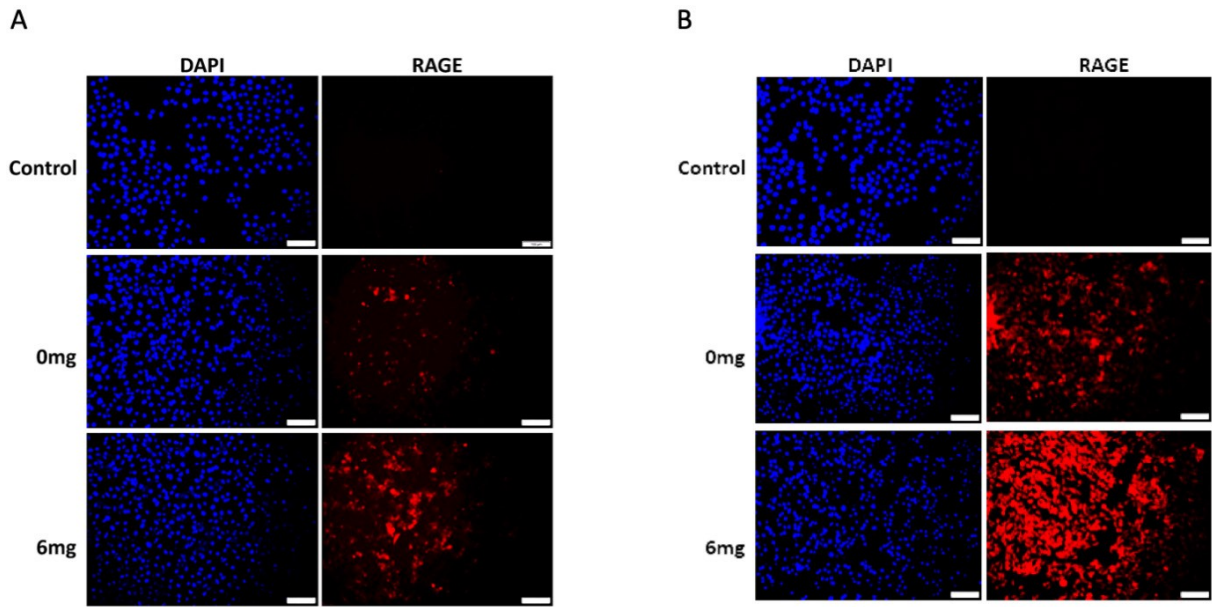Figure B.3: RAGE Expression by Ca9-22 Cells Treated with eCig Liquid.

Cells exposed to Green Apple (A) or Red Hot (B) both increased RAGE expression. Increased RAGE expression was further enhanced when nicotine was included with the eCig flavoring. Experiments were conducted in triplicate and Images (200x original magnification) are representative of the conducted cell culture experiments. Scale bars represent 100 μm.
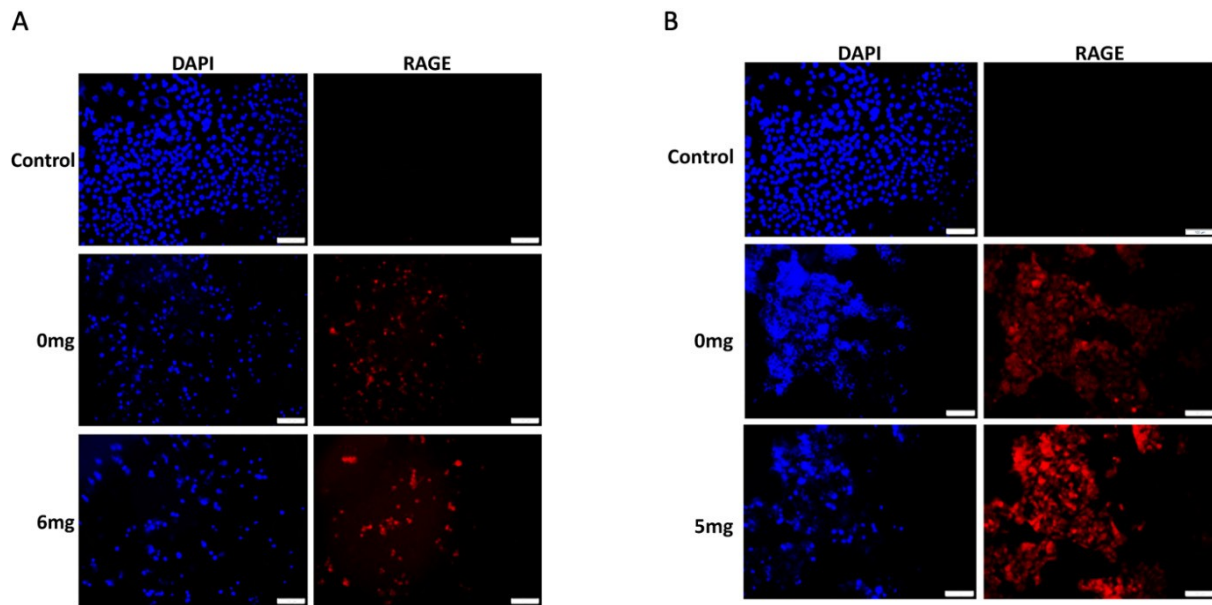
Figure B.4: RAGE Expression by CAL-27 Cells Treated with eCig Liquid.

Cells exposed to Green Apple (A) induced a moderate up-regulation of RAGE expression and CAL-27 cells exposed to Green Apple liquid plus nicotine expressed slightly more RAGE when compared to cells exposed to eCig liquid alone. CAL-27 cells exposed to Red Hot expressed high levels of RAGE with expression further increased when nicotine was added with the Red Hot eCig liquid (B). Experiments were conducted in triplicate and Images (200x original magnification) are representative of the conducted cell culture experiments. Scale bars represent 100 μm.

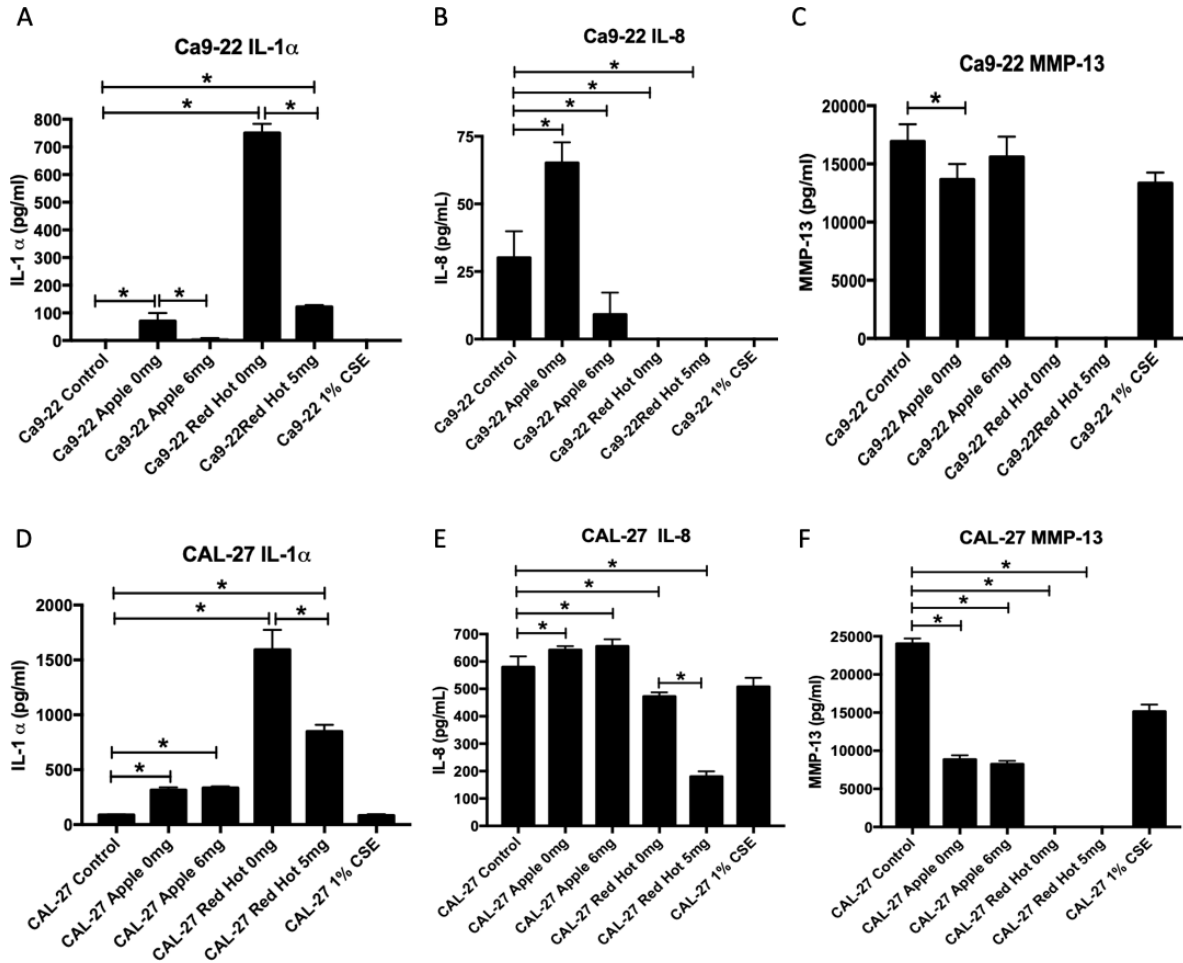Figure B.5: Expression of IL-1α, IL-8, and MMP-13 by Ca9-22 and CAL-27 Cells Treated with eCig Liquid.

Ca9-22 (A, B, C) and CAL-27 (D, E, F) cells were treated as indicated and conditioned cell culture media was screened for IL-1α(A and D), IL-8 B and E), and MMP-13 (C and F). Secreted protein concentrations were obtained in quadruplicate and statistically different values are noted as *$P < .05$.

References

Aberle, D. R., Abtin, F., & Brown, K. (2013). Computed tomography screening for lung cancer: has it finally arrived? Implications of the national lung screening trial. *J Clin Oncol, 31*(8), 1002-1008. doi:10.1200/JCO.2012.43.3110

Alzahrani, T., Pena, I., Temesgen, N., & Glantz, S. A. (2018). Association Between Electronic Cigarette Use and Myocardial Infarction. *Am J Prev Med, 55*(4), 455-461. doi:10.1016/j.amepre.2018.05.004

Bavle, R. M., Venugopal, R., Konda, P., Muniswamappa, S., & Makarla, S. (2016). Molecular Classification of Oral Squamous Cell Carcinoma. *J Clin Diagn Res, 10*(9), ZE18-ZE21. doi:10.7860/JCDR/2016/19967.8565

Bhawal, U. K., Ozaki, Y., Nishimura, M., Sugiyama, M., Sasahira, T., Nomura, Y., Kato, Y. (2005). Association of expression of receptor for advanced glycation end products and invasive activity of oral squamous cell carcinoma. *Oncology, 69*(3), 246-255. doi:10.1159/000087910

Blatt, S., Kruger, M., Ziebart, T., Sagheb, K., Schiegnitz, E., Goetze, E., Pabst, A. M. (2017). Biomarkers in diagnosis and therapy of oral squamous cell carcinoma: A review of the literature. *J Craniomaxillofac Surg, 45*(5), 722-730. doi:10.1016/j.jcms.2017.01.033

Chapman, S., Mick, M., Hall, P., Mejia, C., Sue, S., Abdul Wase, B., . . . Arroyo, J. A. (2018). Cigarette smoke extract induces oral squamous cell carcinoma cell invasion in a receptor for advanced glycation end-products-dependent manner. *Eur J Oral Sci, 126*(1), 33-40. doi:10.1111/eos.12395

Chen, I. L., Todd, I., & Fairclough, L. C. (2019). Immunological and pathological effects of electronic cigarettes. *Basic Clin Pharmacol Toxicol, 125*(3), 237-252. doi:10.1111/bcpt.13225

Deeming Tobacco Products To Be Subject to the Federal Food, D., and Cosmetic Act, as Amended by the Family Smoking Prevention and Tobacco Control Act; Restrictions on the Sale and Distribution of Tobacco Products and Required Warning Statements for Tobacco Products. (2016). [Press release]

Etter, J. F. (2010). Electronic cigarettes: a survey of users. *BMC Public Health, 10*, 231. doi:10.1186/1471-2458-10-231

Gennimata SA, P. A., Kaltsakas G, et al. (2014). Acute effect of e-cigarette on pulmonary function in healthy subjects and smokers. *European Respiratory Journal, 40*(Suppl 56).

Jiang, L., Ji, N., Zhou, Y., Li, J., Liu, X., Wang, Z., . . . Zeng, X. (2009). CAL 27 is an oral adenosquamous carcinoma cell line. *Oral Oncol, 45*(11), e204-207. doi:10.1016/j.oraloncology.2009.06.001

Kong, G., & Krishnan-Sarin, S. (2017). A call to end the epidemic of adolescent E-cigarette use. *Drug Alcohol Depend, 174*, 215-221. doi:10.1016/j.drugalcdep.2017.03.001

Lakhan, S. E., & Kirchgessner, A. (2011). Anti-inflammatory effects of nicotine in obesity and ulcerative colitis. *J Transl Med, 9*, 129. doi:10.1186/1479-5876-9-129

Nagaraj, N. S., & Zacharias, W. (2007). Cigarette smoke condensate increases cathepsin-mediated invasiveness of oral carcinoma cells. *Toxicol Lett, 170*(2), 134-145. doi:10.1016/j.toxlet.2007.02.014

Piao, W. H., Campagnolo, D., Dayao, C., Lukas, R. J., Wu, J., & Shi, F. D. (2009). Nicotine and inflammatory neurological disorders. *Acta Pharmacol Sin, 30*(6), 715-722. doi:10.1038/aps.2009.67

Pisinger, C., Godtfredsen, N., & Bender, A. M. (2019). A conflict of interest is strongly associated with tobacco industry-favourable results, indicating no harm of e-cigarettes. *Prev Med, 119*, 124-131. doi:10.1016/j.ypmed.2018.12.011

Pisinger, C., & Mackay, J. (2019). New Tobacco Products Do Not Protect Public Health. *AnnAm Thorac Soc, 16*(11), 1363-1365. doi:10.1513/AnnalsATS.201905-411PS

Polosa, R., Morjaria, J. B., Caponnetto, P., Campagna, D., Russo, C., Alamo, A., Fisichella, A. (2014). Effectiveness and tolerability of electronic cigarette in real-life: a 24-month prospective observational study. *Intern Emerg Med, 9*(5), 537-546. doi:10.1007/s11739-013-0977-z

Robinson, A. B., Stogsdill, J. A., Lewis, J. B., Wood, T. T., & Reynolds, P. R. (2012). RAGE and tobacco smoke: insights into modeling chronic obstructive pulmonary disease. *Front Physiol, 3*, 301. doi:10.3389/fphys.2012.00301

Rouabhia, M., Park, H. J., Semlali, A., Zakrzewski, A., Chmielewski, W., & Chakir, J. (2017).E-Cigarette Vapor Induces an Apoptotic Response in Human Gingival Epithelial Cells Through the Caspase-3 Pathway. *J Cell Physiol, 232*(6), 1539-1547. doi:10.1002/jcp.25677

Sanders, N. T., Dutson, D. J., Durrant, J. W., Lewis, J. B., Wilcox, S. H., Winden, D. R., Reynolds, P. R. (2017). Cigarette smoke extract (CSE) induces RAGE-mediated inflammation in the Ca9-22 gingival carcinoma epithelial cell line. *Arch Oral Biol, 80*, 95-100. doi:10.1016/j.archoralbio.2017.03.021

Schmidt, A. M., & Stern, D. M. (2001). Receptor for age (RAGE) is a gene within the major histocompatibility class III region: implications for host response mechanisms in homeostasis and chronic disease. *Front Biosci, 6*, D1151-1160. Retrieved from http://www.ncbi.nlm.nih.gov/pubmed/11578972

Singh, T., Arrazola, R. A., Corey, C. G., Husten, C. G., Neff, L. J., Homa, D. M., & King, B. A. (2016). Tobacco Use Among Middle and High School Students--United States, 2011-2015. *MMWR Morb Mortal Wkly Rep, 65*(14), 361-367. doi:10.15585/mmwr.mm6514a1

Sundar, I. K., Javed, F., Romanos, G. E., & Rahman, I. (2016). E-cigarettes and flavorings induce inflammatory and pro-senescence responses in oral epithelial cells and periodontalfibroblasts. *Oncotarget, 7*(47), 77196-77204. doi:10.18632/oncotarget.12857

Uchiyama, S., Senoo, Y., Hayashida, H., Inaba, Y., Nakagome, H., & Kunugita, N. (2016). Determination of Chemical Compounds Generated from Second-generation E-cigarettes Using a Sorbent Cartridge Followed by a Two-step Elution Method. *Anal Sci, 32*(5), 549-555. doi:10.2116/analsci.32.549

Vansickel, A. R., Cobb, C. O., Weaver, M. F., & Eissenberg, T. E. (2010). A clinical laboratory model for evaluating the acute effects of electronic "cigarettes": nicotine delivery profile and cardiovascular and subjective effects. *Cancer Epidemiol Biomarkers Prev, 19*(8), 1945-1953. doi:10.1158/1055-9965.EPI-10-0288

Vardavas, C. I., Anagnostopoulos, N., Kougias, M., Evangelopoulou, V., Connolly, G. N., & Behrakis, P. K. (2012). Short-term pulmonary effects of using an electronic cigarette: impact on respiratory flow resistance, impedance, and exhaled nitric oxide. *Chest, 141*(6),1400-1406. doi:10.1378/chest.11-2443

Wang, T. W., Gentzke, A., Sharapova, S., Cullen, K. A., Ambrose, B. K., & Jamal, A. (2018). Tobacco Product Use Among Middle and High School Students - United States, 2011-2017. *MMWR Morb Mortal Wkly Rep, 67*(22), 629-633. doi:10.15585/mmwr.mm6722a3

Winden, D. R., Barton, D. B., Betteridge, B. C., Bodine, J. S., Jones, C. M., Rogers, G. D., Reynolds, P. R. (2014). Antenatal exposure of maternal secondhand smoke (SHS)increases fetal lung expression of RAGE and induces RAGE-mediated pulmonaryinflammation. *Respir Res, 15*, 129. doi:10.1186/s12931-014-0129-7

World Health Organization. (2013). Questions and answers on electronic cigarettes or electronic nicotine delivery systems (ENDS).

CURRICULUM VITAE

Kary Ya Fang Tsai

1487 Arthur Dr., Provo, UT 84601 U.S.A. • 385-335-7103 • karyyftsai@gmail.com

_____

Education

2017 – 2021   Ph.D. Physiology and Developmental Biology
Brigham Young University, Provo, UT
Dissertation Title: RAGE Implication During DNA-DSBs in
Pathological Placentas and Trophoblast Cells
Ph.D. Advisor: Dr. Juan A. Arroyo
2012 – 2017   B.S. Biomedical science, Biochemistry minor
Brigham Young University - Hawaii, Honolulu, HI

Professional Experience

2019 – 2020   Council Member of Graduate Student Society
Brigham Young University, Provo, UT
2019 – 2020   Department Representative of Graduate Student Society
Brigham Young University, Provo, UT
2017 – 2017   Research Assistant
National Cheng Kung University College of Medicine, Tainan,
Taiwan
2015 – 2016   Quality Assurance Analyst
Honolulu Poi Company, Honolulu, HI
2013 – 2015   Student Researcher
Brigham Young University – Hawaii, Honolulu, HI
2014 – 2015   Vice President of American Society of Biochemistry and Molecular
Biology Undergraduate Affiliate Network of BYU – Hawaii
Brigham Young University – Hawaii, Honolulu, HI

Teaching Experience

2017 – 2020   Teaching Assistant:
1. Science of Biology
2. Cell Biology
3. Advanced Physiology Lab
2020   Lecturer (co-teaching)
1. Advanced physiology Lab Lecture

Awards and Achievements

2017 – 2021	Full Stipend and Tuition Awards
	Brigham Young University, Provo, UT
2020 – 2021	Honor Student
	Delta Alpha Pi International Honor Society
	Brigham Young University, Provo, UT
2019 – 2020	Research Presentation Travel Awards
	Brigham Young University, Provo, UT
2019	University 3MT Competition Department Representative
	Brigham Young University, Provo, UT
2018	2nd place in Department Annual Presentation
	Brigham Young University, Provo, UT
2013 - 2015	Mentored Research Award
	Brigham Young University – Hawaii, Honolulu, HI
2013	General scholarship fund
	Brigham Young University – Hawaii, Honolulu, HI
2012	Monida & Nephi Cummings DOM Scholarship
	Brigham Young University – Hawaii, Honolulu, HI

Oral and Poster Presentations at National and International Meetings

2021	International Association for Dental Research, Virtual Conference. "Acute eCig Vapor or SHS Exposure Induces Inflammatory Signaling in the Adult Murine Lung". Oral Presentation.
2020	Roseman Conference, South Jordan, UT. "RAGE and phospho-ATM Correlation During DNA Double Strand Breaks in Trophoblast Cells". Poster Presentation.
2020	Roseman Conference, South Jordan, UT. "Co-expression of Placental RAGE and g-H2AX During Intrauterine Growth Restriction and Preeclampsia in Rodents". Poster Presentation.
2019	Roseman Conference, South Jordan, UT. "RAGE Implications During DNA Double Strand Breaks in Trophoblast Cells". Poster Presentation.
2019	Roseman Conference, South Jordan, UT. "Differential Expression γ-H2AX and RAGE in the Placenta of Gestational Diabetes Mellitus (GDM), Preterm Labor (PTL) and Preeclampsia patients". Poster Presentation.
2019	Experimental Biology International Meeting, Orlando, FL. "RAGE Implications During DNA Double Strand Breaks in Trophoblast Cells". Oral Presentation.
2019	Experimental Biology International Meeting, Orlando, FL. "Differential Expression γ-H2AX and RAGE in the Placenta of Gestational Diabetes Mellitus (GDM), Preterm Labor (PTL) and Preeclampsia patients". Poster Presentation.

2019	International Federation of Placenta Association, Buenos Aires, Argentina. "Differential Expression γ-H2AX and RAGE in the Placenta of Gestational Diabetes Mellitus (GDM), Preterm Labor (PTL) and Preeclampsia (PE) Patients and Invasive Trophoblast Cells". Oral Presentation.
2019	International Federation of Placenta Association, Buenos Aires, Argentina. "Differential Expression γ-H2AX and RAGE in the Placenta of Gestational Diabetes Mellitus (GDM), Preterm Labor (PTL) and Preeclampsia (PE) Patients and Invasive Trophoblast Cells". Poster Presentation.

Student Grants and Awards

2020	Roseman Conference – 1st Place Poster Presentation J. Taylor Graff: RAGE and phospho-ATM Correlation During DNA Double Strand Breaks in Trophoblast Cells.
2019	Brigham Young University Undergraduate ORCA Award – 2nd Place Sam Llivina: Differential Expression γ-H2AX and RAGE in the Placenta of Gestational Diabetes Mellitus (GDM), Preterm Labor (PTL) and Preeclampsia Patients.
2019	Roseman Conference – 2nd Place Poster Presentation Abby Bennett: RAGE Implications During DNA Double Strand Breaks in Trophoblast Cells.

Publications

1. Hirschi, K. M., Fang Tsai, K. Y., Edwards, M. M., Hall, P., Mejia, J. F., Mejia, C. A., Reynolds, P. R., & Arroyo, J. A. (2019). The mTOR Family of Proteins and the Regulation of Trophoblast Invasion by Gas6. *Journal of Cell Signaling*, *04*(02). https://doi.org/10.35248/2576-1471.19.4.203

2. Mejia, J. F., Hirschi, K. M., Tsai, K. Y. F., Long, M. G., Tullis, B. C., Bitter, E. E. K., Bikman, B. T., Reynolds, P. R., & Arroyo, J. A. (2019). Differential placental ceramide levels during gestational diabetes mellitus (GDM). *Reproductive Biology and Endocrinology*, *17*(1). https://doi.org/10.1186/s12958-019-0523-6

3. Tsai, K. Y. F., Hirschi Budge, K. M., Llavina, S., Davis, T., Long, M., Bennett, A., Sitton, B., Arroyo, J. A., & Reynolds, P. R. (2019). RAGE and AXL expression following secondhand smoke (SHS) exposure in mice. *Experimental Lung Research*, *45*(9–10), 297–309. https://doi.org/10.1080/01902148.2019.1684596

4. Hirschi, K. M., <u>Tsai, K. Y. F.</u>, Davis, T., Clark, J. C., Knowlton, M. N., Bikman, B. T., Reynolds, P. R., & Arroyo, J. A. (2020). Growth arrest-specific protein-6/AXL signaling induces preeclampsia in rats. *Biology of Reproduction*, *102*(1), 199–210. https://doi.org/10.1093/biolre/ioz140

5. <u>Tsai, K. Y. F.</u>, Hirschi Budge, K. M., Lepre, A. P., Rhees, M. S., Ajdaharian, J., Geiler, J., Epperson, D. G., Astle, K. J., Winden, D. R., Arroyo, J. A., & Reynolds, P. R. (2020). Cell invasion, RAGE expression, and inflammation in oral squamous cell carcinoma (OSCC) cells exposed to e-cigarette flavoring. *Clinical and Experimental Dental Research*. https://doi.org/10.1002/cre2.314

6. <u>Tsai, K. Y. F.</u>, Tullis, B., Mejia, J., Reynolds, P. R., & Arroyo, J. A. (2021). Regulation of trophoblast cell invasion by Pyruvate Kinase isozyme M2 (PKM2). *Placenta*, *103*, 24–32. https://doi.org/10.1016/j.placenta.2020.10.019

7. <u>Tsai, K.</u>, Tullis, B., Jensen, T., Graff, T., Reynolds, P., & Arroyo, J. (2021). Differential expression of mTOR related molecules in the placenta from gestational diabetes mellitus (GDM), intrauterine growth restriction (IUGR) and preeclampsia patients. Reproductive Biology, 21(2). https://doi.org/10.1016/j.repbio.2021.100503

8. <u>Tsai, K. Y. F.</u>, Tullis, B., Breithaupt, K. L., Fowers, R., Jones, N., Grajeda, S., Reynolds, P. R., & Arroyo, J. A. (2021). A Role for RAGE in DNA Double Strand Breaks (DSBs) Detected in Pathological Placentas and Trophoblast Cells. Cells, 10(4), 857. https://doi.org/10.3390/cells10040857